UCRL-53779

Hydrology and Radionuclide Migration Program 1985–1986 Progress Report

Compiled by

Robert W. Buddemeier

September 1988

DISCLAIMER

Work performed under the auspices of the U.S. Department of Energy by Lawrence Livermore National Laboratory under Contract W-7405-Eng-48.

UCRL--53779

DE89 010559

Hydrology and Radionuclide Migration Program 1985–1986 Progress Report

Compiled by

Robert W. Buddemeier

Manuscript date: September 1988

LAWRENCE LIVERMORE NATIONAL LABORATORY
University of California • Livermore, California • 94550

Available from: National Technical Information Service • U.S. Department of Commerce
5285 Port Royal Road • Springfield, VA 22161 •A03• (Microfiche A01)

Contents

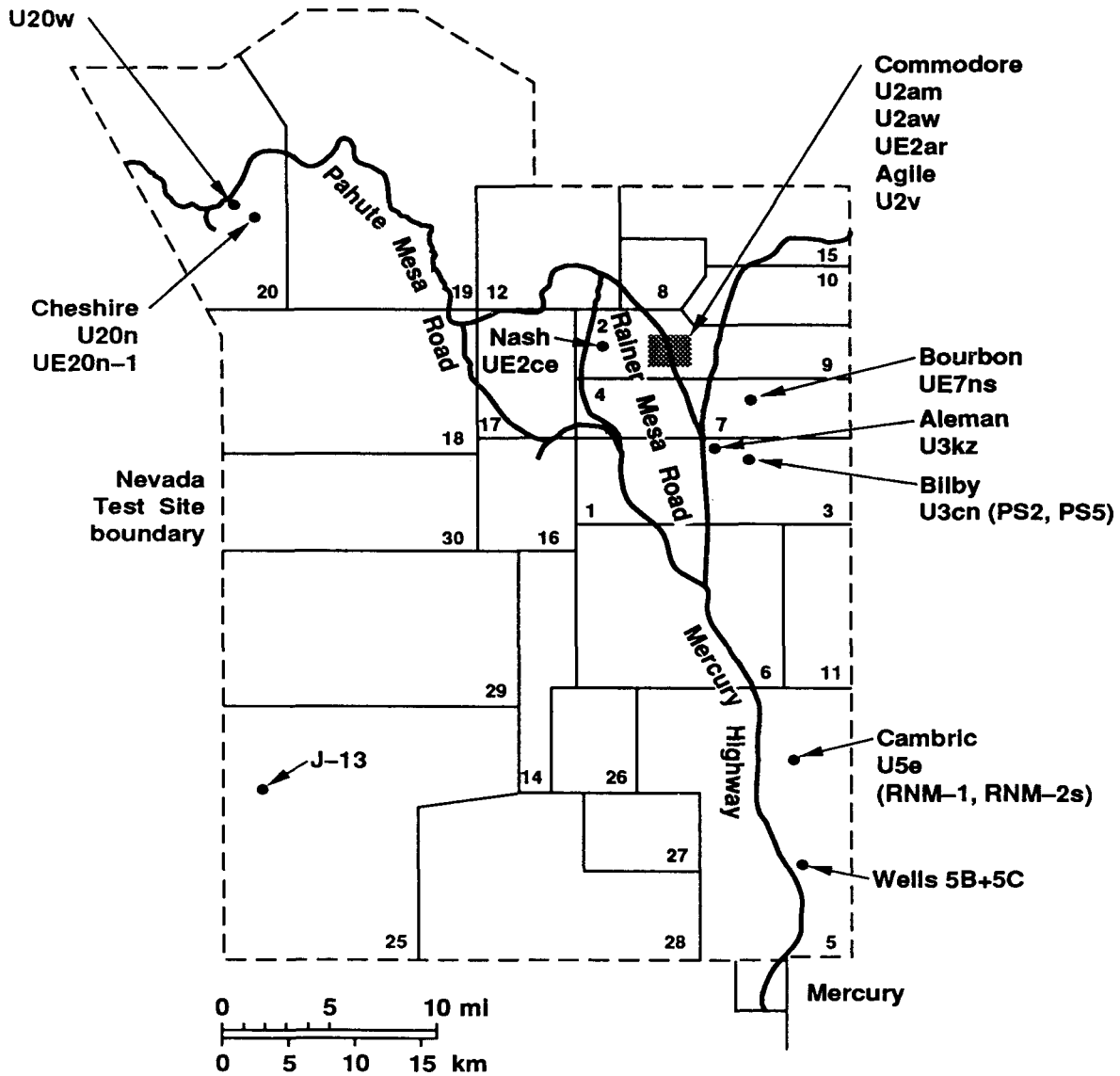

Frontispiece. Locations of wells and events relevant to the Hydrology and Radionuclide Migration Program. Small numbers indicate NTS areas.

Acknowledgments

In the sections of this report that present data or interpretational results, the individuals who made significant scientific or technical contributions to the specific effort are listed as contributors. Many others, however, have provided general support, assistance, and advice important to the overall report. We gratefully acknowledge the contributions of the following organizations and individuals:

Lawrence Livermore National Laboratory: L. Ramspott, C. Martin, N. Crow, D. Isherwood, D. Hansen, C. McGregor, K. Marsh.

Los Alamos National Laboratory: J. Thompson and his coworkers in INC11.

Desert Research Institute (DRI): R. Jacobson, S. Tyler, and the professional and technical staff at both the Reno and Las Vegas offices.

U.S. Geological Survey: Wayne Evert and C. Savard.

Reynolds Electrical and Engineering Co., Inc.: Environmental Science Department personnel.

Department of Energy-Nevada Operations Office: T. Humphrey and J. Burrows.

Dr. Richard C. Evans, of Alabama A&M University, worked on the project while he was a visiting researcher at LLNL supported by the Office of Equal Opportunity.

Hydrology and Radionuclide Migration Program 1985–1986 Progress Report

Abstract

This report presents results from the Lawrence Livermore National Laboratory's participation in the Hydrology and Radionuclide Migration Program (formerly the Radionuclide Migration Project) at the Nevada Test Site (NTS) during fiscal years 1985 and 1986. The report discusses studies of the partitioning and movement of dissolved and colloidal radionuclides at the Cheshire (U20n) site; tracer studies of shallow recharge and of plant-water uptake at the Cambric-site ditch carrying the effluent water pumped from well RNM-2; development of a rapid and sensitive assay for ^{99}Tc in groundwater and its application to a survey of technetium activities at a variety of test wells; and a series of methodological studies directed toward calibrating, understanding, and improving our low-level radionuclide determinations.

Groundwater sampled from the Cheshire cavity and from adjacent aquifers contains substantial concentrations (mg/L) of colloids that appear to consist primarily of natural minerals. These colloids were found to contain detectable amounts of strongly sorbed radionuclides, leading to the hypothesis that radionuclides are being transported by the groundwater in colloidal form.

The RNM ditch at the Cambric site has provided a unique tritium-labeled, irrigated test plot in the desert. One study at this site continued earlier investigations of water and tritium migration in the shallow vadose (unsaturated-soil) zone adjacent to the ditch and extended that study to include using a tracer to determine the velocity of vertical water flow in the recharge zone directly below the ditch. A second investigation employed tritium and deuterium determinations to investigate the water budgets of various plants growing naturally in or near the ditch; it was found that a significant fraction of the free water in plant tissue appeared to be derived from the atmosphere rather than from the soil moisture.

A rapid, simple, and sensitive (detection limit $<10^{-9}$ μCi/mL) method of concentrating TcO_4^- and measuring ^{99}Tc by liquid scintillation spectrometry was developed. The technique was applied to a survey of the various wells that have been sampled for the program; measurable concentrations were detected in the Cheshire cavity well and in the Cheshire, Bilby, and Faultless satellite wells, but not in the Nash, Bourbon, or Cambric satellite wells or in the Cambric cavity well.

Additional investigations included the calibration of Marinelli beaker counting systems and the application of these systems to direct, semi-low-level, prompt characterization of groundwater samples; a sample exchange and intercalibration with the Los Alamos National Laboratory group; a comparison of direct gamma-ray counting of filters with the results of counting ashed-composite filters; and a reanalysis of archived samples relevant to early observations of radionuclide migration in NTS Area 2.

Section 1. Introduction

This report presents the results of technical studies conducted by the Lawrence Livermore National Laboratory (LLNL) as part of the Hydrology and Radionuclide Migration Program (HRMP) at the Nevada Test Site (NTS). The Program, previously known as the Radionuclide Migration Program (RNM), is intended to assess the potential for radionuclide migration away from the underground nuclear test cavities at NTS, with particular emphasis on issues relating to groundwater contamination and transport. The Frontispiece shows the locations of the sites and wells studied at NTS.

The project, which was initiated in 1974, continues as a multi-agency research project [LLNL, Los Alamos National Laboratory (LANL), the Desert Research Institute (DRI) of the University of Nevada, and the U.S. Geological Survey (USGS)] coordinated and funded by the Nevada Operations Office of the U.S. Department of Energy (DOE-NVOO).

The agencies involved in the project issue a variety of letter reports, technical reports, and scientific publications on aspects of HRMP studies. The most recent LLNL report generally available is the 1984 Progress Report (Buddemeier and Isherwood, 1985). The present report is a comprehensive account of LLNL activities and results for the HRM Program for FY85 and FY86.

This report is organized on a topical basis. Section 2 summarizes our current investigations into transport of radionuclides at the Cheshire site. We emphasize findings related to the nature, occurrence, and transport of colloidal radionuclides and include a review of the literature concerning colloid transport in general. Section 3 describes experiments at the Cambric site in which we characterized the flow velocity in a seepage plume from an unlined ditch carrying water pumped from the Cambric cavity. We have also studied water metabolism in plants growing along this ditch by making use of the tritium in the water. Section 4 describes a method we have developed for ^{99}Tc analysis of water samples and presents the results of analysis of samples from both present and historical HRMP sites. Section 5 describes a variety of smaller applied studies, including some new measurements on samples collected in NTS Area 2 in 1975. The report concludes with a description of several methodological investigations relating to analytical techniques and quality assurance.

Section 2. Radionuclide Migration at the Cheshire Event Site

Contributors: R. W. Buddemeier, J. R. Hunt, and J. H. Rego*

Introduction

The Cheshire Event was fired on February 14, 1976, with an announced yield in the 200- to 500-kt range. The site is on the Pahute Mesa (see Frontispiece). The device was detonated at a depth of 1167 m in a rhyolite formation; the preshot water level was at a depth of 630 m. Figure 2-1 shows the stratigraphy and vertical hydraulic gradient prior to detonation of the Cheshire device.

The Cheshire site is of interest to the Hydrology and Radionuclide Migration Program (HRMP) for three reasons:

- It is the only study site in tuff as opposed to alluvium or carbonate aquifers.
- The detonation was more recent and larger than most of the other shots under investigation, thus providing a larger source term and a better opportunity to study the behavior of the short-lived radionuclides.

* University of California, Berkeley.

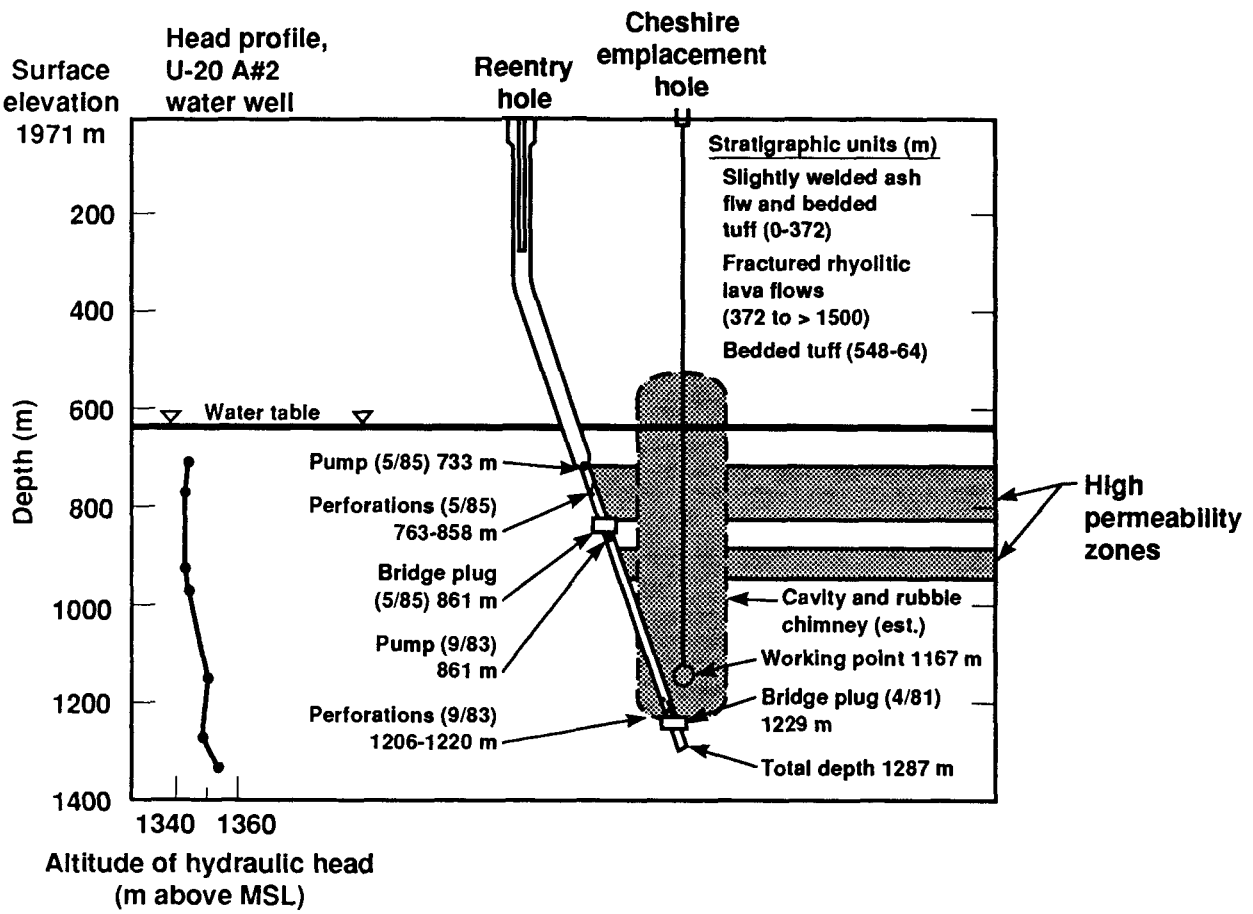

Figure 2-1. Vertical section of Cheshire experimental site showing sampling locations, hydrogeologic stratigraphy, and hydraulic head with depth (Blankennagel and Weir, 1973). Horizontal dimensions are not to scale.

• The site is only 8 km from the western boundary of the Nevada Test Site (NTS) in a permeable formation with a surface water table gradient trending southwest; therefore, this site is a likely candidate for relatively prompt, off-site transport of radionuclides.

Subsurface access was via a slant-drilled reentry hole that was eventually cased and perforated within the cavity. Water was intermittently pumped from the cavity (as indicated in Fig. 2-2 along with tritium activities). In May 1985, the well was plugged (as illustrated in Fig. 2-1) and reperforated in the higher-permeability zones of the formation at a position displaced about 100 m laterally and about 250 m above the upper boundary of the cavity.

Regional groundwater flows are expected to be upward (driven by the vertical hydraulic gradient) and horizontal toward the reperforated zone. For the mesa as a whole, the best estimate of transmissibility is 10^{-3} m²/s (Waddell, 1982), and a pump test near the Cheshire site indicated a transmissibility of 2×10^{-2} m²/s in the most permeable zone. Such a range in values hinders precise estimation of transit times from the cavity to the external sampling location.

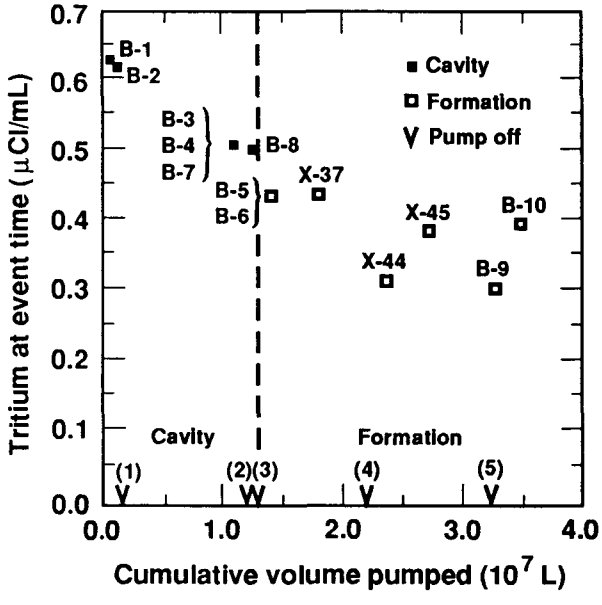

Figure 2-2. Pumping history and tritium activity at the Cheshire site. Tritium counting uncertainties are typically <1%. Samples coded "X" are small-volume samples analyzed for ^{3}H only. Samples B-7 through B-10 are large-volume samples not fully processed at the time of publication. Coded symbols represent intervals when pump was off: 1) 9-9-83 to 8-1-84; 2) 10-25-84 to 4-25-85; 3) 5-14-85 to 5-23-85; 4) 7-20-85 to 9-11-85; 5) 10-1-85 to 10-8-85. (No water has been pumped since 11-7-85.)

Initial studies of the radioactivity of the cavity water were reported by Buddemeier and Isherwood (1985). Included in these findings were the observations that a significant amount of the radioactivity was apparently associated with colloidal particles that passed through conventional filters.

Since many radionuclides strongly adsorb to mineral surfaces, transport with groundwater flow is expected to be limited. One of the key assumptions adopted in transport models is that the radionuclides, once adsorbed, are immobile. However, considerable laboratory and field evidence indicates that colloidal material is mobile in groundwater (McDowell-Boyer et al., 1986), and the initial Cheshire findings revealed a possibility that radionuclides could be transported by these mobile colloids.

This section of the report presents the results of studies conducted to determine the characteristics of colloidal loading, colloidal radionuclide associations, and colloidal transport in and between the groundwater in the cavity and that in the down-gradient external formation (see Fig. 2-1). For completeness and comparison, some of the results presented by Buddemeier and Isherwood (1985) are retabulated and discussed here.

Methods

During the course of pumping from both the cavity and formation locations, water was measured in the field for pH, alkalinity, temperature, dissolved oxygen, and conductivity. Large-volume water samples were collected in new, plastic-lined, 55-gal drums, then sealed and shipped at ambient temperatures to LLNL for analysis. Storage times for the samples (before they were processed) ranged from 1 to 10 months.

In the laboratory, the contents of each drum were vigorously mixed and pumped through various filters (see Table 2-1). The first sample analyzed, B-2, was only filtered to 0.45 μm. Nuclepore polycarbonate filters were used initially for sample B-1. However, because of

Table 2-1. Sample descriptions.

Sample	Location	Date collected	Cumulative water pumped (L)[a]	Filters (retention size, μm)[b]
B-1	Cavity	9/8/83	2.1×10^5	1.0–0.45–0.20–0.006
B-2	Cavity	9/9/83	5×10^5	0.45
B-3	Cavity	10/23/84	1.1×10^7	1.0–0.45–0.20
B-4	Cavity	10/23/84	1.1×10^7	1.0–0.45–0.45–0.20–0.05–0.003
B-5	Formation	5/28/85	1.4×10^7	1.0–0.45–0.20–0.05–0.003
			(1.04×10^6)[c]	
B-6	Formation	5/28/85	1.4×10^7	1.0–0.45–0.20–0.05–0.003
			(1.05×10^6)[c]	

[a]Total volume pumped subsequent to installation of sampling location in cavity.
[b]0.006- and 0.003-μm filters are 100,000- and 10,000-molecular-weight ultrafilters, respectively.
[c]Cumulative volume pumped at formation location after relocation of perforated interval and pump.

clogging and exceedingly slow filtration rates, we completed the sample B-1 filtration using bag-type filters (Fin-L-Filters) with nominal pore sizes of 1.0 and 0.45 μm. All the filters were then counted together and reported as 0.45 μm. For all the other samples, bag-type filters were used for 1.0-, 0.45-, and 0.20-μm nominal pore sizes. The 0.05-μm Millipore filters (293 mm in diameter) were of mixed cellulose acetate and nitrate composition; eight were used in parallel for each sample. Selected serially filtered samples were then ultrafiltered through a Millipore XX42 Pellicon cassette system with either a 100,000- or a 10,000-molecular-weight filter (nomimal pore sizes of 0.006 or 0.003 μm, respectively).

For the first ultrafiltered sample, B-1, the solution was continually pumped through the filters to the ultrafilter, and the ultrafilter retentate was recycled back to the drum until the retentate volume was sufficiently reduced. Subsequent ultrafiltrations were done following a single pass through the filters into a clean drum.

The ultrafiltration system produced about 200 L of ultrafiltrate (that which passed the ultrafilter) and 0.5 L of retentate containing colloids that did not pass the ultrafilter. To determine the activity of gamma-ray—emitting radionuclides, the ultrafiltrates, retentates, and filters were evaporated to dryness, weighed, and counted for 5 days on low-background Ge(Li) detector systems. The overall uncertainties in specific activities were conservatively assumed to be ±25%, which reflects counting statistics, calibration, and the effects of geometry (see Sec. 5 of this report). Tests showed that there was no significant loss of activity to container walls or to the ultrafilter (Buddemeier and Isherwood, 1985).

Selected retentate and ultrafiltrate samples were also analyzed by x-ray diffraction to determine the dominant mineral phases present and by x-ray fluorescence for elemental analysis. Separate analyses were undertaken for tritium and for major anions and cations. All concentrations and activities are reported per liter of original sample volume, activities are decay-corrected to the detonation time of the Cheshire Event, and detection limits are calculated at the time counted.

Details of laboratory methods have been reported previously (Buddemeier and Isherwood, 1985). See also Sec. 5 of this report for discussions on uncertainties, calibration, and specific counting methods.

Results

In this report, we shall emphasize the gamma-spectrometry and chemical results from six large-volume samples designated B-1 through B-6. Additional sample data and supporting analytical work are presented in Secs. 4 and 5 of this report. Descriptions of these samples and the filter series we analyzed are listed in Table 2-1. Well-head measurements indicated that the cavity water had a pH of 8.6, a dissolved oxygen concentration of about 3 mg/L, and a temperature of 40 to 42°C when stabilized by protracted pumping. For the formation samples, the field pH was 8.4 with 5 to 6 mg/L dissolved

oxygen; water temperature was similar to that in the cavity.

Total dissolved solids (TDS) and colloid concentrations were estimated from samples of dried ultrafiltrate and retentate. Table 2-2 summarizes these estimates and indicates the considerable mass of submicrometer colloids present in these pumped groundwaters. The ultrafiltrates were assumed to exclude all colloids; thus, the dried ultrafiltrate is the TDS. Since ultrafiltration was not conducted for all samples, some extrapolation was necessary; this is indicated by the numbers in parentheses in Table 2-2. For example, since the TDS was not available for sample B-2, we assumed the value from B-1. Similarly, sample B-3 was collected on the same date as B-4, so for sample B-3 we assumed the TDS of 263 mg/L from sample B-4.

Dried retentate samples provided estimates of colloid mass concentration. After sample B-4 was filtered through a 0.05-μm filter, the 194.5 L was ultrafiltered, producing a retentate volume of 0.245 L with a dried mass of 2.04 g. Assuming the TDS in the retentate is the same as the ultrafiltrate provides the estimate that 10.1 mg of 0.05- to 0.003-μm colloids are present per liter of the original sample. Samples with different filtrations prior to ultrafiltration provide colloid masses in the various size ranges given in Table 2-2. It is further interesting to note that these original samples were not cloudy despite the high colloid concentrations.

Radionuclide activities retained on various filters and concentrated by ultrafiltration are compiled in Appendix A. Tables 2-3 through 2-8 present the activity data expressed as fraction of total activity of the samples B-1 through B-6, respectively. The actual order of sample processing was B-2, B-1, B-3, B-4, B-5, and B-6; the evolving procedures were dictated by the results of the analysis. For sample B-2, detection of significant activity of the low-solubility, adsorbing nuclides manganese, cobalt, cesium, and europium after the sample was passed through 0.45-μm filters suggested that this filtration did not separate dissolved from particle-associated nuclides. For sample B-3, we switched completely to bag filters (Table 2-3); again, substantial radionuclide activity passed through the 0.20-μm filter for those particle-associated nuclides. The Nuclepore filters used for sample B-2 appear to have been partially plugged because the fraction of europium passing this filter is about 80%; in comparison, about 90% of the europium activity passed through the smaller, 0.20-μm filter used for sample B-3.

Tests of sample B-1 included the ultrafiltration step for the first time, and the analysis showed that colloidal material in the 0.20- to 0.006-μm range had a significant fraction of the radionuclides manganese, cobalt, cesium, cerium, and europium. To provide further information on radionuclide partitioning of the smaller colloids, the final analysis configuration for samples B-4 through B-6 included the 0.05-μm step. For sample B-4, two 0.45-μm filter bags were placed in series, and the second filter had about half the activity of the first. The data for the cesium and europium radioisotopes are very similar in their distribution of activity among

Table 2-2. Dissolved and colloidal material in Cheshire samples.

Sample	Location	TDS[a,b] (mg/L)	Colloid size range (μm)	Colloid mass concentration (mg/L)
B-1	Cavity	256	0.20–0.006	55
B-2	Cavity	(256)	0.45–0.006	(63)
B-3	Cavity	(263)	0.20–0.003	(35)
B-3	Cavity	(263)	0.20–0.05	(25)
B-4	Cavity	263	0.05–0.003	10.1
B-5	Formation	216	0.05–0.003	4.6
B-6	Formation	218	0.05–0.003	4.3

[a]TDS = total dissolved solids.

[b]Parentheses indicate an assumed value based on samples collected close in time to the indicated sample.

Table 2-3. Cheshire nuclide analysis for cavity sample B-1.

Nuclide	Half-life (y)	Total activity (μCi/mL)[a]	Fraction of total activity retained on Prefilter	0.45 μm	0.20 μm	0.006 μm	Fraction dissolved
^{3}H	12.33	0.615 (1)	NA[b]	NA	NA	NA	1.000
^{22}Na	2.605	7.57×10^{-9} (24)	<0.001	0.061	<0.001	<0.06	0.939
^{40}K	1.3×10^{9}	2.67×10^{-9} (18)	<0.02	<0.02	<0.02	0.625	0.375
^{54}Mn	0.855	1.18×10^{-7} (25)	0.503	0.069	0.059	0.369	<0.14
^{60}Co	5.272	5.53×10^{-9} (16)	0.576	0.082	0.071	0.271	<0.004
^{106}Ru	1.020	1.25×10^{-5} (16)	0.189	0.084	0.067	0.578	0.082
^{125}Sb	2.760	5.27×10^{-6} (24)	0.007	0.003	0.002	0.039	0.949
^{134}Cs	2.065	2.18×10^{-8} (17)	0.055	0.020	0.016	0.322	0.587
^{137}Cs	30.170	3.19×10^{-6} (16)	0.084	0.024	0.016	0.326	0.550
^{144}Ce	0.778	1.20×10^{-8} (17)	0.280	0.074	0.055	0.591	<0.01
^{152}Eu	13.40	9.51×10^{-9} (17)	0.281	0.071	0.052	0.596	<0.01
^{154}Eu	8.50	1.64×10^{-8} (17)	0.286	0.073	0.053	0.588	<0.01
^{155}Eu	4.73	4.10×10^{-8} (16)	0.313	0.082	0.059	0.547	<0.01

[a]All activities decay-corrected to T_0 = 14 Feb. 1976. Values in parentheses are the percent uncertainties (±1σ) based on counting uncertainties for the individual samples.
[b]NA = not analyzed.

filter sizes, and the counting statistics for a specific filter were very good. For example, in sample B-4 (Table 2-6) the fractions of total activity recorded on the 1.0-μm pre-filter were 0.111 and 0.116 for ^{134}Cs and ^{137}Cs, respectively; a similarly small variation (0.359, 0.364, and 0.345) was observed for the three europium isotopes. Comparing activity distributions between samples is complicated by the differences in samples and in counting geometry. Sample B-6 measurements had higher detection limits than sample B-5, which hindered comparison of formation samples for homogeneity.

Radionuclide transport from the cavity to the formation is dependent on physical and chemical factors. Figure 2-3 compares the ratio of formation activity to total cavity activity with the fraction dissolved for each nuclide in the cavity sample. One major effect apparent in Fig. 2-3, namely, that the tritium activity in the formation

Table 2-4. Cheshire nuclide analysis for cavity sample B-2.

Nuclide	Half-life (y)	Total activity (μCi/mL)[a]	Fraction of total activity retained on 0.45-μm filter	Fraction of total activity <0.45 μm
^{3}H	12.26	0.614 (1)	NA[b]	1.000
^{22}Na	2.605	9.79×10^{-9} (23)	0.079	0.921
^{40}K	1.3×10^{9}	5.24×10^{-9} (19)	0.269	0.731
^{54}Mn	0.855	1.20×10^{-7} (22)	0.341	0.659
^{60}Co	5.272	6.07×10^{-9} (18)	0.332	0.668
^{106}Ru	1.020	1.48×10^{-5} (21)	0.185	0.815
^{125}Sb	2.760	6.27×10^{-6} (25)	0.007	0.993
^{134}Cs	2.065	2.68×10^{-8} (21)	0.182	0.818
^{137}Cs	30.170	3.40×10^{-6} (20)	0.212	0.788
^{144}Ce	0.778	1.49×10^{-8} (20)	0.209	0.791
^{152}Eu	13.40	1.20×10^{-8} (21)	0.197	0.803
^{154}Eu	8.50	1.90×10^{-8} (21)	0.169	0.831
^{155}Eu	4.73	6.10×10^{-8} (21)	0.191	0.809

[a]All activities decay corrected to T_0 = 14 Feb. 1976. Values in parentheses are the percent uncertainties (±1σ) based on counting uncertainties for the individual samples.
[b]NA = not analyzed.

sample is 86% of that in the cavity sample, shows that very little physical dilution of the cavity water occurs.* For the cobalt and europium nuclides that are more than 98% associated with colloids, the activity at the formation location is only about 2.5% of that at the cavity—indicating significant colloid removal during solution transport. If there were no chemical exchange between dissolved nuclides and suspended colloids or between dissolved nuclides and fracture surfaces, then the other nuclides should fall in the shaded area in Fig. 2-3. Since the other nuclides are not near this mixing line, nuclide exchange among dissolved species, suspended colloids, and fracture surfaces is suggested. ^{40}K is a special case in these results because it is a naturally occurring radionuclide; artificial production by the detonation is not believed to be significant.

The other nuclides show effects of chemical interactions during transit from the cavity to the formation location. For ^{22}Na, ^{125}Sb, ^{134}Cs, and ^{137}Cs, there is lower activity in the formation than expected if only physical dilution and colloid

* A slightly greater dilution, but still less than a factor of two, is suggested by the ^{99}Tc, an anionic species often assumed to act as a conservative tracer.

Table 2-5. Cheshire nuclide analysis for cavity sample B-3.

Nuclide	Half-life (y)	Total activity (μCi/mL)[a]	Fraction of total activity retained on Prefilter	0.45 μm	0.20 μm	Fraction of total activity <0.20 μm
^{3}H	12.26	0.504 (1)	NA[b]	NA	NA	1.000
^{22}Na	2.605	8.02×10^{-9} (25)	0.019	<0.008	<0.002	0.981
^{40}K	1.3×10^{9}	3.58×10^{-9} (24)	[Combined filters, 0.03]			0.097
^{54}Mn	0.855	9.64×10^{-8} (64)	[Combined filters, 0.128]			0.872
^{60}Co	5.272	3.42×10^{-9} (22)	0.068	0.035	0.031	0.866
^{106}Ru	1.020	1.14×10^{-5} (23)	0.029	0.029	0.025	0.917
^{125}Sb	2.760	6.77×10^{-6} (25)	0.001	0.002	0.001	0.996
^{134}Cs	2.065	2.70×10^{-8} (37)	0.008	ND[b]	ND	0.992
^{137}Cs	30.170	4.60×10^{-6} (24)	0.009	0.007	0.008	0.976
^{144}Ce	0.778	1.01×10^{-8} (24)	0.051	<0.004	<0.003	0.949
^{152}Eu	13.40	7.52×10^{-9} (23)	0.047	0.024	0.027	0.902
^{154}Eu	8.50	1.31×10^{-8} (23)	0.044	0.025	0.026	0.905
^{155}Eu	4.73	3.87×10^{-8} (23)	0.044	0.022	0.023	0.911

[a] All activities decay-corrected to T_0 = 14 Feb. 1976. Values in parentheses are the percent uncertainties (±1σ) based on counting uncertainties for the individual samples.
[b] NA = not analyzed; ND = not detected; no limit calculated.

removal were operating, as represented by the shaded region in Fig. 2-3. This suggests either adsorption of dissolved contaminants to fracture surfaces or exchange of a radionuclide with a naturally occurring stable isotope. The result for ^{106}Ru is anomalous in that greater than expected activity is observed at the formation location.

Adsorption and desorption of nuclides can be quantified for nuclides with detectable activities in both the 0.05- to 0.003-μm range and dissolved fractions. If the linear adsorption isotherm is applicable, a distribution coefficient K_d may be expressed as

$$K_d = q/C \quad (1)$$

where q is the activity of the radionuclide adsorbed per unit area of solid, and C is the equilibrium concentration of the dissolved nuclide.

K_d values for ^{106}Ru, ^{125}Sb, ^{134}Cs, and ^{137}Cs are calculated and listed in Table 2-9 for the last cavity sample (B-4) and for the two formation samples (B-5 and B-6). Calculations were

Table 2-6. Cheshire nuclide analysis for cavity sample B-4.

Nuclide	Half-life (y)	Total activity (μCi/mL)[a]	Fraction of total activity retained on					Fraction dissolved
			Prefilter	0.45 μm	0.20 μm	0.05 μm	0.003 μm	
^{3}H	12.36	0.504 (1)	NA[b]	NA	NA	NA	NA	1.000
^{22}Na	2.605	8.5×10^{-9} (23)	<0.18	<0.01	0.022	0.013	0.037	0.928
^{40}K	1.3×10^{9}	4.15×10^{-9} (20)	0.198	0.039	0.079	0.330	0.084	0.270
^{54}Mn	0.855	3.31×10^{-8} (36)	0.750	0.250	<0.14	<0.12	ND[b]	ND
^{60}Co	5.272	3.12×10^{-9}	0.368	0.129	0.155	0.123	0.204	0.021
^{106}Ru	1.020	1.05×10^{-6} (22)	0.321	0.129	0.158	0.070	0.178	0.144
^{125}Sb	2.760	7.30×10^{-6} (24)	0.006	0.005	0.004	0.003	0.014	0.968
^{134}Cs	2.065	2.67×10^{-8} (19)	0.111	0.038	0.048	0.067	0.057	0.679
^{137}Cs	30.170	4.39×10^{-6} (19)	0.116	0.041	0.055	0.068	0.075	0.645
^{144}Ce	0.778	9.56×10^{-9} (25)	0.362	0.132	0.140	0.071	0.295	<0.05
^{152}Eu	13.40	6.75×10^{-9} (25)	0.359	0.127	0.162	0.135	0.209	0.008
^{154}Eu	8.50	1.17×10^{-8} (25)	0.364	0.130	0.161	0.127	0.218	<0.01
^{155}Eu	4.73	3.45×10^{-8} (25)	0.345	0.118	0.148	0.109	0.280	<0.03

[a]All activities decay-corrected to T_0 = 14 Feb. 1976. Values in parentheses are the percent uncertainties (±1σ) based on counting uncertainties for the individual samples.
[b]NA = not analyzed; ND = not detected; no limit calculated.

restricted to those samples because only these samples had corresponding values for colloid mass concentrations (Table 2-2). For ^{106}Ru and ^{125}Sb, the calculated distribution coefficients are close for the cavity sample and the first formation sample. The cesium radioisotopes have a greater spread in K_d values, with greater variability in ^{134}Cs than ^{137}Cs due to poorer counting statistics. For an unknown reason, formation sample B-6 was consistently low in K_d values for all the nuclides. As discussed below, K_d values calculated per mass of solids cannot be extrapolated to submicrometer colloids if they are measured on micrometer and larger particles. Cesium adsorption onto montmorillonite has a measured K_d of 4500 mL/g at 26°C in 2m*M* NaCl (Silva et al., 1979), a sodium concentration similar to that measured in groundwater at this site (3m*M*).

X-ray diffraction studies were undertaken for sample B-4 to gain some insight into the

Table 2-7. Cheshire nuclide analysis for formation sample B-5.

Nuclide	Half-life (y)	Total activity (μCi/mL)[a]	Fraction of total activity retained on					Fraction dissolved
			Prefilter	0.45 μm	0.20 μm	0.05 μm	0.003 μm	
^{3}H	12.36	0.433 (1)	NA[b]	NA	NA	NA	NA	1.000
^{22}Na	2.605	1.07×10^{-9} (24)	<0.02	<0.02	0.057	<0.28	<0.20	0.943
^{40}K	1.3×10^{9}	2.94×10^{-9} (20)	0.047	<0.01	<0.01	0.118	0.083	0.752
^{54}Mn	0.855	7×10^{-9} (72)	[Combined filters, 1.0]					<0.01
^{60}Co	5.272	1.06×10^{-10} (25)	0.441	<0.05	0.097	0.294	0.168	<0.04
^{106}Ru	1.020	2.67×10^{-6} (20)	0.162	0.071	0.055	0.289	0.205	0.217
^{125}Sb	2.760	3.93×10^{-6} (25)	0.003	0.002	0.004	0.004	0.006	0.985
^{134}Cs	2.065	1.91×10^{-9} (25)	ND[b]	ND	ND	ND	0.024	0.976
^{137}Cs	30.170	7.43×10^{-7} (22)	0.018	0.005	0.007	0.050	0.035	0.884
^{144}Ce	0.778	$<7.5 \times 10^{-11}$ (—)	ND[b]	ND	ND	ND	ND	ND
^{152}Eu	13.40	1.65×10^{-10} (25)	0.237	<0.07	<0.08	0.458	0.305	<0.06
^{154}Eu	8.50	2.99×10^{-10} (25)	0.245	<0.02	<0.02	0.466	0.289	<0.07
^{155}Eu	4.73	8.8×10^{-10} (25)	0.173	0.034	0.066	0.382	0.345	<0.13

[a]All activities decay-corrected to T_0 = 14 Feb. 1976. Values in parentheses are the percent uncertainties (±1σ) based on counting uncertainties for the individual samples.
[b]NA = not analyzed; ND = not detected; no limit calculated.

mineral composition of the colloids. The dried ultrafiltrate was composed of evaporite salts (halite, trona, aragonite), whereas the ultrafiltrate solids in the 0.05- to 0.003-μm range were dominated by quartz and (Ca,K) feldspars. About 10% of the dried ultrafilter retentate solids could not be identified by x-ray diffraction, but could be clay minerals formed as secondary minerals during feldspar weathering (Velbel, 1986). Fourier-transform, infrared spectroscopic characterizations being carried out at the Desert Research Institute (DRI) tend to support the hypothesis that clays are present in the colloid fractions (Jacobson, 1986). An equilibrium geochemical model (Wolery et al., 1984) provided further support for this interpretation by predicting chemical speciation using concentration data for 0.45-μm-filtered groundwater from sample B-2 as input.

Table 2-8. Cheshire nuclide analysis for formation sample B-6.

Nuclide	Half-life (y)	Total activity (μCi/mL)[a]	Fraction of total activity retained on					Fraction dissolved
			Prefilter	0.45 μm	0.20 μm	0.05 μm	0.003 μm	
^{3}H	12.36	0.433 (1)	NA[b]	NA	NA	NA	NA	1.000
^{22}Na	2.605	1.49×10^{-9} (19)	[Combined filters, <0.01]				<0.01	>0.99
^{40}K	1.3×10^{9}	2.79×10^{-9} (21)	0.036	<0.01	<0.01	0.094	0.020	0.850
^{54}Mn	0.855	$<6 \times 10^{-9}$	ND[b]	ND	ND	ND	ND	ND
^{60}Co	5.272	5.3×10^{-11} (25)	1.000	<0.01	<0.01	<0.10	<0.05	>0.09
^{106}Ru	1.020	1.79×10^{-6} (12)	0.292	0.084	0.039	0.217	0.053	0.315
^{125}Sb	2.760	3.98×10^{-6} (25)	0.003	0.001	0.001	0.002	0.002	0.991
^{134}Cs	2.065	3.52×10^{-10} (25)	ND[b]	ND	ND	ND	ND	>0.90
^{137}Cs	30.170	5.46×10^{-7} (23)	0.029	0.007	0.005	0.044	0.010	0.905
^{144}Ce	0.778	$<9 \times 10^{-11}$	ND[b]	ND	ND	ND	ND	ND
^{152}Eu	13.40	8.98×10^{-11} (16)	0.404	<0.10	<0.10	0.492	0.104	<0.24
^{154}Eu	8.50	1.92×10^{-10} (15)	0.453	0.120	<0.02	0.342	0.085	<0.12
^{155}Eu	4.73	5.24×10^{-10} (16)	0.367	<0.04	<0.03	0.537	0.096	<0.39

[a] All activities decay-corrected to T_0 = 14 Feb. 1976. Values in parentheses are the percent uncertainties (±1σ) based on counting uncertainties for the individual samples.
[b] NA = not analyzed; ND = not detected; no limit calculated.

The model predicted the following:

- Under field conditions with a pH of 8.5 and a temperature of 45°C—

Calcite	0.49 mg/L
Hausmanite	0.012 mg/L
Muscovite	8.49 mg/L
Phengite	2.57 mg/L
Quartz	49.8 mg/L

- Under laboratory conditions where the measured pH was 7.3 and the temperature was 21°C—

Kaolinite	10.1 mg/L
Nontronite-Ca	0.87 mg/L
Quartz	60.3 mg/L

Although equilibrium is not rapidly achieved in some mineral-alteration reactions, x-ray diffraction studies did observe quartz, and the existence of colloidal aliminum-silicate minerals is strongly suggested by speciation modeling.

We used x-ray fluorescence to measure the distribution of trace elements between the the ultrafilter retentate and the filtrate for sample B-4.

Table 2-9. Calculated K_d values (mL/g) for 0.05- to 0.003-μm-diam colloids.

	Cavity sample	Formation samples	
Nuclide	B-4	B-5	B-6
^{106}Ru	$1.1 \pm 0.4 \times 10^5$	$1.7 \pm 0.6 \times 10^5$	$0.39 \pm 0.14 \times 10^5$
^{125}Sb	$1.3 \pm 0.5 \times 10^3$	$1.3 \pm 0.5 \times 10^3$	$0.41 \pm 0.14 \times 10^3$
^{134}Cs	$7.6 \pm 3.0 \times 10^3$	$5.3 \pm 3.5 \times 10^3$	ND[a]
^{137}Cs	$10.1 \pm 4.1 \times 10^3$	$8.7 \pm 3.1 \times 10^3$	$2.6 \pm 0.9 \times 10^3$

[a]ND = not detected.

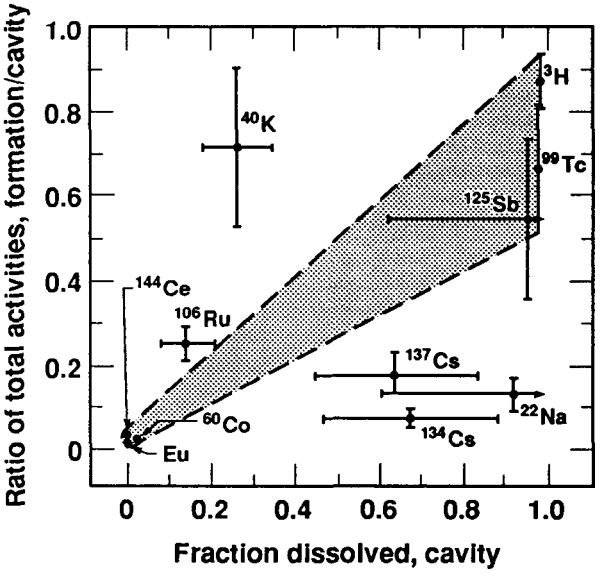

Figure 2-3. Ratio of the total radionuclide activities of formation sample B-5 to those of cavity sample B-4 as a function of dissolved fraction of total activity at the cavity location. Error bars represent cumulative counting uncertainties; data are from Table 2-6 through 2-8. Europium values are an average of the three europium isotopes measured. The shaded area represents the region in which data should fall if the nuclide transport represents a simple combination of the pure particulate (^{60}Co, ^{144}Ce, Eu) and conservative (^{3}H, ^{99}Tc) dissolved cases.

Table 2-10 lists the elements detected, the total concentration per liter of groundwater passing the 0.05-μm filters, and the fraction of that element that was present on 0.05- to 0.003-μm colloids. For potassium, manganese, iron, rubidium, cesium, barium, lanthanum, cerium, and lead, greater than 10% of each element's concentration passing the 0.05-μm filter is present on the small colloids. Detectability problems hinder a comparison of radionuclide association on colloids with elemental association, except that x-ray fluorescence indicates that 36% of the potassium passing through the 0.05-μm filter was colloidal compared to 32% of the ^{40}K detected by gamma-ray counting as passing through the 0.05-μm filter. For ^{134}Cs and ^{137}Cs, 18% and 12%, respectively, of the activity passing the 0.05-μm filters was colloidal, whereas x-ray fluorescence indicated greater than 11% colloidal. Within the uncertainties of these methods, the results are consistent and indicate that trace metals also associate with natural colloids.

Discussion

Background

Colloids have long been recognized as potential carriers of adsorbed radionuclides in the subsurface environment (Champlin and Eicholz, 1968). The potential for transport by colloids is suggested by the colloids' submicrometer sizes, which are far smaller than pore sizes in permeable and fractured media, and by their high surface area per unit mass. Colloid removal from solution by capture onto fixed media surfaces is controlled by the Brownian motion of the colloids and by the attachment efficiency following collision. In general, for natural waters with low ionic strengths, the attachment of colloids to surfaces is hindered by electrostatic repulsion, but predictions based on double-layer theory underpredict attachment by orders of magnitude (McDowell-Boyer, 1986).

Literature on the association of radionuclides with colloids has evolved a unique nomenclature that we have not adopted here. Radionuclides such as plutonium and americium are known to

Table 2-10. The results of x-ray fluorescence analysis of sample B-4.

Element	Concentration passing 0.05-μm filter (μg/L)	Fraction colloidal; 0.05- to 0.003-μm size range
K	735	0.36
Ca	784	0.028
Mn	31	0.18
Fe	140	0.40
Ni	8.6	0.023
Cu	2.9	0.064
Zn	530	0.011
As	13.1	0.016
Br	37	0.004
Rb	7.0	0.28
Mo	10.8	0.004
Cs	<1.5	>0.11
Ba	8.7	0.24
La	<1.5	>0.13
Ce	<2.2	>0.40
Pb	12.5	0.26

form colloids with dimensions of a few nanometers (Davydov, 1967; Benes et al., 1979; Cleveland, 1979). These colloids have been called "true colloids." When radionuclides adsorb onto natural colloidal matter such as clay minerals and hydrated oxides, the resulting particles have been referred to as "pseudo-colloids" (Davydov, 1967; Benes et al., 1979). According to these definitions, a natural colloid becomes a pseudo-colloid when a radionuclide adsorbs. The designation of true versus pseudo-colloid is also inadequate in describing an aggregate composed of a radionuclide colloidal precipitate and a clay colloid. Although the chemical speciation of radionuclides with colloidal material is important, the distinction between true and psuedo-colloids is awkward for application to a broad range of problems. We recommend that the definition of colloids be based on their physical properties (i.e., that they are subject to Brownian motion and have diameters between 0.001 and 1 μm) and not on their chemical history or the scientific discipline of their observer.

The sources and properties of colloids that could transport radionuclides in natural and engineered systems are important. Apps et al. (1982) distinguish two processes for forming suspended colloids:

- Condensation or homogeneous nucleation of dissolved species when a mineral phase is supersaturated, and
- Dispersion of bulk material into suspended solids.

Dispersion of bulk materials actually comprises a number of separate processes because it can include:

- Disruption of fragile aggregates by changes in ionic strength or hydrodynamic force,
- Mechanical grinding of mineral surfaces,
- Mechanical disruption of secondary minerals present at mineral surfaces, and
- Release of less-soluble colloids by dissolution of a more-soluble matrix surrounding these colloids.

Aggregate destruction was suggested when recharge of an aquifer with water having lowered ionic strength resulted in the release of clay minerals into flowing groundwater (Nightingale and Bianchi, 1977). Similarly, infiltrating rain water causes bursts in virus concentration in well waters (Lance and Gerba, 1982). Simmons and Caruso (1983) show photographs of crystalline rocks that have been sealed by new mineral growth. Many sealed cracks have undergone repeated fracturing and sealing because the minerals in the crack are weaker than the rock

and do not completely fill the void space. Similarly, Velbel (1986) presents a review of feldspar-weathering mechanisms that can include the formation of secondary minerals such as clays.

Considerable research is being conducted on the release of colloids when glasses dissolve. For example, Saltelli et al. (1984) measured the size distribution of americium-containing colloids released from a waste container, and Shade et al. (1984) measured radionuclide adsorption onto colloids released from waste-package material. Lutze et al. (1983) report on the rapid surface alteration of borosilicate glass at 165°C in distilled water. After 30 days, there was a 1-μm-thick crystalline outer layer composed of fibers with diameters <0.1 μm.

Thus, submicrometer colloids could easily be released from mineral and glass surfaces when these surfaces are chemically, hydrodynamically, or mechanically stressed.

In spite of the existence of submicrometer colloids in natural systems, there have been few studies of contaminant adsorption to colloids of that size. Experimentally, it is far easier to use large particles that can be efficiently separated from the solution. The presence of colloids is known to interfere with the adsorption of radionuclide and organic contaminants onto micrometer and larger particles. Following conventional filtration or centrifugation, the contaminant remaining in solution is observed to increase as "nonsettleable particles" or "colloidal organic carbon" increase (Sheppard at al., 1980; Gschwend and Wu, 1985; Baker et al., 1986; Higgo and Rees, 1986). Colloidal organic carbon is assumed to be proportional to the amount of dissolved organic matter.

One aspect of the application to colloidal adsorption of adsorption measurements on micrometer and larger particles is that the linear isotherm expressed as Eq. (1) requires reevaluation. Because the isotherm relates solution activity to adsorbed activity per unit mass, experiments with smaller particles would increase the external surface area per unit mass and thus increase K_d if only the external surface area is accessible for adsorption.

James and Parks (1982) have summarized measurements of ionizable-site densities for oxide minerals; their data are spread over a relatively narrow range of 2 to 20 sites per square nanometer. Since these ionizable sites participate in adsorption reactions, relatively little variation in adsorption other than its dependence on surface-group acidity would be expected for minerals when expressed as adsorbed activity per surface area. Therefore adsorption isotherms that are measured on micrometer and larger particles and represented according to Eq. (1) should not be applied to adsorption to colloids.

Quite frequently in the literature there is reference to adsorption onto micrometer and larger particles of species that exist as colloids. Cleveland (1979) has soundly denounced such an interpretation for the interaction of plutonium oxide colloids with glass surfaces. Colloid attachment is irreversible except under aqueous solution conditions that favor dissolution of the colloid. The maximum plutonium loading on glass is 1.6 $\mu g/cm^2$; if the colloids have an average diameter of 1 nm and a density of 11.5 g/cm^3, then the projected area of the colloids is twice the surface area of the glass. This loading is a physical limit of colloid packing on a surface. Cleveland has stressed that such colloid-media association cannot be described as ion-exchange phenomena; therefore, linear adsorption isotherms are completely inadequate mechanistic models. Studies of radionuclide cycling in lakes and oceans have recently acknowledged the importance of radionuclide association with colloids, and models for attachment to settling particles are being developed based on coagulation kinetics (Sanschi et al., 1986).

There are no earlier reports of field sites that demonstrate radionuclide migration by colloid transport. A number of field studies have observed anomalous, rapid, radionuclide transport that suggests mobile colloids as carriers. Travis and Nuttal (1985) have summarized the available data and reference the reports of radionuclide transport from a low-level waste site at Los Alamos National Laboratory. These reports describe how, chiefly during the period 1945–1952, liquid wastes from the plutonium purification plant were sent to adsorption beds overlaying Bandelier tuff. Core samples taken in 1978 revealed that both plutonium and americium had migrated over 30 m downward through the unsaturated tuff. Laboratory experiments on the tuff suggested that colloidal plutonium and americium were responsible for the rapid migration.

Four waste plumes at the Chalk River Nuclear Laboratories in Canada are described by Champ et al. (1984). The analytical procedures for separating gamma-emitting radionuclides distinguished only four forms: particulate species

captured on 0.4-μm filters, species retained on cation- and anion-exchange resins, and nonionic species removed by an aluminum oxide bed. For ^{60}Co, ^{95}Zr, ^{106}Ru, and ^{125}Sb, the anionic forms dominated, and organic ligands were felt to promote mobility for cobalt, cerium, cesium, europium, antimony, and zirconium. Even though the speciation studies would have placed colloidal species <0.4 μm in diameter into cationic, anionic, and nonionic forms, the detection of significant particulate nuclides was reported for ^{60}Co, ^{95}Zr, ^{106}Ru, ^{137}Cs, and ^{144}Ce. The mass of particulate matter in suspension was not reported, but since reported sampling flow rates were about 100 mL/min with 30 min of purging, the solution was probably representative of groundwater and not subject to near-well erosion.

An *in situ* glass-block leaching experiment is one of the four study sites at Chalk River. Field measurements of ^{137}Cs migration indicate transport four times farther than predicted from K_d values (Champ and Merritt, 1981). Soil columns prepared from undisturbed, uncontaminated cores showed cesium transport by 0.2- to 1.0-μm particles. There was also an indication that microorganisms were involved in particulate cesium release and transport.

Colloidal transport is also suggested in the formation of ore bodies. Horzempa and Helz (1979) have found that colloidal copper sulfide prepared by precipitation is destabilized by the ionic composition of natural waters. Transport of the colloids would then be dominated by aggregation and attachment within porous media. On the basis of laboratory experiments, Giblin et al., (1981) argued that uranium adsorbed to hydrous ferric oxide and clay colloids would be mobile in subsurface waters under certain pH and redox conditions. They noted that uranium mobility, once the uranium is adsorbed to submicrometer colloids, is controlled by colloidal stability. That is, if the colloids aggregate, limited mobility is expected.

This Study

Our results are critically dependent on filtration to separate the colloids from solution by size. We recognize a number of well-known problems with using filtration for size characteristics, but these problems do not negate the findings in this work. De Mora and Harrison (1983) have provided an overall evaluation of colloid-solution separation techniques for studies of trace-metal speciation. For depth filters used in this work, particle retention changes slowly with particle size near the stated pore size of the filter. Johnson and Wangersky (1985) have shown that removal efficiency also depends on colloid stability because particles much smaller than the size of a filter pore were removed under the high ionic strength conditions of seawater, but there was no removal when the particles were suspended in distilled water.

Another phenomenon hindering size separation by filtration is the partial clogging of filter pores as the material is retained. As a filter is loaded with particles, its effective pore size is reduced, and smaller particles are retained (Danielsson, 1982). Comparison of results obtained with etched Nuclepore filters (sample B-2) and with bag-type filters (sample B-3) indicates some clogging did occur for the Nuclepore-filtered sample.

Another issue with filtration and ultrafiltration is the intensity of fluid mixing, which could break up fragile aggregates into smaller aggregates or primary particles. Since colloid transport processes are size-dependent, any procedure that alters colloid sizes would give results that could not be used to predict transport. For groundwater samples containing colloids in dilute concentrations on the order of mg/L, there are no alternative procedures for concentrating the colloids to the extent needed for radionuclide detection.

Our experience to date with groundwater samples from the Cheshire site is that serial filtration and ultrafiltration provide consistant results that allow monitoring of radionuclide concentrations.

Deep groundwater from NTS has colloidal material that is far higher in concentration than previously reported in the literature. Apps et al. (1982) reference studies using light scattering and aluminum analysis that report colloid concentration in the μg/L range in samples taken from unperturbed groundwater. Colloid concentrations measured in the present study are in the tens of mg/L range; these could be higher than in other areas because the fractured media of Pahute Mesa is continually subjected to blast-

induced pressure pulses that could erode colloids attached to fracture-wall surfaces. Ultrafiltration can concentrate colloids larger that a few nanometers and is a more sensitive indicator of colloid concentration than methods that depend either on movements of a single element or on light scattering. The scattering effect in particular is very weak for colloids much smaller than the wavelength of the light used; therefore, this technique may tend to underestimate colloid concentrations.

Groundwater at the Cheshire site had radionuclide activity both in the cavity and in the formation. For manganese, cobalt, cerium, and europium nuclides, greater than 98% of their activities were in the colloid fraction, and these radionuclides were detected at the formation location on submicrometer colloidal material. Less strongly sorbing nuclides such as ruthenium, cesium, and antimony are present in both colloidal and dissolved forms at both the cavity and the formation locations.

The data suggest three-phase chemical speciation:

- Dissolved nuclides,
- Nuclides associated with colloidal material with a size range of <0.003 μm to 1 μm, and
- Nuclides associated with immobile fracture surfaces.

Equilibrium-based predictions of contaminant migration are highly suspect in fractured media because adsorption is dependent on accessible surface area, and diffusion into the rock matrix can be very slow (Rasmuson and Neretnieks, 1986). The field data for cesium and sodium suggest some exchange of dissolved radionuclides with the fracture surfaces.

For nuclides that are nearly 100% colloidal, the total activity at the formation location is only 2.5% of the cavity activity. A comparison of colloid mass concentration over the 0.05- to 0.003-μm range shows a much smaller decrease from 10.1 mg/L at the cavity to 4.6 mg/L at the formation location. These results indicate either colloid exchange with fracture surfaces or selective removal of colloids containing radionuclides during fluid flow between the sampling locations. The process of colloid exchange with fixed surfaces is such that a mechanical, hydrodynamic, or chemical shock is required to release colloids once they are attached. Selective removal from NTS groundwater of colloids containing radionuclides is a possibility, but individual colloid minerology and radionuclide content are not at present experimentally accessible.

Issues

Our results raise a number of issues related to sampling, colloid characterization, colloid transport, and modeling radionuclide migration in fractured media. The drilling and well-development activities involved in collecting samples from subsurface environments are mechanically, chemically, and hydraulically disruptive; it is not clear how these factors alter colloid generation, resuspension, and transport. At the Cheshire site, groundwater was pumped at about 30 gal/min from the >20-m-long perforated section of the reentry hole, and more than 50,000 gal were pumped before the first sample was collected. Under these conditions, the aquifer was not hydraulically stressed, and the time between initial drilling and sampling was 7 years. Since the NTS groundwater is oxygenated, sample collection and storage probably did not substantially alter the colloids or radionuclide speciation.

The colloids collected in the NTS groundwater at the Cheshire site are poorly characterized. We estimated colloid mass concentrations over broad colloidal size intervals and detected nuclide activities in these size fractions. X-ray diffraction studies indicated the major mineralogical composition, but these results are only semiquantitative. Equilibrium speciation modeling of NTS groundwater also supported the existence of mineral colloids. Obviously, better colloid characterization is necessary, but because of the dilute colloid concentration and heterogeneous distributions in size and mineralogical composition, advancements in analytical techniques are required. Also unresolved is the question of whether the high colloid loadings observed are natural or are the result of repetitive, blast-induced shocks.

Although a number of colloid-transport models for fractured media have appeared in the literature (Travis and Nuttal, 1985; Bonano and Beyeler, 1985), there is as yet much uncertainty regarding water flow, conservative tracer transport, and mechanisms of colloid generation, deposition, and erosion. Extensive model-development activities are premature without both a fundamental understanding of

mechanisms and data-collection efforts in the laboratory and in the field that can be applied to model calibration and verification.

Summary

Groundwater within the Cheshire cavity contains radionuclides that are associated with submicrometer colloids. Groundwater collected outside the detonation cavity in the formation also contained radionuclides on colloidal matter, but at reduced levels. The majority of the radionuclides associated with suspended colloids passed through conventional 0.45- and 0.20-μm filters. Chemical analysis and equilibrium speciation modeling suggest the colloidal matter is composed of secondary minerals produced by natural weathering of the fractured tuff. Although colloids were observed to transport some of the nuclides, the actual composition of colloids, the mechanisms that control their deposition and erosion, and the potential for long-distance radionuclide transport by colloids are all unknown at this time.

Section 3. Environmental Tritium Transport

Section 3A. Infiltration and Recharge (Cambric Event Site)

Contributors: M. R. Ruggieri, Scott Tyler, and R. W. Buddemeier*

Introduction

The Cambric Event site (see Frontispiece) is the location of a long-term pumping experiment designed to induce and investigate radionuclide migration in the groundwater (Hoffman, 1979; Coles and Ramspott, 1982; Hoffman and Daniels, 1984; Buddemeier and Isherwood, 1985). A result of the primary investigation has been the nearly continuous discharge, over a period in excess of 13 years, of groundwater pumped into an unlined ditch on the desert floor. This water has been continuously monitored; since late 1977 it has contained varying but well-characterized elevated levels of tritium.

In 1983, LLNL and the Desert Research Institute (DRI) cooperated in installing two aids to analysis: flumes to measure flow and infiltration rates and, adjacent to the ditch, an instrumented plot for monitoring the vadose zone. The objective was to exploit as a secondary experiment the steady-state injection of labeled water in order to study recharge and vadose-zone migration in the alluvial soils. A map of the ditch system and plan and vertical views of the vadose-zone study site are shown in Figs. 3A-1 through 3A-3. The details of the installation, sampling, and analysis are reported by Buddemeier and Isherwood (1985), as are the results through 1984.

This report updates the results of the soil-moisture and tritium-monitoring efforts and presents the moisture-transport rates calculated for the vadose zone. We also report on the installation of a deep (ca. 30-m) lysimeter immediately adjacent to the ditch and on the results of its use in a tracer study to determine directly rates of vertical migration beneath the ditch. Additional geophysical, modeling, and hydrologic characterizations have been carried out by DRI; reports on these studies are in preparation.

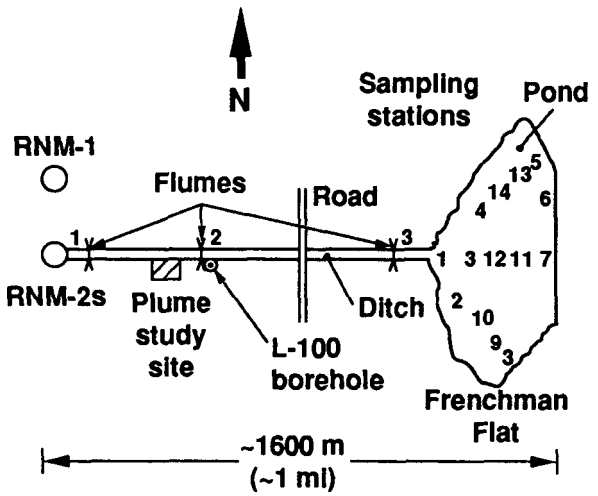

Figure 3A-1. Ditch and pond system carrying water pumped from satellite well RNM-2s. The pump is located 91 m from the working point of the Cambric Event. The numbers in the pond correspond to sampling sites (see data in Appendix B). At the scale of this sketch, the berms along the edges of the ditch cannot be distinguished.

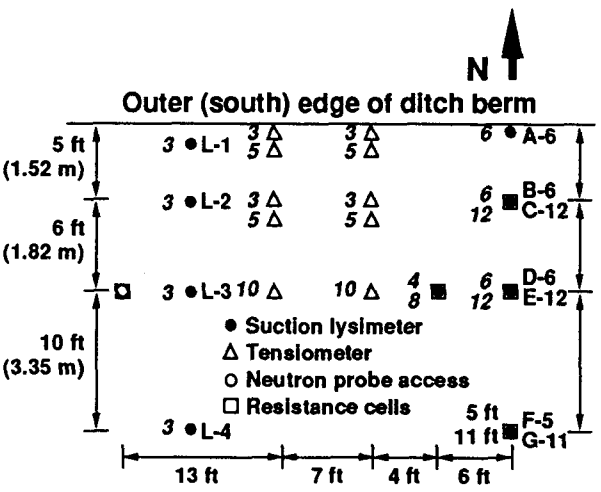

Figure 3A-2. Plan view of the plume study site. The italicized numbers by the instrumentation symbols give the emplacement depth in feet.

* Desert Research Institute, Las Vegas, Nevada.

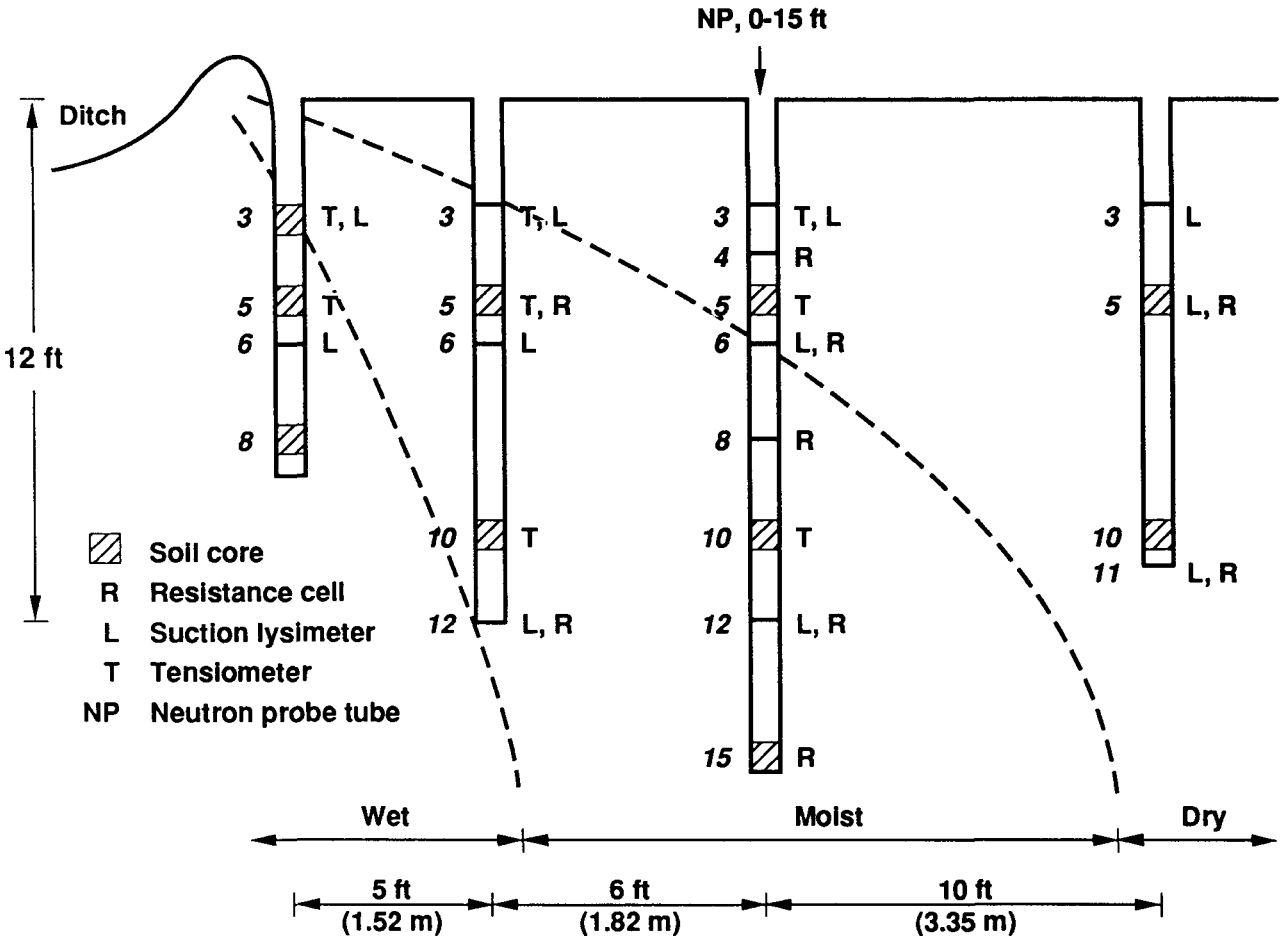

Figure 3A-3. Vertical view of the soil instruments and sample locations used for the vadose-zone study of the Cambric ditch. The italicized numbers give emplacement depth in feet. Contours summarizing the soil-moisture characteristics determined from tensiometer and resistance-cell data are superimposed on the plot.

Vadose-Zone Monitoring and Migration

Moisture and tritium monitoring at the vadose-zone study installation were carried out on a routine basis through late 1986; measurements were then discontinued, but the instruments remain in place, and the site potentially can be refurbished for further investvations. A complete update of the LLNL results (including the data previously published) is contained in Appendix B. LANL also monitors the tritium content of outflow to the ditch from satellite well RNM-2s; their results may be found in their annual project reports. To retain consistency with the previous data reports, the tritium data of Appendix B are reported in units of disintegrations per minute (dpm) per mL, whereas text data are presented in pCi/mL, in keeping with more recent policies to use Curie-based activity units (1 pCi/mL = 10^{-6} μCi/mL). Conversion factors are included in Appendix B.

The data obtained from continued monitoring support and extend the conclusions about tritium and moisture distributions presented in the previous report (Buddemeier and Isherwood, 1985). The outermost installations (3.35 m from the ditch berm; see Figs. 3A-2 and 3A-3) show no indications of elevated moisture or tritium. The soil zones described previously as wet, moist, and dry (see Fig. 3A-3) continued to exhibit those characteristics. The shallowest installations showed fluctuations in both moisture content and tritium activity that appeared to reflect natural

recharge associated with precipitation events. Lysimeter A6, the closest sampling point to the ditch, continued to yield tritium activities very close to equilibrium with concurrently sampled ditch water. Lysimeter C12 continued to exhibit a pattern of tritum activity with time that was parallel to but higher than the trend in tritium activity in the ditch, as shown in Fig. 3A-4 . By contrast, lysimeters D6 and E12 both showed a trend toward increasing tritium activities, suggesting that the water currently sampled at those locations originated in the ditch prior to the occurrence of the peak tritum activity in July 1980.

To determine the transport times between the ditch and the lysimeter locations, we decay-corrected tritium data to a common date (the beginning of the vadose-zone studies), and performed linear regressions of the lysimeter data against a corresponding interval of ditch data, using a range of time lags to test for the best fit. For lysimeter C12, excellent agreement ($r^2 > 0.9$) was found for a time lag of 1.5 years; for E12 the data were somewhat noisier, but yielded a convincing transport time of 6 years. These results demonstrate the potential of the site for long-term research on the unsaturated zone.

Recharge-Plume Investigations

In May 1985, we drilled and sampled a 30.5-m borehole 2.4 m from the berm (see Fig. 3A-1) in order to sample the recharge plume directly beneath the ditch. Core samples were analyzed for tritium and water content, and a lysimeter (designated L-100 in Appendix B) was installed at 28.7 m. Samples were collected from L-100 beginning in July 1985.

Figure 3A-5 shows the sampling and installation pattern of the L-100 borehole. The water content measured in all of the cores indicated unsaturated conditions, consistent with the coarse, porous, high-permeability material. Tritium activities in the core were consistent over the length of the borehole and were close in value to the values measured in the ditch water within the preceding 1 to 2 months. The initial lysimeter samples also suggested a transport time from the ditch to the lysimeter of no more than 1 to 4 months.

Based on these preliminary results, LLNL and DRI planned and carried out a real-time experiment in which the recharge plume was traced in order to

- Compare the results with the tritium observations, and
- Conduct a feasibility study in anticipation of future large-scale tracer studies to investigate the behavior of other tracers, colloids, etc. in the recharge plume.

On March 26, 1986, a 30.5-m segment of the ditch adjacent to the deep lysimeter was dammed at both ends; large plastic tubing was used to divert flow around the blocked section. Into this isolated segment was injected 4000 L of uncontaminated (i.e., having background tritium levels) groundwater from the NTS that had been spiked

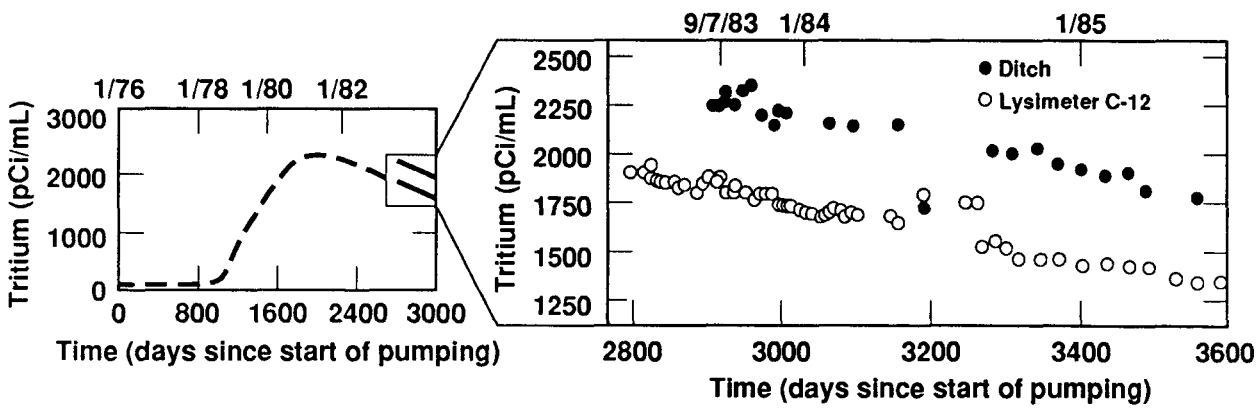

Figure 3A-4. Comparison over time of the tritium content in the surface ditch water with that in samples from lysimeter C12 (expanded plot). The small graph on the left summarizes the complete history of tritium activity in the pumped water.

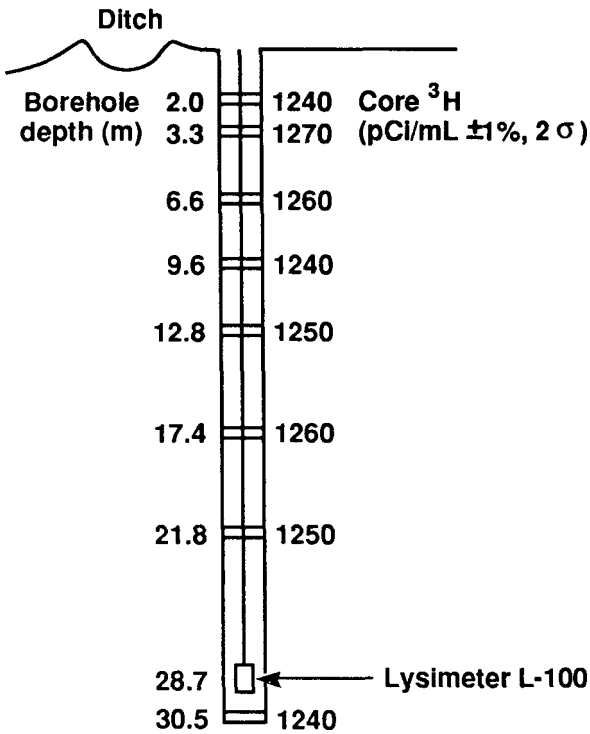

Figure 3A-5. Concentrations of tritium in the core samples from the L-100 borehole, May 1985.

Table 3A-1. Bromide concentrations in deep-lysimeter L-100 samples after injection of the surface tracer.

Date day	Julian injection	Days since (mg/L)	Br^-
3/26/86	85	0	0.15
3/31/86	90	5	0.15
4/10/86	100	15	0.15
4/21/86	111	26	0.17
4/28/86	118	33	0.15
5/15/86	135	50	0.17
6/09/86	160	75	0.27
6/17/86	168	83	0.32
6/26/86	177	92	0.34
7/07/86	188	103	0.32
7/22/86	203	118	0.27
8/04/86	216	131	0.23
9/03/86	246	161	0.20
9/10/86	253	168	0.16
10/09/86	282	197	0.14

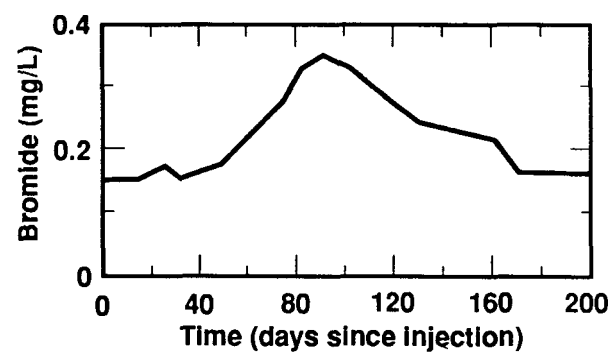

Figure 3A-6. "Breakthrough" of the bromide tracer released into the Cambric ditch, as shown in deep-lysimeter samples taken in 1986.

with LiBr to a concentration of 237 ppm Br^-. After the labeled water had percolated into the ditch bottom, the dams were broken and normal flow was resumed. Lysimeter samples were taken at regular intervals and analyzed for Li^+, Br^-, and tritium.

We found no detectable increase in lithium or decrease in tritium levels. However, the data presented in Table 3A-1 show that bromide levels

- Rose significantly above the consistent background levels by 75 days after tracer injection,
- Peaked at a concentration approximately twice the background level and 750 times lower than the concentrations of the input tracer around 92 days after injection, and
- Returned to background by 168 days after the injection.

The time history of bromide concentration in deep-lysimeter samples taken in 1986 is shown in Fig. 3A-6. The travel time deduced from the bromide tracer, approximately 3 months, is within the range of times deduced from comparing tritium concentrations. The concentration of the tracer observed, less than 0.2% of the input concentration, explains why no reduction in tritium activity was seen as a result of the use of low-tritium water for the tracer; the variation in activity expected would be small compared with the 1% counting statistics for the tritium analyses.

The "unsaturated conditions" noted above, in combination with the shallow soil-moisture

data, the tracer evidence for rapid vertical transport, and the results of other field and model studies by DRI, enhance our understanding of the recharge plume and its utility for possible future tracer work. For the purposes of tracer work and modeling, the quasi-two-dimensional plume is experimentally convenient. In addition, there are a wide range of unsaturated flow velocities within a short and easily measurable distance, and hydrologic transport occurs on a time scale well-suited to field experimentation.

Conclusions

The Cambric ditch and its associated recharge plume provide a unique and valuable opportunity to study the movement of water and radionuclides in alluvium, both as a result of gravity-driven flow and in the form of unsaturated, lateral migration in the vadose zone. Recharge transport has been directly measured at a rate of approximately 0.3 m/day. However, because of the distinctive and well-characterized tritium signature of RNM-2s water, we are not limited by real-time observations. Migration times of up to 6 years have been determined by comparing tritium-activity trends in the vadose zone with the history of ditch activity.

Section 3B. Vegetation Water Budgets

*Contributors: M. R. Ruggieri, R. W. Buddemeier, and R. Jacobson**

Introduction

The unique environment created by the Cambric pumping experiment and described in Sec. 3A provides opportunities for using field tracers to study a variety of natural processes. Because of the long-term, constant irrigation of the desert floor, an extensively vegetated biological community has developed in and near the ditch and pond. The anomalous presence of a well-watered, heavily-vegetated desert community in the midst of an otherwise typically barren location leads directly to the supposition that the plants rely on the ditch water for most if not all of their water needs. Since this water contains a relatively high and time-dependent concentration of tritium, we had the opportunity to perform a variety of large-scale isotopic tracer studies of plant metabolisms, transpiration dynamics, and community water budgets in a natural setting. This section of the report describes the results of some initial hydrogen-isotope studies of vegetation water budgets.

The flux of water through living plants is of interest from a variety of standpoints. The uptake, retention, and release of water are important aspects of plant metabolism because they largely determine a plant's response to environmental stresses such as drought. Vegetational evapotranspiration can be an important factor in local and regional water budgets, with considerable impact on the hydrologic cycle. Finally, the fractionation and incorporation of hydrogen and oxygen isotopes in plant tissues is increasingly studied both as an aid to understanding plant metabolism and as a clue to past climate and environmental conditions that may have left their isotopic signatures in the durable portions of plant tissues.

Isotopic studies have considerable potential for elucidating plant metabolic processes. However, long-term or large-scale environmental studies are generally required to rely on the interpretation of small variations in naturally occurring isotope ratios (Epstein et al., 1977), whereas tracer studies are customarily limited to laboratory settings or to short time periods (IAEA, 1981).

To exploit the uniquely labeled environment of the Cambric ditch, from 1983 through 1985 LLNL and DRI cooperatively sampled and analyzed plants and other environmental media. To address a variety of specific questions, we

- Investigated the degree of isotopic equilibration between the water in the plant tissues and that in the ditch;
- Investigated the relationship between the isotopic ratios of natural deuterium (^2H) and anthropogenic tritium in the water present in the plants, ditch, and air;
- Studied the diurnal variations in the isotopic concentration of the water in plant tissues; and
- Compared the degree of tritium uptake in plants representing two different photosynthetic pathways (C_3 and C_4).

Methods

Initial reconnaissance samples were collected in May 1983, followed by an extensive systematic collection in August 1984. Samples taken in the

* Desert Research Institute, Las Vegas, Nevada.

initial collection were processed by two different methods, and replicate samples were collected and processed for methods comparison. Samples processed by LLNL were cut, bagged, and frozen on dry ice immediately after collection. They were kept frozen until the tissue water was extracted at LLNL by freeze drying. Samples collected by DRI were cut and immediately immersed in flasks of toluene; the flasks were then sealed and the contents subsequently distilled at DRI to remove the water fraction. Water samples were analyzed for tritium at LLNL by liquid scintillation spectrometry and for deuterium at DRI by mass spectrometry.

A second set of samples was collected in August 1984. Plants, which were sampled at different times throughout the day, included the cattail reed *Typha domingensis*, which was repetitively sampled at heights above the water of approximately 0.5, 1, and 2 m (1 to 2, 3 to 4, and 6 to 7 ft, respectively). During this period, air-moisture samples were collected by drawing air through a tube of silica gel, which was subsequently baked out under vacuum in the laboratory to retrieve the water. Nighttime and daytime air-moisture samples were collected at two locations: at about 1 m above the ditch and within the vegetation canopy near where the reeds were being sampled, and approximately 92 ft south (upwind) of the ditch, also at a height of about 1 m.

Throughout the sampling periods, we regularly collected ditch-water and soil-moisture samples (the latter from lysimeters) and analyzed them for tritium.

Results and Discussion

Our results are presented in Appendix B. Included with these analytical data are species identifications and relevant location information. Other sections of the table contain, for the periods in question, data on the tritium content of the ditch water, soil moisture, and air moisture.

The results of methods-comparison samples (splits of the same plants processed by the two different methods) indicate that the two processes produce comparable results; the variability observed is believed to represent intra- and inter-specimen variability rather than systematic effects of the methods.

The transect samples (DRI samples 37 through 50, Appendix B, Tables B2 and B3) produced the expected results: samples in or immediately adjacent to the ditch showed elevated tritium levels, whereas at a distance of a few meters or more the plants showed little if any elevation above the local "background" level. However, the close-in samples did not exhibit tritium activities as high as the ditch-water samples, despite the fact that soil and lysimeter samples from similar locations led us to believe that the soil moisture should be very close in isotopic composition to the ditch water.

Figure 3B-1 summarizes additional results of the 1983 sampling effort. To check for systematic (diel) metabolic effects, we took samples in the early morning (low photosynthesis and transpiration) and at midday (high photosynthesis and transpiration). Two species representing the C_3 photosynthetic pathway and two other species with a C_4 pathway were collected. In Fig. 3B-1, both deuterium and tritium data are presented relative to the ditch-water values for the same time; deuterium values are presented in terms of the Standard Mean Ocean Water (SMOW). Note that one vertical scale in each sub-figure is expressed as percent of ditch water, but that the scales are of very different magnitudes. Although there is no systematic difference in deuterium ratios, at both sampling times the C_3 plants show significantly lower tritium concentrations than the C_4 plants.

The water samples from plants are enriched in deuterium by a few percentage points relative to the ditch water, but are (in some cases) depleted in tritium by over 70%. The deuterium values are reasonable both in magnitude and in time pattern; plant respiration should result in modest enrichments of the liquid phase in the heavier isotope, and the magnitude of this effect should increase as the rate of transpiration increases during the day. Although the tritium values indicate that the plant contains "heavier" water at noon than in the early morning, the tritium is depleted rather than enriched relative to ditch water, and the differences are an order of magnitude greater than for deuterium.

To explore this effect more thoroughly, in 1984 we collected and analyzed additional samples. The plants selected were cattail reeds and salt cedar, both of which were rooted in the bottom of the ditch. Because they were growing out of the flowing water, there could be no question about their root exposure. In addition to further diel sampling, we also sampled the reeds as a function of their height above the surface of the water. Figure 3B-2 presents the results for the cattails and the salt cedar about

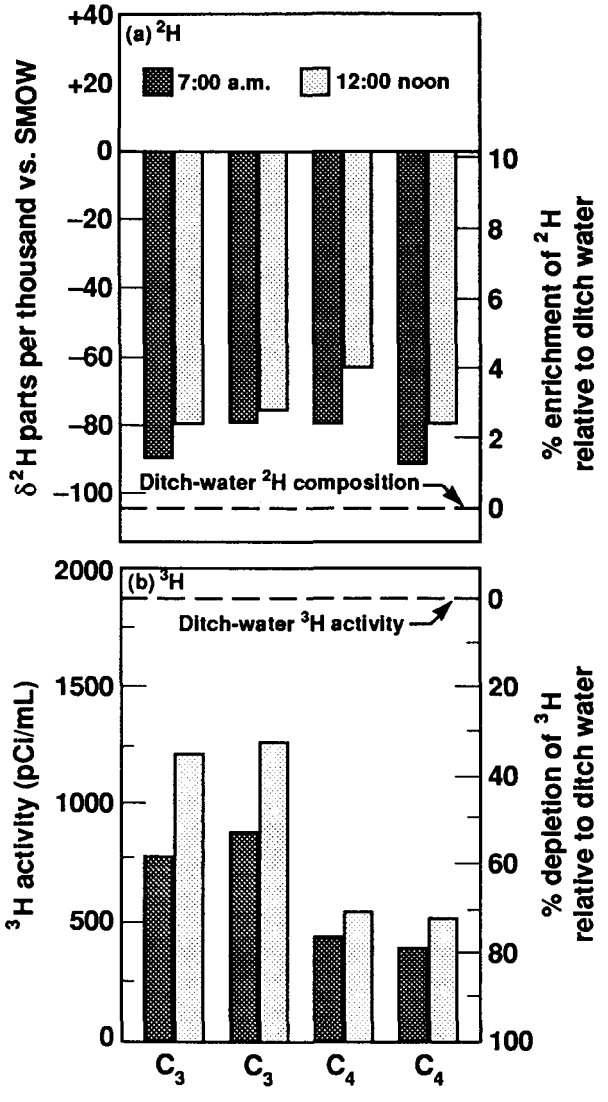

Figure 3B-1. Results of the 1983 sampling effort. Deuterium (a) and tritium (b) concentrations are shown for water extracted from plants having C_3 and C_4 photosynthetic pathways.

1 m above the surface of the water. Here again, we note substantial depletions relative to the tritium levels in the ditch and a trend toward increasing tritium levels (isotopically heavier water in the plants) over the course of the day.

Figure 3B-3 depicts the tritium activity in the cattail stems as a function of both time of day and height above the surface of the water. Air-moisture samples collected within the plant

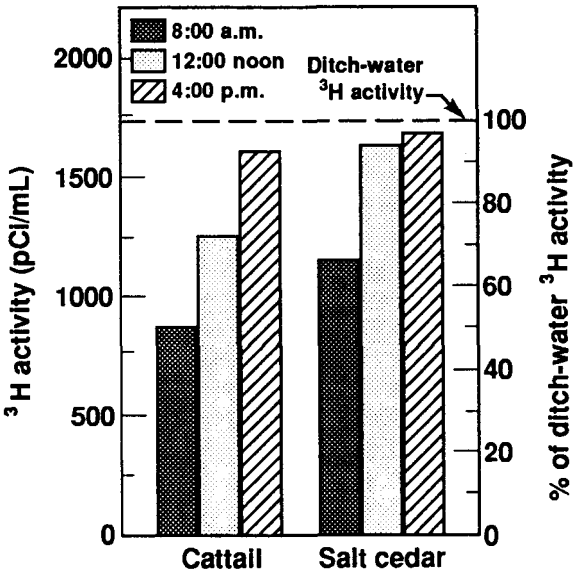

Figure 3B-2. Tritium concentrations as a function of time of day in water extracted from cattail samples taken about 1 m above the surface of the water and from salt-cedar leaf samples.

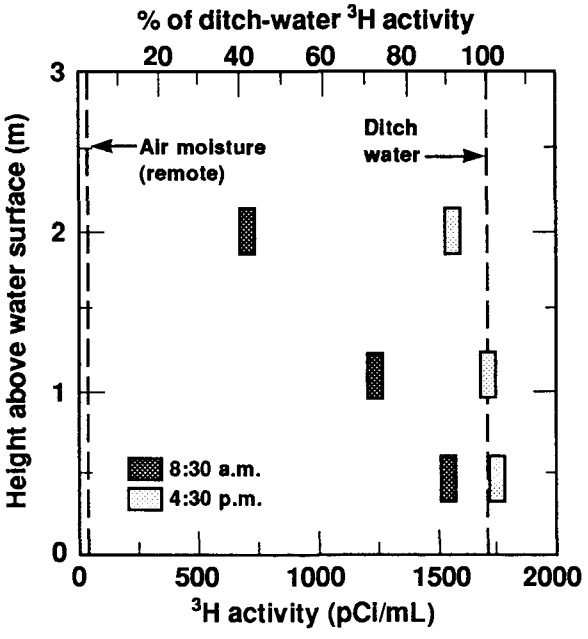

Figure 3B-3. Tritium activity in cattail water as a function of height above water and time of day. Vertical lines show the activities of the ditch water and of air moisture sampled at a location remote from the plant-sampling site.

growth a few feet above the water ranged in activity from about 150 pCi/mL at night to slightly less than 350 pCi/mL during the day.

If we assume that the same mechanisms affect both isotopes, the deuterium enrichments indicate that the reduction in plant-water tritium relative to the ditch water is not caused by any isotope-fractionation process. This leaves dilution as the sole reasonable candidate for consideration, and the only other reservoir of water available to the plants is the atmospheric moisture. This water source is similar in deuterium composition to the ditch and plant water but is initially free of tritium; exchange of water between the plant and the air could therefore dilute the plant-water tritium without dramatic effect on the deuterium composition.

The data permit some rough estimates of the relative amounts of water from the two sources in the plant tissues. If we ignore the effects of isotopic fractionation and treat the remote air and the ditch water as the two end members, the results indicate that approximately 50% of the nighttime water inventory of the cattails and a similar but slightly smaller fraction of the salt-cedar water are derived from the atmosphere. This is a lower limit on the amount of atmosphere-derived moisture, because the tritium activity of the air moisture in the immediate vicinity of the plants is higher than the remote values as a result of local evapotranspiration of the ditch water. The effect of more rapid plant transpiration during the daylight hours is to raise the fraction of ditch water in the total plant tissue to 90% or more, presumably by increasing the rate of transpiration outflow relative to the exchange and back-diffusion of atmospheric moisture at the air-plant interface. The plant data of Fig. 3B-1 show that air moisture must account for up to 70% of the water content of some of the plants growing immediately adjacent to the ditch.

Conclusion

The results are consistent with laboratory studies of HTO-vapor uptake by plants, which indicated that plant water reached tritium values that were 20 to 50% of the vapor-phase values (IAEA, 1981, p. 44). However, the results are somewhat surprising in this case, in view of the low ambient humidity and the ready availability of labeled water from the saturated or nearly saturated soil system. The data do not permit us to identify the mechanism in detail, but they suggest that the air-to-plant exchange of moisture must have rates that can be a significant fraction of the plant's total net water-transpiration flux.

The labeled ecosystem associated with this experiment offers the opportunity for more detailed study of water fluxes and exchange rates, and the results further suggest that interpretation of plant water and tissue must include consideration of possible differences among the isotope ratios in water in the air, soil, and ground.

Section 4. Technetium Migration in Nevada Test Site Groundwater

Contributors: R. J. Silva, R. Evans, J. H. Rego, and R. W. Buddemeier*

Introduction

^{99}Tc is produced in the fission process and is therefore present in both spent nuclear-reactor fuel and in debris from nuclear tests. It is a low-energy beta emitter with a maximum energy of 292 keV and a half-life of $2.13 \pm 0.05 \times 10^5$ y (Kocher, 1981). Because of its long half-life, high solubility, and low sorptive properties under oxidizing conditions, ^{99}Tc is considered a potential hazard if released to environmental waters (Luxenburger and Schuttelkopf, 1984).

Isherwood (1985) and Buddemeier and Isherwood (1985) used the EQ3/6 geochemical computer code developed by LLNL's Earth Sciences Department to predict the chemical speciation and solubility of technetium in groundwater. The groundwater at NTS tends to be oxidizing ($E_h > 250$ mV) and to have pH values between 7 and 9 (Buddemeier and Isherwood, 1985; Ogard and Kerrisk, 1984). It was predicted that TcO_4^- would be the major solution species in these waters, and that technetium concentrations would not be limited by solubility. Because nuclear weapons are tested underground, technetium should be present in small concentrations in some of the water sampled by the Radionuclide Migration (RNM) Project (Isherwood, 1985; Buddemeier and Isherwood, 1985). Laboratory measurements conducted under oxidizing conditions indicate that technetium is not sorbed to any extent in crushed-rock samples from NTS (Daniels and Thompson, 1984). Thus, one would expect technetium to be rather mobile in the environment and to follow tritium rather closely in its migration behavior.

Isolation Technique

For two reasons, we needed to develop a new way to chemically isolate and concentrate the ^{99}Tc before we could perform reliable analyses. First, because there are no gamma rays emitted in the decay of ^{99}Tc, the low-level gamma spectroscopy methods we usually use to analyze NTS samples could not be applied. Second, beta-counting techniques, although applicable, are not as specific as the gamma-ray methods, making chemical analysis necessary for positive isotopic identification.

Therefore, in 1985, we developed and tested a fast and simple chemical-separation scheme for isolating ^{99}Tc from liter quantities of RNM samples. The method is based on a more complex scheme reported by Luxenburger and Schuttelkopf (1984) in which the concentration of ^{99}Tc is determined by liquid-scintillation counting. The steps for testing a 1-L sample are as follows:

- A 1-L sample is acidified and made oxidizing by the addition of 10 cm³ of concentrated HCl and 5 cm³ of 30% H_2O_2. (The HCl and H_2O_2 are scaled up for larger sample volumes.) The solution is stirred with a Teflon-coated magnetic bar for about 1 h.
- About 0.5 g of AG 1 × 8 (100- to 200-mesh) anion resin is added to the solution. (The same amount of resin is added for all sample volumes.) The stirring is continued for 4 h or longer, and the resin is then allowed to settle for 1 h or longer.
- The clear supernate is decanted and the resin is flushed into a 0.5-cm-diam by 10-cm-long glass column. The resulting resin bed is about 4-cm high.
- The resin bed is washed first with 2 cm³ of 0.1*M* HCl and then with 2 cm³ of distilled, deionized water. (If large amounts of tritium are present, additional water washing is necessary.)
- The resin is converted from the chloride form to the perchlorate form by passing 2 cm³ of 1*M* $NaClO_4$ through the resin.
- The technetium is reduced and eluted from the column by passing a 1*M* $NaClO_4$-0.02*M* Na_2SO_3 solution (pH = 12) through the resin.
- Two-cm³ fractions of eluent are collected in glass counting vials, 15 cm³ of scintillation cocktail is added, and the mixture is counted in a liquid-scintillation counter.

* Alabama A&M University, Normal, Alabama.

Preliminary Investigation

The first preliminary tests of this method were reported in 1986 (Silva et al., 1986). In summary, samples were tested from the sites of the Cheshire, Bilby, Nash, and Cambric Events. Although ^{99}Tc was found in most of the samples, none exceeded the maximum permitted concentration for ^{99}Tc of 3×10^{-4} μCi/mL, as given in the United States Nuclear Regulatory Commision (USNRC) *Code of Federal Regulations* (1982). The results from ultrafiltered and normally filtered samples from the Cheshire site showed that the technetium did not appear to be associated to any appreciable extent with particulate material and could be considered primarily dissolved. These results suggested that technetium was indeed present as TcO_4^-, as predicted. However, some of the preliminary results for ^{99}Tc concentrations near the detection limit were inconsistent for the Nash and Cambric samples. Tests performed a few months later on similar but larger-volume samples (thus at higher sensitivities) from these two sites showed no indication of technetium.

Recent Investigation

In early 1987, an improved analysis scheme with ^{95m}Tc as a chemical yield tracer was included in the processing of a second series of samples in order to isolate and determine the concentration of ^{99}Tc in NTS groundwaters (Silva et al., 1988). A secondary goal was to confirm that technetium was not associated with filterable material. Samples from the Faultless site were included in this series.

Test Procedure

Archived samples (in 1- to 4-L volumes) of selected groundwaters from the Cheshire, Bilby, Nash, Bourbon, Cambric, and Faultless Event sites were used in the study. All reagents were of analytical grade and solutions were made with distilled, deionized water. The ^{99}Tc standard used to calibrate the liquid scintillation counter and to test the separation procedures was obtained from and certified by the U.S. National Bureau of Standards. Figure 4-1(a) shows a beta-energy spectrum obtained with the liquid-scintillation counter from an aliquot of the stock solution. The ^{99}Tc standard was counted with a 90.7 ± 1.2% efficiency.

We followed the same chemical separation procedure used for our preliminary migration study except that now the solutions were "spiked" with a known quantity of ^{95m}Tc tracer. The ^{95m}Tc ($T_{1/2}$ = 61 d) was produced by using the Lawrence Berkeley Laboratory's 88-in. cyclotron to irradiate a 0.003-in.-thick niobium foil with 30-MeV alpha particles (Bond and Jha, 1970). After dissolution of the foil in 5 cm^3 of a mixture of 27*M* HF and 1*M* HNO_3, the solution was diluted to 100 cm^3, a stoichiometric amount of H_3BO_3 was added to complex the fluoride ions, and the solution was processed in the same manner described earlier for the NTS samples. Figure 4-1(b) shows an energy spectrum obtained with the liquid scintillation counter from an aliquot of the ^{95m}Tc stock solution.

Data Analysis Procedure

The $NaClO_4$ and the first three $NaClO_4$–Na_2SO_3 2-cm^3 fractions eluted from the

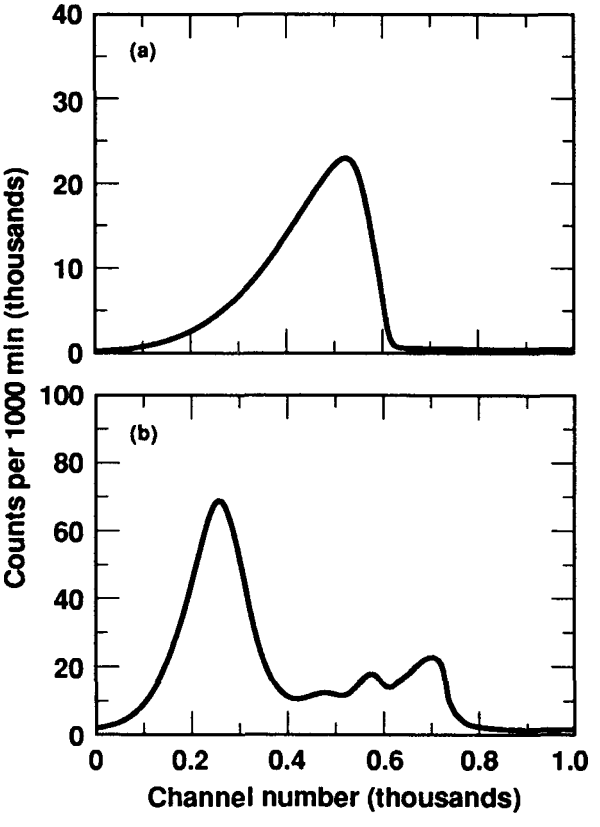

Figure 4-1. Beta-energy spectra obtained with a liquid scintillation counter (a) for the ^{99}Tc stock solution, and (b) for the ^{95m}Tc stock solution.

anion column for each sample were counted for 1000 to 2000 minutes in a liquid scintillation counter. The resulting 1000-channel energy spectra were collected, and the background was subtracted. A typical spectrum for the Cheshire sample and a typical background spectrum are shown in Figs. 4-2(a) and 4-2(b), respectively. The concentrations of ^{99}Tc and the yield tracer ^{95m}Tc were determined by spectra-stripping techniques using standard spectra for these isotopes. The ^{99}Tc and ^{95m}Tc were finally identified from their characteristic energy spectra and their column elution behaviors; i.e., both energy spectra (after background subtraction) and elution behavior were required to be the same as those determined for the standards of these isotopes. The detection limit is 9×10^{-7} μCi for the 1-L samples, or 2.3×10^{-7} μCi for the 4-L samples.

Results

Using ^{99}Tc standards, we found that on the average 93.0 ± 7.0% of the tracer was recovered and that 87.0 ± 5.0% of the tracer was eluted in the first 4 cm^3 of eluent. We thus had confidence in the relative accuracy of our results. Figure 4-3 shows a typical elution curve.

The results of the analyses of samples obtained in and near the six event sites are shown in Table 4-1. The error limits represent one standard deviation and result from uncertainties associated with chemical yields, counting, and data analysis. The tritium contents, corrected back to the time of the event ($T = 0$), are included for comparison.

Conclusions

^{99}Tc was detected in water samples taken in or near the cavity regions of the Cheshire, Bilby, and Faultless Event sites. However, none exceeded the maximum permissible concentration for water of 3×10^{-4} μCi/mL as given in the Code of Federal Regulations (USNRC, 1982). None of the satellite well waters contained ^{99}Tc above our detection limit. The ^{99}Tc detected in the Faultless sample is the first radionuclide other than tritium reported in water from this event site (see Buddemeier and Isherwood, 1985, for a

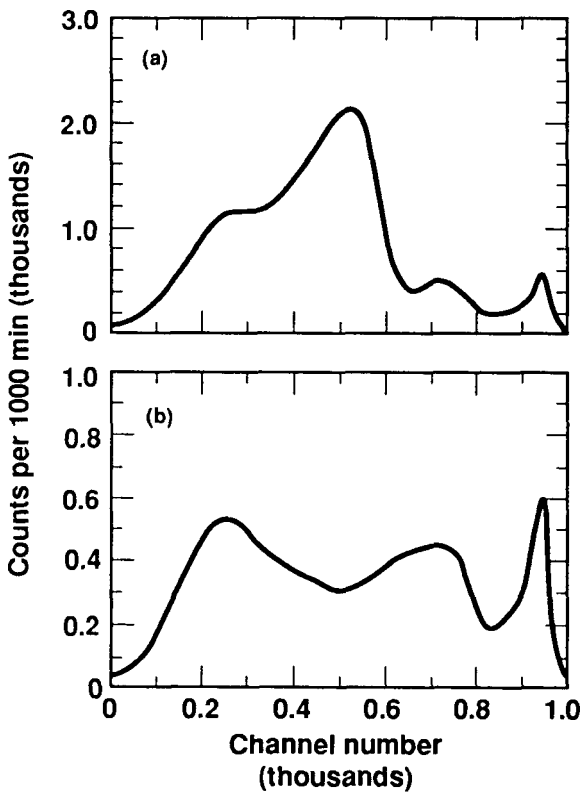

Figure 4-2. Typical energy spectra (a) for the Cheshire sample, and (b) for the background.

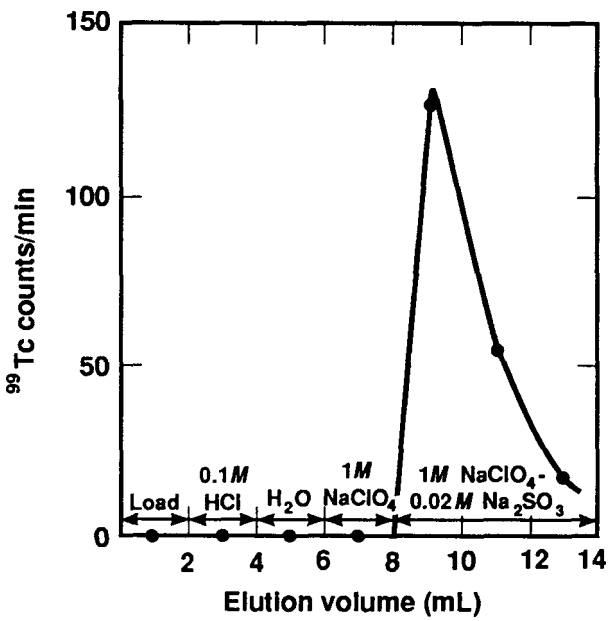

Figure 4-3. Typical elution behavior of ^{99}Tc from an anion resin column (AG 1 × 8, 100–200 mesh, 0.5-cm diam by 6-cm long).

Table 4-1. Results of technetium analyses.

Experimental site	Sample location	Sampling date	Sample volume (L)	Filter size (μm)	^{99}Tc Count (μCi/mL)	^{99}Tc % SD	^{3}H (μCi/mL at T_0)
Cheshire (U20n)	Cavity	5/09/85	1.17	0.003	5.11×10^{-8}	11.5	5.0×10^{-1}
		10/23/84	1.00	None	4.90×10^{-8}	10.6	4.1×10^{-1}
	Above cavity	5/29/85	1.00	0.05	3.83×10^{-8}	12.5	4.3×10^{-1}
		5/29/85	1.20	0.003	2.73×10^{-8}	11.6	4.3×10^{-1}
Bilby (U3cn)	Chimney	7/19/82	1.00	0.45	4.05×10^{-8}	5.0	9.9×10^{-2}
		6/18/85	1.00	0.20	5.87×10^{-8}	4.0	9.5×10^{-2}
Faultless (UCP1P2SR)	Well (2590 ft)	7/21/83	3.10	0.45	4.77×10^{-9}	10.4	5.0×10^{-2}
	(2390 ft)		1.75	0.45	1.49×10^{-9}	12.1	5.0×10^{-2}
Nash (U2ce)	Satellite well	4/18/84	4.0	0.45	$<2.3 \times 10^{-10}$		6.3×10^{-2}
Bourbon (U7n)	Satellite well	6/24/83	4.0	0.45	$<2.3 \times 10^{-10}$		$<3.3 \times 10^{-6}$
Cambric (U5e)	Lower cavity	1/06/75	1.0	0.45	$<9.0 \times 10^{-10}$		9.9
	Chimney	8/07/75	4.0	0.45	$<2.3 \times 10^{-10}$		1.4×10^{-1}
	Chimney & adjacent	4/10/85	4.0	0.20	$<2.3 \times 10^{-10}$		7.2×10^{-5}
	Satellite well	11/8/82–11/10/82	3.5	0.45	$<2.3 \times 10^{-10}$		6.3×10^{-3}

description of the Faultless site and previous sampling efforts there).

Laboratory measurements conducted under oxidizing conditions yield K_d values near zero for technetium (Daniels and Thompson, 1984; Serne and Relyea, 1982). Thus, one would expect technetium to follow tritium rather closely in its migration behavior. Because water samples can be obtained from both the cavity area (RNM-1) and a satellite well (RNM-2), the Cambric site would seem to provide a unique opportunity for testing migration patterns in the field. Unfortunately for this purpose, none of the Cambric samples indicated ^{99}Tc above our detection limit. Samples obtained from the cavity did have higher-than-normal detection limits. These were caused by the large amount of tritium in these waters which, because it could not be totally removed during the chemical processing, caused background subtraction problems.

The results for ^{99}Tc, obtained from Cheshire samples passed through filters of different pore sizes, confirm our earlier expectations that technetium would exhibit a behavior similar to Na and Sb. There was not clear evidence that technetium is sorbed to any appreciable extent on filterable material in the water samples. This result could be expected if the technetium is indeed present as TcO_4^- as predicted. Most naturally occurring colloids, e.g., clays, iron hydroxides, etc., have a negative surface charge at neutral and alkaline pH values (Yariv and Cross, 1979). These colloidal particles would tend to sorb positively charged solution species and not negatively charged ones (Yariv and Cross, 1979).

Section 5. Other Studies

Section 5A. Further Data on 1974 Study of Radionuclide Migration at Yucca Flat

Contributors: J. H. Rego, R. W. Buddemeier, and K. V. Marsh

Introduction

Early in 1986, LANL reported unexpected tritium and fission product activity in the water flowing into the proposed emplacement hole for the Aleman test (Area 3, Yucca Flat). In order to relate these results (Sewell, 1987) to earlier observations of apparent rapid transport of radionuclides, we reviewed the earlier work done at LLNL and published by Crow (1976).

Crow (1976) reported on the observations of tritium in three holes in Area 2 (see Frontispiece). The first hole, U2aw, was found to have an initial inflow of 28.6 m^3 of groundwater per day, with tritium concentrations ranging from 2 to 12×10^{-3} μCi/mL over the period of observation (April through September, 1974). Water from this hole had also been analyzed for gamma emitters with negative results, but the analytical procedure and sensitivity were not reported. The suspected source of the tritium was the Commodore Event, which had been fired on 20 May 1967 in hole U2am, 465 m south east of U2aw. Water from the second exploratory drill hole (UE2aw) also had an elevated tritium concentration (approx. 10^{-4} μCi/mL). A third exploratory hole, UE2ar, was drilled 981 m south of U2aw and 361 m from a second possible source, the Agile Event, that had been fired in February 1967 with a working point at 733 m.

Crow (1976) reported that four water samples were bailed from hole UE2ar on May 10, 1975. At the time of sampling, the hole had caved in nearly to the level of the water table (544 m below ground surface). The samples showed tritium activities ranging from 1.1 to 5.0×10^{-4} μCi/mL, with an average of 3×10^{-4} μCi/mL. Crow concluded that Agile was the probable source of the tritium observed in UE2ar.

Experimental

A search of the Nuclear Chemistry Division's sample archives located four 1-L sample bottles labeled "H_2O–UE2ar–1790 ft–5/10/75," "(1 of 4)" through "(4 of 4)." The sample liquid was brown and appeared to contain considerable sediment. Sample (3 of 4) was gamma counted without filtration. Sample (4 of 4) was centrifuged, filtered through a 0.45-μm filter and gamma counted as (a) filter+sediment and (b) filtrate. The filtrate was also analyzed for tritium. The filtrate and the unfiltered, sediment+water samples were counted in a Marinelli beaker (see Sec. 5B); the filter+sediment sample was counted in a standard 25 cm^3 counting vial.

Results and Discussion

Table 5A-1 lists the radionuclide concentrations observed; all have been decay corrected to the 1975 sampling date. The tritium value is within the range previously measured (Crow, 1976). It is significant, however, that ^{125}Sb was found in the filter+sediment sample and ^{137}Cs was found in all three sample fractions analyzed. These nuclides were not originally detected and were not found in the U2aw groundwater; they are, however, observed to undergo hydrologic transport at the Cheshire site and in Area 3.

It is interesting to note that for both of the gamma-emitting nuclides detected in the UE2ar samples, the largest fraction of the total activity was found in the filterable materials rather than in the filtrate. The samples from Cheshire (see Sec. 2) indicate that antimony is almost completely dissolved and cesium is predominantly so. However, the UE2ar samples are substantially older than the Cheshire samples, both in terms of the time elapsed since detonation and in terms of the time stored as a mixed sediment+water system. These results hint at the possibility that the kinetics of sorption equilibrium for these species are very slow, producing different distribution coefficients as a function of time over periods much longer than those of typical lab or field experiments. Another possibility, of course, is that the chemical characteristics of either the groundwater or the solids in Area 2 are very different from conditions near the Cheshire site; we know, for example, that groundwater temperatures on Pahute Mesa are significantly higher than in Yucca Flat. As we concern ourselves with longer-term migration issues, these matters would seem to merit further attention.

If the source of the UE2ar activity is the Agile Event, and if the transport mechanism is hydrologic migration, the indication is that some

Table 5A-1. Radionuclides in groundwater samples from hole UE2ar at NTS: comparison between measurements made in 1975 and recent measurements corrected to 1975.

Nuclide	Recent measurements: Sample (3 of 4) Nonfiltered (μCi/mL/% error)	Recent measurements: Sample (4 of 4) Filter + sediment (μCi/mL/% error)	Recent measurements: Sample (4 of 4) Filtrate (μCi/mL/% error)	Range of 1975 measurements[a] (10^{-4} μCi/mL)
^{3}H	NA[b]	NA	2.68×10^{-4}/1.0	1 to 5
^{40}K	2.81×10^{-7}/6.17	1.40×10^{-7}/5.6	1.6×10^{-7}/50	NA
^{125}Sb	ND[b]	6.02×10^{-8}/16.4	ND	NA
^{137}Cs	2.14×10^{-8}/5.55	5.67×10^{-8}/1.3	1.29×10^{-9}/51.4	NA

[a] From Crow (1976).

[b] NA = not analyzed; ND = not detected.

radionuclides are being transported in tuff more rapidly than at first expected. A transit time of 8 y or less over a distance of about 360 m implies a migration rate of at least 45 m/y. Initial estimates of groundwater flow velocities were in the range of 30 m/y (Crow, 1976).

Conclusions

The results of our review of earlier work and our examination of preserved groundwater samples tend to reinforce the conclusions drawn from the Cheshire site and Area 3 observations, i.e., that antimony and cesium are relatively mobile and may be expected to undergo reasonably prompt migration with moving groundwater. The Area 2 and Area 3 results, obtained from regions of tuffaceous alluvium, raise the question of why similar radionuclide movements have not been seen in the induced-migration experiment at the Cambric site.

Section 5B. Calibration and Applications of Marinelli Beakers

Contributors: R. A. Failor, J. Beiriger, J. H. Rego, R. W. Buddemeier, and K. V. Marsh

Introduction

Marinelli beakers are frequently used to obtain preliminary analyses of very low-level, large-volume samples, especially liquids. The GAMANAL program (Gunnink and Niday, 1972) is not able to handle the geometry of these beakers, so special efficiency calibrations are necessary. We have performed detector-specific calibrations for our systems that allow us to account for counting geometry and for gamma-ray absorption effects on both the sample and background activities.

Initially, we intended to use the Marinelli counting method to scan incoming samples to detect gross differences in concentration and to choose samples for more precise workup. However, we found that a simple calibration allowed the Marinelli beakers to be used for semi-quantitative analyses. In this discussion, we include results from an analysis of samples from the Cheshire site.

Calibrations

Procedure. We used a National Bureau of Standards (NBS) standard reference solution containing ^{125}Sb, ^{125m}Te, ^{154}Eu, and ^{155}Eu as the calibration solution. NBS suggests that this solution be used as the mixed-radionuclide solution standard for efficiency calibration of germanium-spectrometer systems.

The reference solution was diluted to produce a reduced-activity solution in sufficient volume to fill two 1-L Marinelli beakers (manufactured by GA-MA Associates, Inc.) and to provide 50 mL for small-volume measurements in a standard geometry.

The activity of the diluted solution was measured using the small-volume samples and compared to the values calculated from the NBS reference values. The measured and calculated values agreed to within less than 3%. Duplicate counts were made of both Marinelli beakers containing the diluted standard. These values agreed to within counting uncertainty (<5%).

To account for possible absorption of ambient gamma rays by the water-filled Marinelli beakers, long background measurements were

made for each detector with and without the Marinelli beaker in place.

Results. The energy-dependent efficiency was calculated for each detector separately. Reciprocal efficiency as a function of energy is shown in Table 5B-1 and plotted in Fig. 5B-1. The deviations from linearity at low energies can be accounted for by absorption of the gamma rays in the sample. The deviations from linearity at the high energies are due to summing of the gamma rays from a given isotope. Summing corrections for the NBS nuclides resulted in linear high-energy values. Although this method gives us a general calibration of efficiency versus gamma-ray energy, it is not applicable to radionuclides from which cascade gamma rays produce large summing effects. We intend to perform specific empirical calibrations for all such nuclides of interest to the HRMP program.

The absorption of the gamma rays by a Marinelli beaker filled with water also results in a reduction in the background activity seen by the detector. We have measured the effect for each detector. At energies below 1 MeV, the changes were up to 10%. This was greater than the counting uncertainty. For this reason, we used "Marinelli background values" for all the analyses presented here.

Analysis of Cheshire Samples

To investigate the association of radionuclides with colloidal particles, as well as the size distribution of small particles (<1.0 to >0.003 μm), we ultrafiltered two 1-L samples and used the calibrated Marinelli beakers to analyze the filtrates. Results for these two samples (identified as 0.003-μm filter size) were compared with those for nonfiltered and conventionally filtered samples and with the results of large-volume sample processing.

Table 5B-2 shows the results of this experiment. If we compare the ^{125}Sb concentrations for nonfiltered and ultrafiltered 1-L portions of sample B-8, we see no significant difference in the values. This information supports the results obtained from large-volume samples (see Sec. 2 and Appendix A); namely, ^{125}Sb in these samples is almost completely dissolved (>97%). The same comparison for ^{137}Cs shows a difference of 60%, indicating that 60% of the activity is in solution (passing through a 0.003-μm membrane) and 40% of the activity is attached to particles greater than 0.003 μm. This is consistent with the 0.003-μm cutoff observed from evaporation of our large-volume (194.5-L) B-8 sample, which excluded about 35% of the total ^{137}Cs.

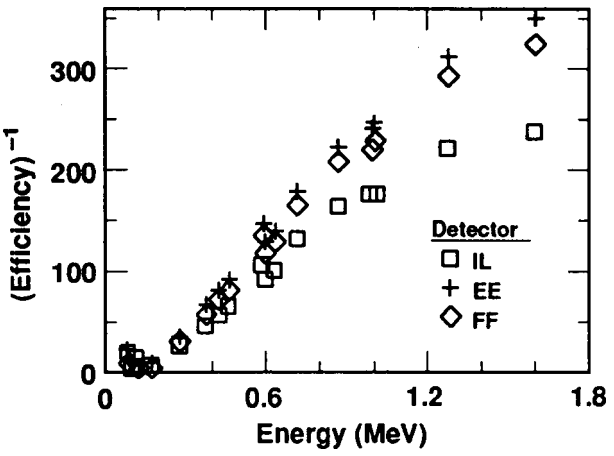

Figure 5B-1. Marinelli counting efficiency for three detectors.

The remainder of the table presents the results of Marinelli beaker counts of other samples passed through filters of various pore sizes. They are included to indicate the general accuracy and limits of detection of the technique. The ^{85}Kr results merely indicate the concentration present in the sample when counted; no attempt was made to take or preserve these samples for quantitative determination of the ^{85}Kr.

Conclusion

This technique has been shown to be useful and accurate in its present form, but can be refined considerably (Zimmer, 1980), and work is in progress to do so. At present, we must take the output of a computer analysis of the spectrum calculated as counts per minute (cpm) of each gamma ray and, using plots similar to that shown in Fig. 5B-1, perform calculations by hand to convert the cpm to the desired concentration units. In the future, we will incorporate in the computer program a table of "pseudo-branching intensities" that will permit the GAMANAL code to identify isotopes and calculate concentrations directly. These pseudo-branching intensities will combine the actual nuclear decay branching intensities with correction factors for absorption of the gamma rays by the sample and for coincidence summing effects. In the meantime, the disposable Marinelli beakers give us a very fast and convenient means of analyzing up to 1-L volumes of liquid with accuracy and sensitivity suitable for many HRMP applications.

Table 5B-1. Details of gamma-ray Marinelli calibration.

Radionuclide	Photon energy (keV)	(Efficiency)$^{-1}$[a] Det L-01	Det E-01	Det F-01
^{155}Eu	86.6	58	59.64	47.49
^{155}Eu	105.3	41.09	50.17	42.68
^{154}Eu	123.1	53.73	49.2	43.85
^{125}Sb	176.4	47.16	50.4	45.89
^{154}Eu	280	64.59	72.69	68.15
^{125}Sb	380.5	81.8	100.4	91.4
^{125}Sb	427.9	91.42	112.4	105
^{125}Sb	463.9	98.24	122.2	113
^{154}Eu	591.7	135.6	169.6	160.2
^{125}Sb	600.6	122.6	154.6	145.3
^{125}Sb	635.9	129.4	164.6	154.6
^{154}Eu	723.3	156.8	198.2	186.3
^{154}Eu	873.2	184.8	237.7	224.7
^{154}Eu	996.4	196.6	254.1	235.5
^{154}Eu	1004.8	196.2	258.7	243.3
^{154}Eu	1274.4	235.9	317.1	299.2
^{154}Eu	1596.5	250.8	350.5	327.7

[a] (Efficiency)$^{-1}$ = photons/min emitted ÷ counts/min observed.

Section 5C. Determination of Particulate Activity: Bulk Filters versus Ashed Filters

Contributors: J. H. Rego, R. W. Buddemeier, and K. V. Marsh

Introduction

Standard LLNL procedures for the determination of particulate activity in large-volume water samples rely on direct counting of the filters used to process the sample. The filters representing each size fraction are drained, cut or folded as necessary, and then packed into a standard container (usually a sealed aluminum can, 8.5 cm i.d. by 4 cm i.h., commonly referred to as a "tuna can"). These containers are counted directly on low-background Ge(Li) detectors, and the gamma-ray activity is calculated using the GAMANAL code (Gunnink & Niday, 1972). The process is convenient, involves little risk of sample loss or contamination, and provides data on the distribution of activity as a function of particle size. However, there are at least two potential disadvantages, both related to the extended-source geometry of the tuna can. First, because an extended-source geometry reduces counting efficiency relative to smaller sources, sensitivity is reduced. Second, we know that the filter material is not uniformly distributed throughout the tuna can, and we have every reason to believe that the particulate material is not uniformly distributed on the filter. The extended source is therefore inhomogeneous to some degree, but the GAMANAL code necessarily treats it as a homogeneous source.

For studies focused on the distribution of activity between the dissolved and total-particulate phases, it seemed clear that combined filters reduced to a relatively small volume would provide more favorable geometry (in terms of both size and homogeneity) and higher total activity per sample. In principle, this should result in greater sensitivity and more accurate determinations of total particulate activity. To test these hypotheses, we compared the activities obtained the traditional way, by counting filters directly, with the activities measured by counting ashed composites obtained by ashing and then combining all of the ashed filters from a given sample.

Table 5B-2. Results of calibrated Marinelli beaker scans of water samples from the Cheshire site (μCi/mL).

Date collected	09/—/76	09/09/83	09/09/83	10/23/84	10/23/84	05/09/85	05/09/85	05/25/85	06/19/85	09/11/85	10/01/85
Detector	L-01	L-01	L-01	L-01	L-01	F-01	E-01	L-01	L-01	L-01	L-01
Sample label	S-0	S-1	S-1	B-3	B-4	B-8	B-8	S-38	S-31	S-36	S-37
Sample size (L)	1.0169	0.950	0.950	0.980	0.898	1.0366	1.03412	0.998	1.0124	0.9231	1.063
Filter cutoff (μm)	(None)	0.45	0.006	0.20	0.003	(None)	0.003	(None)	(None)	0.45	0.45
Nuclide	Cavity							Formation			
^{22}Na	ND[a]	1.11×10^{-8} 55%[b]	1.13×10^{-8} 26%	3.31×10^{-8} 17.8%	1.47×10^{-8} 33.2%	6.09×10^{-8} 20.3%	ND[a]	ND	ND	ND	ND
^{40}K	5.06×10^{-5} 8.0%	ND	ND	ND	ND	ND	ND	ND	ND	ND	ND
^{85}Kr	ND	8.17×10^{-5}	ND	5.22×10^{-6} 28.1%	ND	ND	ND	2.62×10^{-5} 6.6%	2.40×10^{-5} 7.2%	1.83×10^{-5} 1.5%	2.54×10^{-5} 1.3%
^{125}Sb	1.78×10^{-6} 1.7%	8.81×10^{-6} 4%	7.74×10^{-6} 4%	5.74×10^{-6} 1.4%	6.17×10^{-6} 1.2%	5.14×10^{-6} 1.8%	5.17×10^{-6} 1.8%	3.75×10^{-6} 1.2%	3.97×10^{-6} 1.0%	2.67×10^{-6} 1.3%	3.46×10^{-6} 1.2%
^{137}Cs	5.13×10^{-9} 9.2%	2.06×10^{-7} 2%	1.62×10^{-6} 2%	3.94×10^{-6} 1.6%	2.87×10^{-6} 1.3%	3.42×10^{-6} 0.4%	2.03×10^{-6} 0.5%	4.30×10^{-7} 1.2%	7.32×10^{-7} 1.2%	2.25×10^{-7} 1.3%	6.41×10^{-7} 1.2%

[a] ND = not detected; no limit calculated.

[b] % uncertainties are based on counting statistics, ±1 standard deviation.

Procedures

The samples used for the comparison were the filters from Cheshire samples B-1 through B-6 (see Sec. 1 and Appendix A), all of which had received long counts on low-background detectors in the standard tuna-can configuration.

The sample cans were opened, and the filter pieces were placed in a porcelain crucible and heated in a small muffle furnace at about 475°C for 8 hours or until the filters were completely ashed. The ashed filter fractions were then combined into a composite for each sample, and the composite ash sample was counted on a low-background Ge(Li) gamma-ray spectrometry system. A set of unused filters was also ashed and counted to determine whether the filters themselves contributed to the measured activities.

For purposes of comparison, the activities of the individually counted unashed filters were summed for each sample, and the percent standard deviation of the sum was calculated according to the formula

$$\%SD = \frac{\left[(SD_1)^2 + (SD_2)^2 + (SD_3)^2 \ldots\right]^{1/2}}{(A_1 + A_2 + A_3 + \ldots)} \times 100,$$

where %SD = the percent standard deviation of a given activity A, and SD = (%SD × A)/100. Limit values were omitted from the sums when discrete values were available for any of the fractions, but when only limits were available, they were summed and their sum was listed as an upper limit for the total activity.

Results

Complete data for the individual filters and ashed composites of samples B-1 through B-6 are tabulated in Appendix A. Table 5C-1 presents a summary of the summed-filter and ashed-composite results for the major radionuclides in all six samples and in a set of unused filters. The sample counts were corrected to activity at time zero (T_0) for the detonation; the counting data for the unused filters were presented as activity (limits) at the time of the count, since nearly all the activity reflects background counts and therefore would not vary with time. Contributions to the sample activities by the unused filters can be seen to be negligible.

Table 5C-2 presents for each of the major nuclides in each sample the ratio of the ashed-composite activity to the summed-filter activity. The uncertainties associated with these ratios are calculated from the counting uncertainties in Table 5C-1. To facilitate comparisons, two further sets of calculations are presented in Table 5C-2: at the bottom of the table are the means of the ratios averaged across all nuclides in a give sample, and in the right-hand column are the means of the ratios averaged across all samples for a given nuclide. In these two cases, the standard deviations presented are calculated from the set of ratios averaged and do not reflect the counting statistics. For reasons discussed below, ratios with a compounded counting uncertainty in excess of 10% were excluded for the calculation of the means; these values are marked with a superscript "c" in the table.

Several conclusions can be based on Table 5C-1. First, we note that the summed and ashed values are generally reasonably close. We can also see that the ashed sample values usually have lower counting uncertainties, and that the difference in the counting uncertainties increases as the level of activity decreases (see, for example, the europium isotopes and ^{60}Co in samples B-5 and B-6). Related to this is the observation that sensitivities are improved by counting the ash; several nuclides that are shown only as limits in the sums appear as real (albeit very uncertain) numbers in the ash counts.

The ashed-composite samples from both B-5 and B-6 were counted twice in order to obtain an estimate of the reproducibility of the results for an individual ash sample; the data are presented in Appendix A and in Table 5C-3. For the major nuclide activities and ratios listed in Table 5C-3, the mean absolute difference between counts was 3±9% for the B-5 comparison and 11±10% for the B-6 comparison.

Table 5C-2 indicates that the ashing procedures introduced no major biases into the relative concentrations of the nuclides in a given sample. Nuclide yields from the ashed samples (relative to the summed values) were reasonably consistent within a sample; results for B-1, B-2, and B-5 indicate good total recovery; results for B-4 and possibly B-3 suggest the possibility of sample loss; and the few reasonably precise values for sample B-6 indicate that the values for the ashed sample were higher.

Table 5C-1. Activity comparisons of directly counted and ashed filters (μCi/mL at T_0).[a]

Sample ID	Cheshire B-1				Cheshire B-2				Cheshire B-3				Cheshire B-4			
Collection date	9/8/83				9/9/83				10/23/84				10/23/84			
Volume (L)	188				200				166				194.5			
Nuclide	Summed fractions	% SD[b]	Combined ashed	% SD	Summed fractions	% SD	Combined ashed	% SD	Summed fractions	% SD	Combined ashed	% SD	Summed fractions	% SD	Combined ashed	% SD
^{54}Mn	7.4×10^{-8}	12.0	5.8×10^{-8}	34	4.1×10^{-8}	23.9	2.9×10^{-8}	46.4	NL[c]	—	1.2×10^{-8}	64	3.3×10^{-8}	45	3.3×10^{-8}	67
^{60}Co	4.0×10^{-9}	1.1	3.6×10^{-9}	0.7	2.0×10^{-9}	2.6	1.9×10^{-9}	0.9	4.6×10^{-10}	6.4	3.7×10^{-10}	1.5	2.4×10^{-9}	3.6	1.9×10^{-9}	0.9
^{106}Ru	4.3×10^{-6}	2.3	3.7×10^{-6}	2.5	2.7×10^{-6}	3.0	2.5×10^{-6}	4.8	9.5×10^{-7}	8.2	7.4×10^{-7}	3.4	7.1×10^{-6}	4.4	5.7×10^{-6}	2.9
^{125}Sb	6.6×10^{-8}	2.2	6.1×10^{-8}	1.5	4.4×10^{-8}	3.1	4.5×10^{-8}	1.7	2.6×10^{-8}	2.2	2.1×10^{-8}	1.6	1.3×10^{-7}	2.2	1.1×10^{-7}	1.2
^{137}Cs	3.9×10^{-7}	0.8	3.7×10^{-7}	0.8	7.2×10^{-7}	0.9	6.7×10^{-7}	1.1	1.0×10^{-7}	0.9	9.5×10^{-8}	0.8	1.2×10^{-6}	1.0	1.0×10^{-6}	0.7
^{144}Ce	4.9×10^{-9}	7.8	5.2×10^{-9}	7.1	3.1×10^{-9}	10.7	3.8×10^{-9}	25.6	5.1×10^{-10}	17.5	8.5×10^{-10}	12.5	6.7×10^{-9}	15.9	5.6×10^{-9}	8.5
^{152}Eu	3.8×10^{-9}	1.9	3.5×10^{-9}	1.2	2.4×10^{-9}	3.7	2.4×10^{-9}	1.3	7.4×10^{-10}	5.9	6.0×10^{-10}	2.4	5.3×10^{-9}	2.5	4.2×10^{-9}	1.2
^{154}Eu	6.7×10^{-9}	1.4	6.2×10^{-9}	1.2	3.2×10^{-9}	3.2	4.2×10^{-9}	1.1	1.2×10^{-9}	4.0	1.1×10^{-9}	1.8	9.1×10^{-9}	2.1	7.2×10^{-9}	1.0
^{155}Eu	1.9×10^{-8}	2.1	2.0×10^{-8}	2.2	1.2×10^{-8}	2.8	1.2×10^{-8}	1.4	3.4×10^{-9}	4.9	3.6×10^{-9}	2.3	2.5×10^{-8}	2.5	1.9×10^{-8}	1.9

[a] Corrected to 2/14/76.

[b] Standard deviation.

[c] NL = not calculated.

Table 5C-1. (Continued)

Sample ID	Cheshire B-5				Cheshire B-6				Blank Filterbags[d]			
Collection date	5/28/85				5/28/85							
Volume (L)	184				200				200			
Nuclide	Summed fractions	% SD	Combined ashed	% SD	Summed fractions	% SD	Combined ashed	% SD	Summed fractions	% SD	Combined ashed	% SD
^{54}Mn	$<6.5\times10^{-10}$	—	7.0×10^{-9}	71	$<3.0\times10^{-7}$	—	$<2.0\times10^{-7}$	—	$<2.3\times10^{-12}$	—	$<9.0\times10^{-13}$	—
^{60}Co	7.8×10^{-11}	15.8	8.7×10^{-11}	4.4	5.3×10^{-11}	11.5	$<7.9\times10^{-11}$	5.2	$<2.7\times10^{-12}$	—	$<9.0\times10^{-13}$	—
^{106}Ru	1.5×10^{-6}	5.9	1.4×10^{-6}	2.2	1.1×10^{-6}	6.3	1.3×10^{-6}	3.9	$<2.3\times10^{-11}$	—	$<2.0\times10^{-12}$	—
^{125}Sb	3.7×10^{-8}	1.6	3.6×10^{-8}	0.7	2.8×10^{-8}	1.6	3.2×10^{-8}	0.9	$<6.3\times10^{-12}$	—	$<2.0\times10^{-12}$	—
^{137}Cs	6.0×10^{-8}	0.8	5.8×10^{-8}	0.8	4.6×10^{-8}	1.1	5.4×10^{-8}	1.0	$<2.7\times10^{-12}$	—	4.6×10^{-12}	24
^{144}Ce	$<8.8\times10^{-12}$	—	3.3×10^{-10}	31	$<1.8\times10^{-12}$	—	$<1.8\times10^{-11}$	—	$<1.4\times10^{-11}$	—	$<4.0\times10^{-11}$	—
^{152}Eu	1.1×10^{-10}	22.5	1.2×10^{-10}	4.8	8.0×10^{-11}	12.6	1.0×10^{-10}	8.1	$<4.6\times10^{-12}$	—	$<2.0\times10^{-12}$	—
^{154}Eu	2.1×10^{-10}	7.4	2.1×10^{-10}	4.9	1.8×10^{-10}	14.2	2.0×10^{-10}	3.8	$<7.7\times10^{-12}$	—	$<9.0\times10^{-13}$	—
^{155}Eu	5.8×10^{-10}	13.1	7.5×10^{-10}	4.9	4.8×10^{-10}	9.2	6.9×10^{-10}	7.3	1.0×10^{-11}	27	$<2.0\times10^{-12}$	—

[d] Activity at count time.

Table 5C-2. Ratios of combined ashed-composite to summed-filter activities.

Nuclide	B-1	(%)[a]	B-2	(%)	B-3	(%)	B-4	(%)	B-5	(%)	B-6	(%)	$\bar{x} \pm SD$[b]
^{54}Mn	0.74[c]	(0.27)	0.60[c]	(0.32)	—	—	1.00[c]	(0.80)	—	—	—	—	—
^{60}Co	0.90	(0.01)	0.95	(0.03)	0.80	(0.05)	0.79	(0.03)	1.12[c]	(0.18)	1.49[c]	(0.18)	0.86 ± 0.08
^{106}Ru	0.86	(0.03)	0.93	(0.05)	0.78	(0.07)	0.80	(0.04)	0.93	(0.06)	1.18	(0.09)	0.91 ± 0.15
^{125}Sb	0.92	(0.02)	1.02	(0.04)	0.81	(0.02)	0.85	(0.02)	0.97	(0.02)	1.14	(0.02)	0.95 ± 0.12
^{137}Cs	0.95	(0.01)	0.93	(0.01)	0.95	(0.01)	0.83	(0.01)	0.97	(0.01)	1.17	(0.02)	0.97 ± 0.11
^{144}Ce	1.06	(0.11)	1.23[c]	(0.34)	1.67[c]	(0.36)	0.84[c]	(0.15)	—	—	—	—	—
^{152}Eu	0.90	(0.02)	1.00	(0.04)	0.81	(0.05)	0.79	(0.02)	1.09[c]	(0.25)	0.80	(0.02)	0.88 ± 0.10
^{154}Eu	0.93	(0.02)	1.00	(0.03)	0.92	(0.04)	0.79	(0.02)	1.00	(0.09)	0.90[c]	(0.13)	0.93 ± 0.09
^{155}Eu	1.05	(0.03)	1.00	(0.03)	1.06	(0.06)	0.76	(0.02)	1.29[c]	(0.18)	1.44[c]	(0.17)	0.97 ± 0.14
$\bar{y} \pm SD$	0.95 ± 0.07		0.98 ± 0.04		0.88 ± 0.10		0.80 ± 0.03		0.97 ± 0.03		1.16 ± 0.02		0.92 ± 0.04

[a] The % counting error for that nuclide in the sample.
[b] Standard deviation.
[c] Omitted from calculation of means.

Table 5C-3. Repeat count comparisons, ashed composite filters (units: μCi/mL ± 1 SD).[a]

Nuclide	$B\text{-}5_1$	(%)[b]	$B\text{-}5_2$	(%)	$B\text{-}5_1/B\text{-}5_2$	$B\text{-}6_1$	(%)	$B\text{-}6_2$	(%)	$B\text{-}6_1/B\text{-}6_2$
^{40}K	5.61×10^{-10}	(5.0)	5.21×10^{-10}	(5.0)	1.08	4.30×10^{-10}	(7.9)	3.91×10^{-10}	(4.8)	1.09
^{60}Co	8.68×10^{-11}	(4.4)	7.21×10^{-11}	(5.1)	1.20	7.86×10^{-11}	(5.2)	8.10×10^{-11}	(4.9)	0.97
^{106}Ru	1.34×10^{-6}	(2.2)	1.36×10^{-6}	(3.5)	0.98	1.30×10^{-6}	(3.9)	1.26×10^{-6}	(5.3)	1.03
^{125}Sb	3.61×10^{-8}	(0.7)	3.60×10^{-8}	(0.7)	1.00	3.24×10^{-8}	(0.9)	2.96×10^{-8}	(0.8)	1.09
^{137}Cs	5.84×10^{-8}	(0.8)	5.67×10^{-8}	(1.1)	1.03	5.36×10^{-8}	(1.0)	4.94×10^{-8}	(0.7)	1.09
^{152}Eu	1.23×10^{-10}	(4.8)	1.16×10^{-10}	(5.4)	1.06	1.00×10^{-10}	(8.1)	9.03×10^{-11}	(5.0)	1.11
^{154}Eu	2.06×10^{-10}	(4.9)	2.24×10^{-10}	(2.7)	0.92	1.99×10^{-10}	(3.8)	1.75×10^{-10}	(3.1)	1.14
^{155}Eu	7.50×10^{-10}	(4.9)	7.99×10^{-10}	(5.2)	0.94	6.86×10^{-10}	(7.3)	5.20×10^{-10}	(5.0)	1.32
Mean (±SD) ratio					1.03 ± 0.09					1.11 ± 0.10

[a] Standard deviation.
[b] The % counting error for that nuclide in the sample.

Discussion

A review of the process suggests that, if there are any predictable differences between the values for the summed and ashed-composite samples, one would expect the ash values to be lower. The two possible sources of loss are in the increased manipulation involved in transferring and combining the relatively small ash samples and in the possibility of loss by spattering or volatilization. There are no systematic differences between the refractory nuclides (e.g., the lanthanides) and those which might be imagined to have some potential for volatilization (cesium, antimony, and ruthenium), so we can eliminate that consideration. Between-sample ratio comparisons suggest that some total loss did occur in the case of sample B-4, and this is supported by the laboratory records. This was the first sample ashed and the only sample that included flat Millipore filters with the bag filters that were subsequently used exclusively. On heating, these filters formed small pellets that could not be reduced to ash. We suspect that the difference is due to loss incurred in the extended efforts to ash these pellets or is a result of the altered geometry when we counted them.

Somewhat less obvious is the source of the apparent gain on ashed-composite sample B-6. Some, but not all, of this systematic difference could be removed if either the second ash count or the mean of the two counts had been used in the comparison (see Table 5C-3). We also note, however, that a majority of the high uncertainty ratios from all samples (compounded counting uncertainty >10% in Table 5C-2) have ratios greater than 1.0. The decision to exclude from the averages ratios with an uncertainty in excess of 10% was based on substantial semi-empirical experience; we have found that values with high calculated uncertainties are likely to present Compton and background correction problems and that the actual uncertainties are often greater than the calculated values. As can be seen from Table 5C-2, this group of ratios contains most of the extreme outliers. We have already noted that precision and sensitivity are superior for the ash samples, so these ratios are typically derived from a low-precision summed value and a significantly more precise ash value. This suggests that the values for the upper limits and barely detectable concentrations calculated by GAMANAL are systematically too low, since even the addition of the upper-limit values into the sums does not raise the values enough to bring the ash/sum ratio reasonably close to unity. We consider this possibility intriguing but not conclusive (the cesium and antimony values for B-6, for example, involve no limits or high uncertainties and still yield high ratios). On the whole, it tends to support the utility of the ashing process as an approach to improving sensitivity and precision.

The results presented in Table 5C-3 indicate that the actual precision, as determined by reproducibility, of the ash activity determinations is about ±10%. This is consistent with our general experience on the replicability of counting data, and also with the observed distribution of data summarized in Table 5C-2. This does not address the question of absolute accuracy, and it should be noted that the ashed-composite samples are probably compact and homogeneous relative to the bulk-filter samples in the tuna-can configuration.

Conclusions

The ashing procedure provides results that are consistent with the results obtained from a direct count of the filters. Although probably not justified for routine applications, ashing does provide increased sensitivity and precision in the determination of very low levels of particulate activity. Although the increased manipulation carries with it the potential for sample loss, this does not appear to be a significant problem with samples using the bag filters.

Comparison of the data sets suggests the following conclusions concerning the accuracy and precision of the gamma-ray counting data:

- Activities with GAMANAL-calculated counting uncertainties of 10% or more may be considerably less precise than the counting statistics indicate.
- There is the possibility that GAMANAL underestimates both the very-low-level activities and the upper limits it calculates.
- Although counting statistics appreciably less than 10% are required for a reliable determination, the actual reproducibility of the values obtained is probably best represented by an uncertainty of approximately 10%.

Section 5D. Gamma-Ray Spectrometry Intercalibration with LANL

Contributors: J. H. Rego, R. W. Buddemeier, and K. V. Marsh

Introduction

Both the Lawrence Livermore and the Los Alamos National Laboratories analyze large-volume, low-radioactivity groundwater samples from HRMP sites. In order to investigate possible biases occurring as a result of different processing and analysis methods, we exchanged samples from water collections at the Cheshire site. These were not duplicate samples and were, in fact, processed by different techniques, but both samples were counted on both laboratories' systems and so are directly comparable on an individual sample basis. In each case, the selected sample had been filtered, evaporated to dryness, and the remaining salt packaged for counting in each laboratory's standard form.

LLNL Sample Preparation

The LLNL salt sample from Cheshire cavity sample B-3 (see Appendix A and Sec. 1) was homogenized and sealed in our standard "tuna-can" counting container, a geometry well-calibrated for our gamma-ray spectroscopy measurements. It was counted on four different Ge-Li spectrometers, and average values were calculated (see Table 5D-1). The standard deviation of the mean value was calculated without regard to statistical counting errors. The sample and our analytical results were sent to LANL. The results of the LANL measurements are reported by Thompson (1987); generally, all their measurements except for ^{40}K agreed with ours within 25% or better.

LANL Sample Preparation

LANL prepared the dried salt from their sample 852-9-85-004, which had been collected from the Cheshire formation (above the cavity) on 18 June 1985. Their standard procedure is to use hydraulic pressure to compact the sample into a plastic-bagged "hockey puck" configuration—a solid disk slightly smaller than the LLNL "tuna can." This sample was sent to LLNL along with two gamma-ray spectrometry printouts (one for a 500-minute "short" count and one for a 4000-minute "long" count) and the results of a radiochemical separation determination of ^{137}Cs.

LLNL Measurements and Results

On receiving the Los Alamos sample, we x-rayed it (top, bottom, and side views at 0 and 90 degrees) to determine packing uniformity. There were no large voids or asymmetries noted. The x-ray procedure was suggested because (as described below) the sample would be repackaged during our analysis: documentation of its original condition would aid in verifying any counting discrepancies or in answering any questions regarding differences in geometry and void areas.

The LANL sample was then counted twice in the "hockey puck" configuration, the second time after rotation through 90 deg in the detection chamber, and the results of these two counts were averaged. The sample was then carefully removed from the plastic bags, broken up into particle sizes comparable to the original salt sample, repacked in one of our standard tuna cans, and counted again. Results of these counts, along with LANL's analyses, are shown in Table 5D-2. Table 5D-3 presents the ratios of the LANL activity to the LLNL activity, both for the LLNL determinations described and for the LANL determinations previously reported by Thompson (1987).

Discussion

In Sec. 5C, we discussed the fact that the reproducibility of the activity values using the same sample and calculation procedures is on the order of 10% for samples with calculated counting uncertainties significantly less than 10%, and is substantially greater for values with higher calculated uncertainties. The calculated counting uncertainty is typically lower than the actual experimental precision, and for relatively high counting uncertainties the calculated value may be a very poor estimate of the accuracy of the determination. This is due to a number of factors such as the large size of the sample and its lack of homogeneity, detector size (which affects peak/Compton ratios) and calibration, and counting geometry variations due to positioning errors from count to count. The interlaboratory comparison, although not conducted with "known" or independently determined activities, gives us at least some information about the accuracy as well as the precision of our determinations. Table 5D-1 presents the results of careful replicate counts on a relatively high-activity (cavity) sample; we consider the uncertainties in the absolute activities to

Table 5D-1. LLNL-measured nuclides in sample B3 (LANL intercomparison sample).[a]

Nuclide	λ/yr	Det. AA[b]	(%)[c]	Det. VV[b]	(%)	Det. EE[b]	(%)	Det. R7[b]	(%)	Average	(%) SD[d]
^{22}Na	0.269	6.27×10^{-9}	12.5	7.82×10^{-9}	11.6	8.21×10^{-9}	10	9.89×10^{-9}	13	8.05×10^{-9}	16
^{40}K	5.4×10^{-10}	3.66×10^{-9}	8.5	3.25×10^{-9}	8.5	3.33×10^{-9}	5.7	3.82×10^{-9}	10.8	3.56×10^{-9}	6.6
^{60}Co	0.132	2.94×10^{-9}	1.3	2.62×10^{-9}	1.6	2.95×10^{-9}	1.4	3.22×10^{-9}	1.6	2.98×10^{-9}	4.9
^{106}Ru	0.690	1.14×10^{-5}	4	1.13×10^{-5}	5.2	1.12×10^{-5}	5	1.17×10^{-5}	4.9	1.14×10^{-5}	1.6
^{125}Sb	0.250	6.60×10^{-6}	1.3	6.36×10^{-6}	0.6	6.73×10^{-6}	0.5	7.02×10^{-6}	0.7	6.68×10^{-6}	3.6
^{134}Cs	0.340	8.08×10^{-9}	5.3	2.59×10^{-8}	6.5	2.72×10^{-8}	5.1	2.96×10^{-8}	7.3	2.27×10^{-8}	37.7
^{137}Cs	0.023	4.55×10^{-6}	0.7	4.23×10^{-6}	0.7	4.46×10^{-6}	0.7	4.72×10^{-6}	0.8	4.49×10^{-6}	3.9
^{152}Eu	0.052	6.76×10^{-9}	2.4	6.52×10^{-9}	2.6	6.77×10^{-9}	2.1	7.14×10^{-9}	3.1	6.80×10^{-9}	3.2
^{154}Eu	0.082	1.23×10^{-8}	2.3	1.14×10^{-8}	2.6	1.17×10^{-8}	2	1.22×10^{-8}	2.9	1.19×10^{-8}	3.1
^{155}Eu	0.147	3.90×10^{-8}	2.1	3.33×10^{-8}	5	3.38×10^{-8}	3.2	3.57×10^{-8}	7.5	3.55×10^{-8}	6.3

[a] Units in μCi/mL, corrected for decay to 2/14/76.

[b] Detector configurations: AA is a sidelooker; VV is a downlooker; and EE and R7 are uplookers.

[c] The percent counting error for that nuclide in the sample.

[d] Standard deviation on the mean of four counts.

Table 5D-2. LANL and LLNL determinations of LANL intercomparison sample (units: μCi/mL ± 1 SD).

	LANL determinations[a,b]					LLNL determinations			
Nuclide	Short count	SD	Long count	SD	Radiochemistry	LANL form[c]	SD	LLNL form[a]	SD
^{40}K	3.8×10^{-9}	10.6	3.8×10^{-9}	3.9	—	2.0×10^{-9}	0.8	2.4×10^{-9}	3.1
^{60}Co	—	—	1.1×10^{-10}	17.2	—	$<2.7 \times 10^{-12}$	—	$<1.7 \times 10^{-11}$	—
^{106}Ru	2.5×10^{-8}	14.9	1.1×10^{-6}	45.0	—	8.2×10^{-7}	19.3	1.6×10^{-6}	19.2
^{125}Sb	3.0×10^{-6}	4.9	3.0×10^{-6}	2.5	—	2.9×10^{-6}	2.8	4.0×10^{-6}	0.5
^{137}Cs	4.7×10^{-7}	0.5	—	—	7.1×10^{-7}	4.9×10^{-7}	0.1	6.3×10^{-7}	0.7
^{152}Eu	5.5×10^{-8}	36.3	4.2×10^{-11}	8.0	—	5.7×10^{-11}	67.5	$<1.0 \times 10^{-11}$	—
^{154}Eu[d]	6.7×10^{-10}	21.9	—	—	—	1.5×10^{-10}	31.7	$<1.5 \times 10^{-11}$	—
^{155}Eu	—	—	5.9×10^{-9}	36.3	—	8.4×10^{-10}	13.1	$<8.3 \times 10^{-11}$	—

[a] Uncertainties based on counting statistics.

[b] LANL form; long-count value used for comparisons if available.

[c] Uncertainties based on mean if two replicate counts.

[d] LANL determination questionable.

Table 5D-3. Ratio of LANL counts in LANL form to LLNL counts.

Nuclide	LANL determination of B-3		LLNL determination[a] of 852-9-85-004	
	RAYGUN code	SPECANL code	LANL configuration	LLNL configuration
^{40}K	1.42	1.48	1.90	1.58
^{60}Co	1.09	1.04	—	—
^{106}Ru	1.00	1.21	1.34	0.69
^{125}Sb	0.85	0.80	1.03	0.75
^{134}Cs	0.93	1.01	—	—
^{137}Cs	0.75	0.75	0.96 1.45[b]	0.75 1.13[b]
^{152}Eu	0.93	0.89	0.74	—
^{154}Eu	1.15	1.12	4.47	—
^{155}Eu	1.15	1.18	7.02	—

[a] "Long count" value from Table 5D-1 used for ratios, if available.

[b] Relative to radiochemical separation value in Table 5D-1.

represent the best precision that can be achieved, and we would normally consider ±5–10% to be a more conservative value.

Because the activity of the LANL-supplied formation sample was so much lower than the LLNL-supplied cavity sample analyzed by LANL, there are only three nuclides for which both the LANL and the LLNL analyses achieved counting statistics less than 10%—^{40}K, ^{125}Sb, and ^{137}Cs (see Table 5D-2). If we compare the activity ratios for these nuclides (LANL count in LANL form to LLNL count in LLNL form) for the two different sample intercomparisons in Table 5D-2, we see that they are quite similar. At the level of upper-limit and/or highly imprecise determinations, agreement is no better than to within an order of magnitude. The results do not contain any indication of which set of numbers is more accurate, although the radiochemical ^{137}Cs result is somewhat closer to the LLNL gamma-ray spectrometry value.

Although the LLNL intercomparison set is too small to be treated as statistically significant, most of the ratios that are not based on imprecise determinations (and some that are) deviate from unity by 25–35%—similar to the 25% range noted for the LANL intercomparison set. We may ask what sort of distribution of ratios we would expect to see as a function of the uncertainties of the individual numbers (considering accuracy as well as precision). If two numbers both have an associated (one standard deviation) uncertainty of 25%, then their ratio will have an uncertainty of 35%; the comparable ratio uncertainties for component number uncertainties of 20, 15, and 10% are 28, 21, and 14%. Although the ratio consistency for individual nuclides may suggest that we are dealing with biases rather than random errors, this analysis indicates that, in the absence of better data, an appropriate conservative value to assign as the actual uncertainty of an activity value with counting statistics <10% is probably in the range of 20 to 25%.

Conclusions

The LANL-LLNL intercomparison efforts indicate that the two laboratories agree to within 25% on the activities of nuclides with counting uncertainties <10%, although the reproducibility of individual numbers by an individual laboratory may be considerably better. There is a suggestion that some of the differences between the LANL and LLNL determinations for individual nuclides may represent systematic biases rather than random errors; however, pending further calibration results, we suggest that a conservative approach to data interpretation is to assign an absolute uncertainty of ±25% to all gamma-ray spectrometry results based on counting statistics <10%, and to treat all values with higher uncertainties as order-of-magnitude estimates. If this is done, the LANL and LLNL results will generally be in complete agreement for the same sample, and differences beyond these levels of uncertainty can normally be ascribed to the sample rather than to the techniques.

References

Apps, J. A., G. L. Carnahan, P. C. Lichtner, M. C. Michel, D. Perry, R. J. Silva, O. Weres, and A. F. White (1982), *Status of Geochemical Problems Relating to the Burial of High-Level Radioactive Waste*, Lawrence Berkeley Laboratory, Berkeley, Calif., LBL-15103.

Baker, J. E., P. D. Capel, and S. J. Eisenreich (1986), "Influences of Colloids on Sediment-Water Partition Coefficients of Polychlorobiphenyl Cogeners in Natural Waters," *Environ. Sci. Technol.* **20**, pp. 1136–1143.

Benes, P., J. Glos, and A. Gosman (1979), "Radiochemical Study of the Physicochemical State of Trace Cerium in Aqueous Solutions," *Radiochim. Acta* **26**, 55–58.

Blankennagel, R. K., and J. E. Weir, Jr. (1973), *Geohydrology of the Eastern Part of Pahute Mesa, Nevada Test Site, Nye County, Nevada*, U. S. Geological Survey, Professional Paper 712-B, U. S. Government Printing Office.

Bonano, E. J., and W. E. Beyeler (1985), "Transport and Capture of Colloidal Particles in Single Fractures," in *The Scientific Basis for Nuclear Waste Management VIII*, C. M. Jantzen, J. A. Stone, and R. C. Ewing, Eds. (Materials Research Society, Pittsburg, Pa.), pp. 385–392.

Bond, P., and S. Jha (1970), "Nuclear-Structure and Hyperfine-Field Studies with Mo95," *Phys. Rev. C* **12**, 1887.

Buddemeier, R. W., and D. Isherwood (1985), *Radionuclide Migration Project 1984 Progress Report*, Lawrence Livermore National Laboratory, Livermore, Calif., UCRL-53628, pp. 57–59.

Buddemeier, R. W., M. R. Ruggieri, and J. H. Rego (1984), "Studies of Radionuclide Migration at the Nevada Test Site," *Nuclear Chemistry Division FY 84 Annual Report*, Lawrence Livermore National Laboratory, Livermore, Calif., UCAR 10062-84/1, pp. 4–21.

Champ, D. R., and W. F. Merritt (1981), "Particulate Transport of Cesium in Groundwater," in *Proc. Canadian Nuclear Society, Second Annual Conference*, F. N. McDonnell, Ed. (Canadian Nuclear Society, Toronto, Canada), pp. 66–69.

Champ, D. R., J. L. Young, D. E. Robertson, and K. H. Abel (1984), "Chemical Speciation of Long-Lived Radionuclides in a Shallow Groundwater Flow System," *Water Pollution Res. J. Canada* **19**(2), 35–54.

Champlin, J. B. F., and G. G. Eicholz (1968), "The Movement of Radioactive Sodium and Ruthenium Through a Simulated Aquifer," *Water Resour. Res.* **4**, 147–58.

Cleveland, J. M., (1979), "Critical Review of Plutonium Equilibria of Environmental Concern," in *Chemical Modeling in Aqueous Systems*, E. A. Jenne, Ed., ACS Symp. Ser. 93, (American Chemical Society, Washington, D.C.), pp. 321–328.

Coles, D., and L. Ramspott (1982), "Migration of Ruthenium-106 in a Nevada Test Site Aquifer: Discrepancy Between Field and Laboratory Results," *Science* **125**, 1235–1237.

Crow, N. B. (1976), *First Observations of Tritium in Ground Water Outside Chimneys of Underground Nuclear Explosions, Yucca Flat, Nevada Test Site*, Lawrence Livermore National Laboratory, Livermore, Calif., UCRL-52073.

Daniels, W. R. , and J. L. Thompson (1984), *Laboratory and Field Studies Related to the Radionuclide Migration Project*, Los Alamos National Laboratory, Los Alamos, N.Mex., LA-10121-PR, p. 29.

Danielsson, L. G. (1982), "On the Use of Filters for Distinguishing Between Dissolved and Particulate Fractions in Natural Waters," *Water Res.* **16**, 179–182.

Davydov, Yu. P. (1967), "Nature of Colloids of Radioactive Elements," *Radiokhimiya* **9**, 94–105.

de Mora, S. J., and R. M. Harrison (1983), "The Use of Physical Separation Techniques in Trace Metal Speciation Studies," *Water Res.* **17**, 723–733.

Epstein, S., P. Thompson, and C. J. Yapp (1977), "Oxygen and Hydrogen Isotopic Ratios in Plant Cellulose," *Science* **198**, 1209–1205.

Giblin, A. M., B. D. Batts, and D. J. Swaine (1981), "Laboratory Simulation Studies of Uranium Mobility in Natural Waters," *Geochim. Cosmochim. Acta* **45**, 699–709.

Gschwend, P. M. and S. Wu (1985), "On the Constancy of Sediment-Water Partition Coefficients of Hydrophobic Organic Pollutants," *Environ. Sci. Technol.* **19**, 90–96.

Gunnink, R. and J. B. Niday (1972), *Computerized Quantitative Analysis by Gamma-Ray Spectrometry*, Lawrence Livermore National Laboratory, Livermore, Calif., UCRL-51061.

Higgo, J. J. W., and L. V. C. Rees (1986), "Adsorption of Actinides by Marine Sediments: Effect of the Sediment/Seawater Ratio on the Measured Distribution Ratio," *Environ. Sci. Technol.* **20**, 483–490.

Hoffman, D. C., and W. R. Daniels (1984), "Assessment of the Potential for Radionuclide Migration from a Nuclear Explosion Cavity," in *Groundwater Contamination*, National Research Council, National Academy Press, Washington, D.C., 139–146.

Hoffman, D. C. (1979), "A Field Study of Radionuclide Migration in Radioactive Waste in Geologic Storage," S. Fried, Ed., *AGS Symposium Series* **100**, p. 149.

Horzempa, L. M., and G. R. Helz (1979), "Controls on the Stability of Sulfide Sols: Colloidal Covellite as an Example," *Geochim. Cosmochim. Acta* **43**, 1645–1650.

International Atomic Energy Agency (1981), *Tritium in Some Typical Ecosystems*, IAEA, Vienna, Austria, Technical Report No. 207.

Isherwood, D. (1985), *Application of the Ruthenium and Technetium Thermodynamic Data Bases Used in the EQ3/6 Geochemical Codes*, Lawrence Livermore National Laboratory, Livermore, Calif., UCRL-53594.

Jacobson, R. (1986), Desert Research Institute, Reno, Nevada, personal communication.

James, R. O., and G. A. Parks (1982), "Characterization of Aqueous Colloids by their Electrical Double-Layer and Intrinsic Surface Chemical Properties," *Surf. Colloid Sci.* **12**, 119–216.

Johnson, B. D., and P. J. Wangersky (1985), "Seawater filtration: Particle Flow and Impaction Considerations," *Limnol. Oceanogr.* **30**, 966–971.

Kocher, D. C. (1981) *Radioactive Decay Data Tables*, National Technical Information Service, Springfield, Va., DOC/TIC-11026.

Lance, J. C., and C. P. Gerba (1982), "Virus Removal with Land Filtration," in *Water Reuse*, E. J. Middlebrooks, Ed. (Ann Arbor Science, Ann Arbor, Mich.), pp. 641–660.

Lutze, W., G. Malow, H. Rabe, and T. J. Headley (1983), "Surface Layer Formation on a Nuclear Waste Glass," in *Scientific Basis for Nuclear Waste Management VI*, D. G. Brookins, Ed. (Elsevier, New York), pp. 37–45.

Luxenburger, H. J., and H. Schuttelkopf (1984), "A Fast Radiochemical Procedure to Measure Tc-99 in Environmental Samples and Gaseous and Liquid Effluents," *Proc. 5th Intern. Conf. on Nuclear Methods in Environmental and Energy Research*, National Technical Information Service, Springfield, Va., CONF/TIC-840408, pp. 376–384.

McDowell-Boyer, L. M., J. R. Hunt, and N. Sitar (1986), "Particle Transport through Porous Media," *Water Resour. Res.* **22**, 1901–1921.

Nightingale, H. I., and W. C. Bianchi (1977), "Ground-Water Turbidity Resulting from Artificial Recharge, " *Ground Water* **15**, 146–152.

Ogard, A. E., and J. F. Kerrisk (1984), *Groundwater Chemistry Along the Flow Path Between a Proposed Repository Site and the Accessible Environment*, Los Alamos National Laboratory, Los Alamos, N.Mex., LA-10188-MS, pp. 9–10.

Rasmuson, A., and I. Neretnieks (1986), "Radionuclide Transport in Fast Channels in Crystalline Rock," *Water Resour. Res.* **22**, 1247–1256.

Saltelli, A., A. Avogadro, and G. Bidoglio (1984), "Americium Filtration in Glauconitic Sand Columns," *Nucl. Technol.* **67**, 245–254.

Sanschi, P. H., U. P. Nyffeler, Y. -H. Li, and P. O'Hara (1986), "Radionuclide Cycling in Natural Waters: Relevance of Scavenging Kinetics," in *Sediments and Water Interaction*, P. G. Sly, Ed. (Springer-Verlag, New York), pp. 183–191.

Serne, R. J., and J. F. Relyea (1982), *The Status of Radionuclide Sorption-Desorption Studies Performed by the WRIT Program*, Pacific Northwest Laboratory, Richland, Wash., PNL-3997, p. 28.

Sewell, D. (1987), *Aleman Radionuclide Migration Panel Final Report, 22 Jan 87*, Department of Energy, Nevada Operations Office, Las Vegas, Nev.

Shade, J. W., L. L. Ames, and J. E. McGarrah (1984), "Actinide and Technetium Sorption on Iron-Silicate and Dispersed Clay Colloids," in *Geochemical Behavior of Disposed Radioactive Waste, ACS Symp. Series 246*, G. S. Barney, J. D. Nauratil, and W. W. Schulz, Eds. (American Chemical Society, Washington, D.C.), pp. 67–77.

Sheppard, J. C., M. J. Campbell, T. Cheng, and J. A. Kittrick (1980), "Retention of Radionuclides by Mobile Humic Compounds and Soil Particles," *Environ. Sci. Technol.* **14**, 1349–1353.

Silva, R. J., L. V. Benson, A. W. Yee, and G. A. Parks (1979), *Waste Isolation Safety Assessment Program, Task 4: Collection and Generation of Transport Data, Theoretical and Experimental Evaluation of Waste Transport in Selected Rocks*, Annual Progress Report, Lawrence Berkeley Laboratory, Berkeley, Calif., LBL-9945.

Silva, R. J., R. Evans, J. H. Rego, and R. W. Buddemeier (1986), "Technetium Analysis in the Radionuclide Migration Project," *Nuclear Chemistry Division FY 86 Annual Report*, Lawrence Livermore National Laboratory, Livermore, Calif., UCAR 10062/86, pp. 3-14 through 3-16.

Silva, R. J., R. Evans, J. H. Rego, and R. W. Buddemeier (1988), "Methods and Results of Tc-99 Analysis of Nevada Test Site Groundwaters," *J. Radioanal. Nucl. Chem.* **124** (2), 397–405; also Lawrence Livermore National Laboratory, Livermore, Calif., UCRL-96399.

Simmons, G., and L. Caruso (1983), "Microcracks and Radioactive Waste Disposal," in *Scientific Basis for Nuclear Waste Management, Vol. VI*, D. G. Brookins, Ed. (Elsevier, New York), pp. 331–338.

Thompson, J. L. (1987), *Laboratory and Field Studies Related to the Radionuclide Migration Project, October 1, 1985 to September 30, 1986—Progress Report*, Los Alamos National Laboratory, Los Alamos, N.Mex., LA-11081-PR.

Travis, B. J., and H. E. Nuttal (1985), "A Transport Code for Radiocolloid Migration: With an Assessment of an Actual Low-Level Waste Site," in *Scientific Basis for Nuclear Waste Management VIII*, C. M. Jantzen, J. A. Stone, and R. C. Ewing, Eds. (Materials Research Society, Pittsburg, Pa.), pp. 969–976.

U.S. Nuclear Regulatory Commission (1982), *Code of Federal Regulations*, Title 10, Part 20, p. 206.

Velbel, M. A. (1986), "Influence of Surface Area, Surface Characteristics, and Solution Composition on Feldspar Weathering Rates," in *Geochemical Processes at Mineral Surfaces*, J. A. Davis and K. F. Hayes, Eds., ACS Symp. Series 323 (American Chemical Society, Washington, D.C.), pp. 615–634.

Waddell, R. K. (1982), *Two-Dimensional, Steady-State Model of Ground-Water Flow, Nevada Test Site and Vicinity, Nevada-California*, U. S. Geological Survey, Water Resources Investigations 82–4085.

Wolery, T. J., D. Isherwood, K. J. Jackson, J. M. Delany, and I. Puigdomenech (1984), *EQ3/6: Status and Applications*, Lawrence Livermore National Laboratory, Livermore, Calif., UCRL-91884.

Yariv, S., and H. Cross (1979), *Geochemistry of Colloid Systems* (Springer-Verlag, New York), pp. 210–219.

Zimmer, W. H. (1980), "Marinelli Beaker Calibration," in *Effluent and Environmental Radiation Surveillance*, J. J. Kelly, Ed., ASTM STP 698, pp. 297–308.

CKM:slk

Appendix A. Analytical Data Used in Study of Radionuclide Migration, Cheshire Area

Table A-1. Cheshire (U20n) sample B-1 nuclide analyses.[a]

Fraction ID		Prefilter		0.45-μm filter		0.20-μm filter		Ashed composite filters		Retentate >0.006 μm		Filtrate (salt) <0.006 μm	
Isotope	$t_{1/2}$ (yr)	Value	%SD	Value	%SD	Value	%SD	Value	%SD	Value	%SD	Value	%SD
^{3}H	12.26	—	—	—	—	—	—	—	—	—	—	0.615	1.0
^{22}Na	2.605	$<9.6\times10^{-13}$	—	4.63×10^{-10}	37.8	$<9.6\times10^{-13}$	—	3.35×10^{-10}	70.5	$<4.5\times10^{-11}$	—	7.11×10^{-9}	3.8
^{40}K	1.3×10^{9}	$<4.8\times10^{-11}$	—	$<4.1\times10^{-11}$	—	$<3.9\times10^{-11}$	—	3.60×10^{-10}	14.8	1.67×10^{-9}	19.7	1.00×10^{-9}	18.9
^{54}Mn	0.855	5.92×10^{-8}	8.5	8.11×10^{-9}	21.1	6.88×10^{-9}	31	5.77×10^{-8}	33.8	4.34×10^{-8}	57	$<1.6\times10^{-11}$	—
^{60}Co	5.272	3.18×10^{-9}	0.9	4.56×10^{-10}	2.1	3.93×10^{-10}	1.9	3.61×10^{-9}	0.7	1.50×10^{-9}	3	$<6.7\times10^{-12}$	—
^{106}Ru	1.020	2.37×10^{-6}	2	1.05×10^{-6}	2.6	8.34×10^{-7}	2.8	3.73×10^{-6}	2.5	7.25×10^{-6}	3.2	1.03×10^{-6}	26.4
^{125}Sb	2.760	3.89×10^{-8}	2.2	1.58×10^{-8}	3	1.14×10^{-8}	1.3	6.07×10^{-8}	1.5	2.07×10^{-7}	2.6	5.00×10^{-6}	1.2
^{134}Cs	2.065	1.19×10^{-9}	20.5	4.37×10^{-10}	3.9	3.47×10^{-10}	14.5	1.87×10^{-9}	9.7	7.02×10^{-9}	9.3	1.28×10^{-8}	3.6
^{137}Cs	30.170	2.68×10^{-7}	0.8	7.57×10^{-8}	0.9	5.11×10^{-8}	0.8	3.72×10^{-7}	0.8	1.04×10^{-6}	1.1	1.76×10^{-6}	0.8
^{144}Ce	284	3.37×10^{-9}	6.4	8.86×10^{-10}	10.6	6.57×10^{-10}	11	5.20×10^{-9}	7.1	7.08×10^{-9}	9.2	ND[b]	—
^{152}Eu	13.400	2.67×10^{-9}	1.7	6.73×10^{-10}	2.5	4.98×10^{-10}	2	3.54×10^{-9}	1.2	5.67×10^{-9}	2.8	$<3.2\times10^{-11}$	—
^{154}Eu	8.500	4.69×10^{-9}	1.2	1.19×10^{-9}	2.2	8.77×10^{-10}	1.4	6.18×10^{-9}	1.2	9.64×10^{-9}	2	$<7.2\times10^{-11}$	—
^{155}Eu	4.730	1.28×10^{-8}	1.7	3.34×10^{-9}	2.9	2.42×10^{-9}	2.9	2.00×10^{-8}	2.2	2.24×10^{-8}	5.4	$<1.5\times10^{-10}$	—

[a] t_0 = detonation time (day 45, 1976). Values are in μCi/mL $\pm$ 1 SD (%) at t_0. Date collected: 9/8/83; sample volume: 188 L; pumped volume: 56,790 gal; location: cavity. Detection limits are calculated at count time. Evaporation after filtration through 0.006-μm UF. Filtered 364 days after collection. Sample recycled through entire filter series during ultrafiltration.

[b] Not detected. No limit calculated for this nuclide.

Table A-2. Cheshire (U20n) sample B-2 nuclide analyses.[a]

Fraction ID		Prefilter		0.45-μm filter		Ashed composite filters		Filtrate (salt[b]) <0.20 μm	
Isotope	$t_{1/2}$ (yr)	Value	%SD	Value	%SD	filters	%SD	Value	%SD
^{3}H	12.33	—	—	—	—	—	—	0.614	1.0
^{22}Na	2.605	4.71×10^{-10}	37.8	3.04×10^{-10}	36.2	2.29×10^{-10}	75.9	9.01×10^{-9}	8.7
^{40}K	1.3×10^{9}	1.41×10^{-9}	11.6	ND[c]	—	1.22×10^{-9}	6.1	3.83×10^{-9}	6.8
^{54}Mn	0.855	3.01×10^{-8}	21.1	1.09×10^{-8}	31.4	2.89×10^{-8}	46.4	7.93×10^{-8}	32.1
^{60}Co	5.272	1.52×10^{-9}	2.1	4.96×10^{-10}	4.3	1.93×10^{-9}	0.9	4.05×10^{-9}	1.3
^{106}Ru	1.020	2.31×10^{-6}	2.6	4.35×10^{-7}	4.9	2.46×10^{-6}	4.8	1.21×10^{-5}	1.7
^{125}Sb	2.760	3.65×10^{-8}	3	7.65×10^{-9}	3.4	4.47×10^{-8}	1.7	6.23×10^{-6}	0.8
^{134}Cs	2.065	4.66×10^{-9}	3.9	2.20×10^{-10}	41.4	4.32×10^{-9}	4.4	2.19×10^{-8}	5.2
^{137}Cs	30.170	6.76×10^{-7}	0.9	4.38×10^{-8}	0.7	6.74×10^{-7}	1.1	2.68×10^{-6}	0.7
^{144}Ce	284	2.65×10^{-9}	10.6	4.69×10^{-10}	11	3.79×10^{-9}	25.6	1.18×10^{-8}	6.1
^{152}Eu	13.400	2.05×10^{-9}	2.5	3.14×10^{-10}	11.3	2.38×10^{-9}	1.3	9.64×10^{-9}	2.1
^{154}Eu	8.500	2.75×10^{-9}	2.2	4.58×10^{-10}	9.5	4.22×10^{-9}	1.1	1.58×10^{-3}	2.1
^{155}Eu	4.730	9.87×10^{-9}	2.9	1.75×10^{-9}	2	1.24×10^{-9}	1.4	4.94×10^{-8}	2.5

[a] t_0 = detonation time (day 45, 1976). Values are in μCi/mL $\pm$ 1 SD (%) at t_0. Date collected: 9/9/83; sample volume: 200 L; pumped volume: 131,860 gal; location: cavity. Detection limits are calculated at count time. Filtered 87 days after collection.

[b] Evaporation after filtration through 0.45-μm filter.

[c] Not detected. No limit calculated for this nuclide.

Table A-3. Cheshire (U20n) sample B-3 nuclide analyses.[a]

Fraction ID		Prefilter		0.45-μm filter		0.20-μm filter		Ashed composite filters		(salt) <0.20 μm	
Isotope	$t_{1/2}$ (yr)	Value	%SD	Value	%SD	Value	%SD	filters	%SD	Value	%SD
^{3}H	12.33	—	—	—	—	—	—	—	—	0.504	1.0
^{22}Na	2.605	1.55×10^{-10}	37.3	$<6.0 \times 10^{-12}$	—	$<1.1 \times 10^{-12}$	—	2.32×10^{-10}	31.6	7.87×10^{-9}	16
^{40}K	1.3×10^{9}	$<4.9 \times 10^{-11}$	—	$<2.2 \times 10^{-10}$	—	$<6.1 \times 10^{-11}$	—	1.19×10^{-10}	20.6	3.46×10^{-9}	6.6
^{54}Mn	0.855	$<7.6 \times 10^{-12}$	—	$<4.6 \times 10^{-12}$	—	$<2.2 \times 10^{-12}$	—	1.23×10^{-8}	64.3	8.40×10^{-8}	72.3
^{60}Co	5.272	2.33×10^{-10}	3.8	1.20×10^{-10}	17.3	1.05×10^{-10}	16.9	3.75×10^{-10}	1.5	2.96×10^{-9}	4.89
^{106}Ru	1.020	3.37×10^{-7}	6.8	3.32×10^{-7}	10	2.80×10^{-7}	7.9	7.45×10^{-7}	3.4	1.05×10^{-5}	1.58
^{125}Sb	2.760	7.40×10^{-9}	2.2	1.05×10^{-8}	2.3	8.40×10^{-9}	2.1	2.14×10^{-8}	1.6	6.74×10^{-6}	3.58
^{134}Cs	2.065	2.29×10^{-10}	20.1	ND[b]	—	ND	—	4.27×10^{-10}	19.2	2.68×10^{-8}	37.6
^{137}Cs	30.170	3.99×10^{-8}	0.8	3.18×10^{-8}	0.9	3.54×10^{-8}	1	9.47×10^{-8}	0.8	4.49×10^{-6}	3.92
^{144}Ce	284	5.12×10^{-10}	17.5	$<4.5 \times 10^{-11}$	—	$<2.9 \times 10^{-11}$	—	8.49×10^{-10}	12.5	9.54×10^{-9}	15.2
^{152}Eu	13.400	3.55×10^{-10}	4.3	1.81×10^{-10}	10.3	2.02×10^{-10}	4.8	6.01×10^{-10}	2.4	6.78×10^{-9}	3.22
^{154}Eu	8.500	5.79×10^{-10}	3.4	3.28×10^{-10}	6.2	3.37×10^{-10}	2.9	1.10×10^{-9}	1.8	1.19×10^{-8}	3.1
^{155}Eu	4.730	1.68×10^{-9}	3.7	8.59×10^{-10}	7.9	9.08×10^{-10}	4.3	3.63×10^{-9}	2.3	3.53×10^{-8}	6.3

[a] t_0 = detonation time (day 45, 1976). Values are in μCi/mL $\pm$ 1 SD (%) at t_0. Date collected: 10/23/84; sample volume: 166 L; pumped volume: 3.0×10^{6} gal; location: cavity. Detection limits are calculated at count time. Evaporation after filtration through 0.20-μm filter. Filtered 134 days after collection.

[b] Not detected. No limit calculated for this nuclide.

Table A-4. Cheshire (U20n) sample B-4 nuclide analyses.[a]

Fraction ID		Prefilter[b]		0.45-μm filter		0.20-μm filter		0.05-μm filter	
Isotope	$t_{1/2}$ (yr)	(Sum)	%SD	Value	%SD	(Sum)	%SD	Value	%SD
^{3}H	12.33	—	—	—	—	—	—	—	—
^{22}Na	2.605	$<1.3 \times 10^{-10}$	—	$<9.3 \times 10^{-12}$	—	1.88×10^{-10}	54.4	1.11×10^{-10}	87.5
^{40}K	1.3×10^{9}	8.23×10^{-10}	16.1	1.61×10^{-10}	27.4	3.26×10^{-10}	24	1.37×10^{-9}	4.5
^{54}Mn	0.855	2.48×10^{-8}	45.8	8.26×10^{-9}	44.9	$<2.7 \times 10^{-12}$	—	$<2.3 \times 10^{-12}$	—
^{60}Co	5.272	1.15×10^{-9}	1.8	4.01×10^{-10}	7.7	4.82×10^{-10}	2.1	3.82×10^{-10}	6.4
^{106}Ru	1.020	3.39×10^{-6}	2.8	1.36×10^{-6}	7.7	1.66×10^{-6}	3.5	7.32×10^{-7}	8
^{125}Sb	2.760	4.70×10^{-8}	2.1	3.33×10^{-8}	2.3	2.62×10^{-8}	2.1	2.41×10^{-8}	2.8
^{134}Cs	2.065	2.97×10^{-9}	7.3	1.00×10^{-9}	16.8	1.29×10^{-9}	9.8	1.79×10^{-9}	21
^{137}Cs	30.170	5.11×10^{-7}	1.1	1.78×10^{-7}	1.1	2.40×10^{-7}	0.8	3.00×10^{-7}	1
^{144}Ce	284	3.46×10^{-9}	12.4	1.26×10^{-9}	34.2	1.34×10^{-9}	13.5	6.75×10^{-10}	4.2
^{152}Eu	13.400	2.42×10^{-9}	1.8	8.59×10^{-10}	4.2	1.09×10^{-9}	2	9.12×10^{-10}	3.5
^{154}Eu	8.500	4.24×10^{-9}	1.2	1.51×10^{-9}	2.6	1.88×10^{-9}	1.6	1.48×10^{-9}	5
^{155}Eu	4.730	1.19×10^{-8}	1.7	4.08×10^{-9}	4.3	5.11×10^{-9}	2.1	3.75×10^{-9}	3.8

[a] t_0 = detonation time (day 45, 1976). Values are in μCi/mL $\pm$ 1 SD (%) at t_0. Date collected: 10/23/84; sample volume: 194.5 L; pumped volume: 3.0×10^{6} gal; location: cavity. Evaporation after filtration to 0.003 μm. Filtered 193 days after collecion. Detection limits are calculated at count time.

[b] Possible prefilter bag split.

Table A-4. (Continued)

Fraction ID		Ashed composite filters		Retentate >0.003 μm		Recount retentate >0.003 μm		Filtrate (salt[a]) <0.003 μm	
Isotope	$t_{1/2}$ (yr)	Value	%SD	Value	%SD	Value	%SD	Value	%SD
^{3}H	12.33	—	—	—	—	—	—	0.504	1.0
^{22}Na	2.605	6.95×10^{-10}	38.2	3.18×10^{-10}	69	—	—	7.91×10^{-9}	3.3
^{40}K	1.3×10^{9}	2.12×10^{-9}	3.6	3.50×10^{-10}	24.2	5.17×10^{-10}	8.0	1.12×10^{-9}	8.1
^{54}Mn	0.855	3.33×10^{-8}	67.2	ND[b]	—	—	—	$<2.0 \times 10^{-11}$	—
^{60}Co	5.272	1.94×10^{-9}	0.9	6.37×10^{-10}	6.3	6.95×10^{-10}	3	6.40×10^{-11}	30
^{106}Ru	1.020	5.71×10^{-6}	2.9	1.87×10^{-6}	7.6	2.34×10^{-6}	7.8	1.52×10^{-6}	24.4
^{125}Sb	2.760	1.06×10^{-7}	1.2	1.03×10^{-7}	1.1	1.21×10^{-7}	1	7.07×10^{-6}	0.4
^{134}Cs	2.065	5.40×10^{-9}	4.5	1.53×10^{-9}	14.6	2.06×10^{-9}	13.4	1.81×10^{-8}	5
^{137}Cs	30.170	1.02×10^{-6}	0.7	3.28×10^{-7}	0.8	3.78×10^{-7}	0.7	2.83×10^{-6}	0.7
^{144}Ce	284	5.57×10^{-9}	8.5	2.82×10^{-9}	19.7	—	—	$<5.1 \times 10^{-10}$	—
^{152}Eu	13.400	4.16×10^{-9}	1.2	1.41×10^{-9}	3.4	1.68×10^{-9}	1.8	5.52×10^{-11}	60.1
^{154}Eu	8.500	7.22×10^{-9}	1	2.54×10^{-9}	3.1	3.02×10^{-9}	1.3	$<7.6 \times 10^{-11}$	—
^{155}Eu	4.730	1.93×10^{-8}	1.9	9.67×10^{-9}	2.8	9.21×10^{-9}	3.8	$<2.9 \times 10^{-10}$	—

[a] Evaporation after ultrafiltration to 0.003 μm.

[b] Not detected. No limit calculated for this nuclide.

Table A-5. Cheshire (U20n) sample B-5 nuclide analyses.[a]

Fraction ID		Prefilter[b]		0.45-μm filter		0.20-μm filter		0.05-μm filter	
Isotope	$t_{1/2}$ (yr)	(Sum)	%SD	Value	%SD	(Sum)	%SD	Value	%SD
^{3}H	12.26	—	—	—	—	—	—	—	—
^{22}Na	2.605	$<2.1 \times 10^{-12}$	—	$<2.0 \times 10^{-12}$	—	6.13×10^{-11}	84.8	$<2.4 \times 10^{-11}$	—
^{40}K	1.3×10^{9}	1.34×10^{-10}	23.6	$<3.4 \times 10^{-11}$	—	$<3.3 \times 10^{-11}$	—	3.48×10^{-10}	16.2
^{54}Mn	0.855	$<1.4 \times 10^{-12}$	—	$<1.2 \times 10^{-12}$	—	$<1.5 \times 10^{-12}$	—	$<1.7 \times 10^{-12}$	—
^{60}Co	5.272	4.66×10^{-11}	12	$<1.5 \times 10^{-12}$	—	1.03×10^{-11}	8.8	3.11×10^{-11}	23.8
^{106}Ru	1.020	4.37×10^{-7}	1.2	1.72×10^{-7}	20	1.29×10^{-7}	9.3	7.69×10^{-7}	4.5
^{125}Sb	2.760	9.67×10^{-9}	5.5	6.40×10^{-9}	1.4	5.44×10^{-9}	2.7	1.52×10^{-8}	1.6
^{134}Cs	2.065	ND[c]	—	ND	—	ND	—	ND	—
^{137}Cs	30.170	1.36×10^{-8}	0.8	3.95×10^{-9}	0.9	5.56×10^{-9}	0.8	3.68×10^{-8}	0.7
^{144}Ce	284	$<1.4 \times 10^{-11}$	—	$<8.3 \times 10^{-12}$	—	$<9.8 \times 10^{-12}$	—	$<2.2 \times 10^{-11}$	—
^{152}Eu	13.400	3.89×10^{-11}	30.7	$<6.6 \times 10^{-12}$	—	$<7.6 \times 10^{-12}$	—	7.55×10^{-11}	18.3
^{154}Eu	8.500	7.33×10^{-11}	19.2	$<2.5 \times 10^{-12}$	—	$<3.4 \times 10^{-12}$	—	1.39×10^{-10}	1.2
^{155}Eu	4.730	1.52×10^{-10}	18.2	3.00×10^{-11}	43.2	5.81×10^{-11}	0.8	3.36×10^{-10}	10.2

[a] t_0 = detonation time (day 45, 1976). Values are in μCi/mL $\pm$ 1 SD (%) at t_0. Date collected: 5/28/85; sample volume: 184 L; pumped volume: 3.7×10^{6} gal; location: outside cavity. Detection limits are calculated at count time. Filtered 85 days after collection.

[b] Possible prefilter bag split.

[c] Not detected. No limit calculated for this nuclide.

Table A-5. (Continued)

Fraction ID		Ashed composite filters		Ashed composite filters		Retentate >0.003 μm		Filtrate (salt[d]) <0.003 μm	
Isotope	$t_{1/2}$ (yr)	Value	%SD	Recount	%SD	Value	%SD	Value	%SD
^{3}H	12.33	—	—	—	—	—	—	0.433	1.0
^{22}Na	2.605	5.96×10^{-11}	54.6	—	—	$<1.7 \times 10^{-11}$	—	1.01×10^{-9}	5.8
^{40}K	1.3×10^{9}	5.61×10^{-10}	5.0	5.21×10^{-10}	5	2.45×10^{-10}	9.4	2.21×10^{-9}	2
^{54}Mn	0.855	7.00×10^{-9}	71.2	—	—	$<7.3 \times 10^{-13}$	—	$<2.0 \times 10^{-12}$	—
^{60}Co	5.272	8.68×10^{-11}	4.4	7.21×10^{-11}	5.1	1.78×10^{-11}	16	$<1.2 \times 10^{-12}$	—
^{106}Ru	1.020	1.37×10^{-6}	2.2	1.34×10^{-6}	3.9	5.13×10^{-7}	4.4	6.52×10^{-7}	17.2
^{125}Sb	2.760	3.61×10^{-8}	0.7	3.60×10^{-8}	0.7	2.37×10^{-8}	0.6	3.87×10^{-6}	0.6
^{134}Cs	2.065	5.75×10^{-11}	76.6	6.18×10^{-11}	9.4	4.51×10^{-11}	61	1.86×10^{-9}	7.7
^{137}Cs	30.170	5.84×10^{-8}	0.8	5.67×10^{-8}	1.1	2.63×10^{-8}	0.7	6.57×10^{-7}	0.7
^{144}Ce	284	3.35×10^{-10}	30.9	—	—	$<1.2 \times 10^{-11}$	—	$<7.5 \times 10^{-11}$	—
^{152}Eu	13.400	1.23×10^{-10}	4.8	1.16×10^{-10}	5.4	5.03×10^{-11}	7.4	$<5.6 \times 10^{-12}$	—
^{154}Eu	8.500	2.06×10^{-10}	4.9	2.24×10^{-10}	2.7	8.63×10^{-11}	4.5	$<1.0 \times 10^{-11}$	—
^{155}Eu	4.730	7.50×10^{-10}	4.9	7.99×10^{-10}	5.2	3.04×10^{-10}	8.2	$<2.7 \times 10^{-11}$	—

[d] Evaporation after ultrafiltration to 0.003 μm.

Table A-6. Cheshire (U20n) sample B-6 nuclide analyses.[a]

Fraction ID		Prefilter[b]		0.45-μm filter		0.20-μm filter		0.05-μm filter	
Isotope	$t_{1/2}$ (yr)	(Sum)	%SD	Value	%SD	(Sum)	%SD	Value	%SD
^{3}H	12.33	—	—	—	—	—	—	—	—
^{22}Na	2.605	3.36×10^{-10}	18.0	$<1.5 \times 10^{-12}$	—	1.32×10^{-10}	72.2	$<1.1 \times 10^{-12}$	—
^{40}K	1.3×10^{9}	1.01×10^{-10}	31.3	$<4.0 \times 10^{-11}$	—	$<2.6 \times 10^{-11}$	—	2.61×10^{-10}	11.1
^{54}Mn	0.855	$<1.4 \times 10^{-12}$	—	$<1.3 \times 10^{-12}$	—	$<1.4 \times 10^{-11}$	—	$<6.8 \times 10^{-13}$	—
^{60}Co	5.272	5.26×10^{-11}	11.5	$<1.5 \times 10^{-12}$	—	$<1.4 \times 10^{-12}$	—	$<1.4 \times 10^{-12}$	—
^{106}Ru	1.020	5.23×10^{-7}	4.6	1.50×10^{-7}	10.9	7.04×10^{-8}	19.1	3.89×10^{-7}	4.6
^{125}Sb	2.760	1.06×10^{-8}	1.4	4.08×10^{-9}	1.8	3.74×10^{-9}	2.9	9.26×10^{-9}	1.2
^{134}Cs	2.065	ND[c]	—	ND	—	ND	—	ND	—
^{137}Cs	30.170	1.56×10^{-8}	1.6	3.86×10^{-9}	1.0	2.82×10^{-9}	0.8	2.42×10^{-8}	0.8
^{144}Ce	284	$<1.3 \times 10^{-11}$	—	$<8.9 \times 10^{-12}$	—	$<7.2 \times 10^{-12}$	—	$<1.3 \times 10^{-11}$	—
^{152}Eu	13.400	3.63×10^{-11}	16.4	$<5.6 \times 10^{-12}$	—	$<5.2 \times 10^{-12}$	—	4.42×10^{-11}	9.4
^{154}Eu	8.500	8.69×10^{-11}	16.4	2.30×10^{-11}	25.1	$<2.0 \times 10^{-12}$	—	6.56×10^{-11}	7.4
^{155}Eu	4.730	1.92×10^{-10}	13.2	$<5.0 \times 10^{-12}$	—	$<3.2 \times 10^{-12}$	—	2.81×10^{-10}	6.5

[a] t_0 = detonation time (day 45, 1976). Values are in μCi/mL $\pm$ 1 SD (%) at t_0. Date collected: 5/28/85; sample volume: 200 L; pumped volume: 3.7×10^{6} gal; location: outside cavity. Detection limits are calculated at count time. Filtered 181 days after collection.

[b] Possible prefilter bag split.

[c] Not detected. No limit calculated for this nuclide.

Table A-6. (Continued)

Fraction ID		Ashed composite filters		Ashed composite filters		Retentate >0.003 μm		Filtrate (salt[d]) <0.003 μm	
Isotope	$t_{1/2}$ (yr)	Value	%SD	Recount	%SD	Value	%SD	Value	%SD
^{3}H	12.33	—	—	—	—	—	—	0.433	1.0
^{22}Na	2.605	$<7.1 \times 10^{-11}$	—	$<7.1 \times 10^{-11}$	—	$<9.0 \times 10^{-13}$	—	1.02×10^{-9}	4.7
^{40}K	1.3×10^{9}	4.30×10^{-10}	7.9	3.94×10^{-10}	4.8	5.61×10^{-11}	15.4	2.37×10^{-9}	2.2
^{54}Mn	0.855	$<9.0 \times 10^{-13}$	—	—	—	$<4.5 \times 10^{-13}$	—	$<2.2 \times 10^{-12}$	—
^{60}Co	5.272	7.86×10^{-11}	5.2	8.10×10^{-11}	4.9	$<6.8 \times 10^{-13}$	—	$<1.3 \times 10^{-12}$	—
^{106}Ru	1.020	1.30×10^{-6}	3.9	1.26×10^{-6}	5.3	9.56×10^{-8}	11.4	5.66×10^{-7}	24.3
^{125}Sb	2.760	3.24×10^{-8}	0.9	2.96×10^{-8}	0.8	6.88×10^{-9}	1.2	3.95×10^{-6}	0.5
^{134}Cs	2.065	ND	—	—	—	ND	—	3.52×10^{-10}	25.7
^{137}Cs	30.170	5.36×10^{-8}	1	4.94×10^{-8}	0.7	5.45×10^{-9}	0.7	4.94×10^{-7}	0.7
^{144}Ce	284	$<1.6 \times 10^{-11}$	—	—	—	$<4.3 \times 10^{-12}$	—	$<9.4 \times 10^{-11}$	—
^{152}Eu	13.400	1.00×10^{-10}	8.1	9.03×10^{-11}	5	9.30×10^{-12}	26.3	$<1.3 \times 10^{-11}$	—
^{154}Eu	8.500	1.99×10^{-10}	3.8	1.75×10^{-10}	3.1	1.63×10^{-11}	11.9	$<1.0 \times 10^{-11}$	—
^{155}Eu	4.730	6.86×10^{-10}	7.3	5.20×10^{-10}	5	5.05×10^{-11}	20.3	$<4.8 \times 10^{-11}$	—

[d] Evaporation after ultrafiltration to 0.003 μm.

Appendix B. Soil Moisture Data and Environmental Tritium and Deuterium Analyses, Cambric Area

Key to Abbreviations used in Appendix B Tables

AMS: Air-moisture sample. Surface-air moisture was collected using silica-gel traps; one sampling was within the ditch vegetation and one was 92 ft south (upwind) of the ditch. Both were in the vicinity of Flume 1; both had air intakes about 3 ft above the surface. The first of the two numbers for each location represents a daytime sample; the second, a nighttime sample. Silica-gel samples were freeze dried at LLNL, with tritium analysis done at LLNL and deuterium analysis done at the University of Nevada, Las Vegas, Nevada. See Fig. 3A-1.

CCW: Cambric canal water. Grab samples were collected at several locations along the ditch during the course of the study.

CPW: Cambric pond water. Two surface-water sample surveys were conducted to identify temporal and spatial variation of tritium within the discharge pond and between the ditch and pond. The numerical suffixes in the W-series samples correspond to the locations mapped in Fig. 3A-1; other location designators are defined below.

EEOL: East end of lake. Several grab samples were collected along the eastern edge of the pond (lake) prior to the pond-sampling surveys.

F: Flume. Three calibrated Parshal flumes were installed in the ditch in order to estimate flow rates, percolations, and evaporative rates. Ditch-water grab samples were collected at each of these three locations over time. See Fig. 3A-1.

FDPW: Freeze-dried plant water. Plant material was sampled and freed dried, and the extracted water was analyzed for tritium and deuterium. For the samples collected on 83271, the numbers after the "/" in the code column are the DRI TPS (see Table B3 for numbers that are field-collection replicates of the LLNL sample). For the samples collected on 84220, SC = salt cedar and CT = cattail; numbers after the CT designator indicate the height in feet above the water surface from which the reed sample was collected.

FDSW: Freeze-dried soil water. Soil-core water samples were extracted by freeze drying for tritium analysis. Location codes: for codes of the form 5-10, the first number is the distance in feet from the edge of the ditch berm; the second number is the depth in feet of the sample below ground surface. All were taken in or near the instrumented plot. The FF sample series was submitted by DRI. All samples of the form L-100-15 were from the L-100 installation borehole (see Fig. 3A-1 and 3A-5), with the final number indicating depth.

Isotopic concentration units:

Deuterium:
%SMOW = [D/H(sample)]/[D/H(std)] × 100
D(‰SMOW) = {1 – [D/H(sample)]/[D/H(std)]} × 1000

Tritium:
1 dpm/mL = 4.50×10^{-1} pCi/mL
= 4.50×10^{-7} μCi/mL = 1.4×10^{-2} T.U.
1 p/Ci/mL = 10^{-6} μCi/mL
= 2.22 dpm/mL = 3.10×10^{2} T.U.
1 T.U. (tritium unit) = 1 atom of ^{3}H per 10^{18} H atoms
= 3.23×10^{-3} pCi/mL
= 7.17×10^{-3} dpm/mL

Decay-correction date is 7 Sept. 1983 (83250).

L: Lysimeter samples. Several types of suction lysimeters, installed at various depths, were sampled and the water was analyzed for tritium. A6, C12, D6, E12, F5, G11, and L-100 are fully buried units with access lines to the surface. L-1 and L-2 are partially buried units that allow full inspection of the lysimeter interior.

ND–Not determined—Within the extensive number of samples collected and analyzed, several could not be finalized due to field or laboratory complications.

LANL CCW: LANL analyses of CCW excerpted from their progress reports for comparison purposes. See subsequent LANL reports for additional data.

NP: Neutron probe.

OUT: Outflow. Ditch-water samples were collected near the outflow pipe for RNM-2s.

RC: Resistance cell. Readings normally were the average of a pair of cells at the same location.

RW: Rainwater. Rainwater was collected in a rain gauge located on the instrumented plot.

SAW: Soil-atmosphere water. Soil-atmosphere (gas) moisture was collected at the instrumented plot using a low-flow, gas-extraction system and silica-gel traps. The extraction systems were installed in place of lysimeters L-3 and L-4 (see Fig. 3A-2) after the lysimeters consistently failed to produce moisture samples.

SEOL: Southeastern side of the lake. Pond grab samples were collected prior to the systematic survey of the pond. See Fig. 3A-1.

SOL: Southern side of the lake. Pond grab samples were collected prior to the survey of the pond. See Fig. 3A-1.

T: Tensiometer.

TPS: Toluene plant samples. Plant samples were collected on 83271 and analyzed for tritium using a toluene water-extraction technique. Samples were processed by DRI and analyzed by LLNL; location numbers tabulated are described above. Replicate field samples processed by LLNL are indicated in the FDPW table.

%VM: Percent of water by volume of soil (approximate).

Table B1: Soil moisture data, Cambric area.

(a) Type: RC

Julian date	Sample#[a]	Reading (Ω)	Julian date	Sample#[a]	Reading (Ω)
83192	13,14-5-11	7750	84072	13,14-5-11	6950
83200	13,14-5-11	6900	84079	13,14-5-11	7100
83206	13,14-5-11	6700	84086	13,14-5-11	7200
83213	13,14-5-11	6700	84093	13,14-5-11	7200
83220	13,14-5-11	6250	84100	13,14-5-11	7250
83227	13,14-5-11	6050	84107	13,14-5-11	7100
83241	13,14-5-11	6000	84052	13,14-5-11	6950
83250	13,14-5-11	6000	84114	13,14-5-11	7350
83255	13,14-5-11	6000	84121	13,14-5-11	7800
83262	13,14-5-11	6100	84128	13,14-5-11	7650
83271	13,14-5-11	6100	84135	13,14-5-11	7300
83283	13,14-5-11	6150	84142	13,14-5-11	7500
83297	13,14-5-11	6150	84151	13,14-5-11	7300
83305	13,14-5-11	6400	84156	13,14-5-11	7250
83311	13,14-5-11	5900	84163	13,14-5-11	7250
83318	13,14-5-11	6100	84170	13,14-5-11	7350
83325	13,14-5-11	5850	84177	13,14-5-11	7250
83332	13,14-5-11	6150	84184	13,14-5-11	7100
83339	13,14-5-11	6250	84191	13,14-5-11	7250
83346	13,14-5-11	6250	84198	13,14-5-11	7400
83353	13,14-5-11	6250	84205	13,14-5-11	7400
83361	13,14-5-11	6200	84212	13,14-5-11	7800
84003	13,14-5-11	6350	84219	13,14-5-11	7400
84009	13,14-5-11	6350	84226	13,14-5-11	6350
84016	13,14-5-11	6350	84241	13,14-5-11	7000
84030	13,14-5-11	6700	84248	13,14-5-11	6600
84037	13,14-5-11	6500	84254	13,14-5-11	6350
84044	13,14-5-11	7000	84261	13,14-5-11	6800
84052	13,14-5-11	6950	84268	13,14-5-11	6800
84058	13,14-5-11	7150	84275	13,14-5-11	7000
84065	13,14-5-11	7150	84282	13,14-5-11	9900

[a] Final two numbers of the Sample # identify the location and depth of the instrument. See Sec. 3 and references cited therein for details of locations and descriptions.

Table B1, Type: RC, continued.

Julian date	Sample#[a]	Reading (Ω)
84290	13,14-5-11	6500
84296	13,14-5-11	6500
84303	13,14-5-11	6575
84310	13,14-5-11	6500
84318	13,14-5-11	6500
84324	13,14-5-11	6500
84331	13,14-5-11	6600
84338	13,14-5-11	6500
84345	13,14-5-11	6500
84352	13,14-5-11	6500
84361	13,14-5-11	6500
85002	13,14-5-11	7200
85009	13,14-5-11	6700
85014	13,14-5-11	6850
85021	13,14-5-11	6800
85029	13,14-5-11	6950
85035	13,14-5-11	7250
85042	13,14-5-11	7500
85056	13,14-5-11	7500
85062	13,14-5-11	7500
85070	13,14-5-11	7800
85077	13,14-5-11	7600
85084	13,14-5-11	8200
85091	13,14-5-11	8250
85098	13,14-5-11	8150
85112	13,14-5-11	8050
85119	13,14-5-11	8050
85126	13,14-5-11	7750
85133	13,14-5-11	7750
85140	13,14-5-11	7900
85148	13,14-5-11	8100
85154	13,14-5-11	8550
85161	13,14-5-11	8450
85168	13,14-5-11	8500
85182	13,14-5-11	7950
85189	13,14-5-11	8000
85196	13,14-5-11	7000
85217	13,14-5-11	6250
85224	13,14-5-11	6150
85231	13,14-5-11	6400
85238	13,14-5-11	6100
85246	13,14-5-11	5550
85252	13,14-5-11	5250
85259	13,14-5-11	5650
85266	13,14-5-11	5450
85273	13,14-5-11	5200
85287	13,14-5-11	5300
85294	13,14-5-11	5400
85301	13,14-5-11	4900
85308	13,14-5-11	5200
85316	13,14-5-11	5000
85322	13,14-5-11	5550
85329	13,14-5-11	5000
85343	13,14-5-11	4900
85350	13,14-5-11	3300
85357	13,14-5-11	5450
85364	13,14-5-11	4850
86006	13,14-5-11	5550
86013	13,14-5-11	5700
86027	13,14-5-11	5950
86034	13,14-5-11	5750
86041	13,14-5-11	5300
86049	13,14-5-11	5900
86055	13,14-5-11	6400
86062	13,14-5-11	6250
86069	13,14-5-11	6250
86076	13,14-5-11	5050
86083	13,14-5-11	6500
86090	13,14-5-11	6500
86097	13,14-5-11	7050
86104	13,14-5-11	6800
86111	13,14-5-11	6800
86118	13,14-5-11	6850
83192	22-5-5	7750
83200	22-5-5	6800
83206	22-5-5	6000
83213	22-5-5	6000
83220	22-5-5	6000

Table B1, Type: RC, continued.

Julian date	Sample#[a]	Reading (Ω)
83227	22-5-5	5500
83241	22-5-5	3500
83250	22-5-5	3300
83255	22-5-5	3300
83262	22-5-5	3200
83271	22-5-5	3300
83283	22-5-5	3400
83297	22-5-5	3400
83305	22-5-5	3200
83311	22-5-5	3200
83318	22-5-5	3200
83325	22-5-5	3200
83332	22-5-5	3400
83339	22-5-5	3400
83346	22-5-5	3500
83353	22-5-5	3500
83361	22-5-5	3600
84003	22-5-5	3600
84009	22-5-5	3500
84016	22-5-5	3600
84030	22-5-5	3700
84037	22-5-5	3500
84044	22-5-5	3600
84052	22-5-5	3600
84058	22-5-5	3600
84065	22-5-5	3500
84072	22-5-5	3500
84079	22-5-5	3400
84086	22-5-5	3400
84093	22-5-5	3200
84100	22-5-5	3400
84107	22-5-5	3500
84114	22-5-5	3500
84121	22-5-5	3500
84128	22-5-5	3500
84135	22-5-5	3200
84142	22-5-5	3000
84151	22-5-5	3000
84156	22-5-5	2800
84163	22-5-5	2800
84170	22-5-5	2800
84177	22-5-5	2800
84184	22-5-5	2700
84191	22-5-5	2300
84198	22-5-5	2700
84205	22-5-5	2700
84212	22-5-5	2500
84219	22-5-5	2500
84226	22-5-5	2400
84241	22-5-5	2100
84248	22-5-5	2100
84254	22-5-5	2200
84261	22-5-5	2200
84268	22-5-5	2200
84275	22-5-5	2300
84282	22-5-5	2500
84290	22-5-5	2400
84296	22-5-5	3600
84303	22-5-5	2700
84310	22-5-5	2800
84318	22-5-5	2800
84324	22-5-5	2800
84331	22-5-5	3000
84338	22-5-5	3000
84345	22-5-5	3000
84352	22-5-5	3000
84361	22-5-5	3000
85002	22-5-5	3000
85009	22-5-5	3000
85014	22-5-5	3000
85021	22-5-5	3000
85029	22-5-5	3100
85035	22-5-5	3200
85042	22-5-5	3200
85056	22-5-5	3200
85062	22-5-5	3000
85070	22-5-5	3100
85077	22-5-5	3000

Table B1, Type: RC, continued.

Julian date	Sample#[a]	Reading (Ω)	Julian date	Sample#[a]	Reading (Ω)
85084	22-5-5	3100	86041	22-5-5	4200
85091	22-5-5	3000	86049	22-5-5	4500
85098	22-5-5	3100	86055	22-5-5	4500
85112	22-5-5	2900	86062	22-5-5	4200
85119	22-5-5	2900	86069	22-5-5	4000
85126	22-5-5	2800	86076	22-5-5	4000
85133	22-5-5	2800	86083	22-5-5	3800
85140	22-5-5	3000	86090	22-5-5	3600
85148	22-5-5	3400	86097	22-5-5	3500
85154	22-5-5	3100	86104	22-5-5	3500
85161	22-5-5	3400	86111	22-5-5	3500
85168	22-5-5	3500	86118	22-5-5	3400
85182	22-5-5	3300	83192	15,16-11-11	20400
85189	22-5-5	3500	83200	15,16-11-11	11650
85196	22-5-5	3600	83206	15,16-11-11	10400
85217	22-5-5	6900	83213	15,16-11-11	6550
85224	22-5-5	10000	83220	15,16-11-11	6250
85231	22-5-5	20000	83227	15,16-11-11	4800
85238	22-5-5	15000	83241	15,16-11-11	3950
85246	22-5-5	79000	83250	15,16-11-11	3750
85252	22-5-5	5800	83255	15,16-11-11	3700
85259	22-5-5	5500	83262	15,16-11-11	3450
85266	22-5-5	4700	83271	15,16-11-11	3150
85273	22-5-5	4400	83283	15,16-11-11	3100
85287	22-5-5	4100	83297	15,16-11-11	3100
85294	22-5-5	3600	83305	15,16-11-11	3050
85301	22-5-5	3900	83311	15,16-11-11	3000
85308	22-5-5	3900	83318	15,16-11-11	3000
85316	22-5-5	3800	83325	15,16-11-11	2900
85322	22-5-5	4300	83332	15,16-11-11	2900
85329	22-5-5	4200	83339	15,16-11-11	2900
85343	22-5-5	4000	83346	15,16-11-11	2900
85350	22-5-5	4200	83353	15,16-11-11	2900
85357	22-5-5	4400	83361	15,16-11-11	2900
85364	22-5-5	4400	84003	15,16-11-11	2900
86006	22-5-5	4400	84009	15,16-11-11	2900
86013	22-5-5	4400	84016	15,16-11-11	2900
86027	22-5-5	4600	84030	15,16-11-11	3150
86034	22-5-5	4500	84037	15,16-11-11	3000

Table B1, Type: RC, continued.

Julian date	Sample#[a]	Reading (Ω)	Julian date	Sample#[a]	Reading (Ω)
84044	15,16-11-11	3050	84324	15,16-11-11	2450
84052	15,16-11-11	3000	84331	15,16-11-11	2600
84058	15,16-11-11	3050	84338	15,16-11-11	2750
84065	15,16-11-11	3100	84345	15,16-11-11	2650
84072	15,16-11-11	2950	84352	15,16-11-11	2650
84079	15,16-11-11	3050	84361	15,16-11-11	2650
84086	15,16-11-11	3100	85002	15,16-11-11	2900
84093	15,16-11-11	3000	85009	15,16-11-11	2700
84100	15,16-11-11	3300	85014	15,16-11-11	2950
84107	15,16-11-11	3000	85021	15,16-11-11	2950
84114	15,16-11-11	3000	85029	15,16-11-11	2950
84121	15,16-11-11	3000	85035	15,16-11-11	3000
84128	15,16-11-11	3000	85042	15,16-11-11	3100
84135	15,16-11-11	3000	85056	15,16-11-11	3150
84142	15,16-11-11	2950	85062	15,16-11-11	3150
84151	15,16-11-11	2950	85070	15,16-11-11	3150
84156	15,16-11-11	2900	85077	15,16-11-11	3100
84163	15,16-11-11	2800	85084	15,16-11-11	3200
84170	15,16-11-11	2850	85091	15,16-11-11	3150
84177	15,16-11-11	2800	85098	15,16-11-11	3150
84184	15,16-11-11	2600	85112	15,16-11-11	3100
84191	15,16-11-11	2750	85119	15,16-11-11	3100
84198	15,16-11-11	2800	85126	15,16-11-11	3050
84205	15,16-11-11	2800	85133	15,16-11-11	3250
84212	15,16-11-11	2700	85140	15,16-11-11	3050
84219	15,16-11-11	2700	85148	15,16-11-11	3100
84226	15,16-11-11	2650	85154	15,16-11-11	3050
84241	15,16-11-11	2500	85161	15,16-11-11	3100
84248	15,16-11-11	2650	85168	15,16-11-11	3100
84254	15,16-11-11	2550	85182	15,16-11-11	3000
84261	15,16-11-11	2650	85189	15,16-11-11	3000
84268	15,16-11-11	2650	85196	15,16-11-11	3000
84275	15,16-11-11	2600	85217	15,16-11-11	2900
84282	15,16-11-11	2650	85224	15,16-11-11	2950
84290	15,16-11-11	2500	85231	15.16-11-11	2900
84296	15,16-11-11	2600	85238	15,16-11-11	2900
84303	15,16-11-11	2500	85246	15,16-11-11	2950
84310	15,16-11-11	2600	85252	15,16-11-11	2750
84318	15,16-11-11	2600	85259	15,16-11-11	3050

Table B1, Type: RC, continued.

Julian date	Sample#[a]	Reading (Ω)	Julian date	Sample#[a]	Reading (Ω)
85266	15,16-11-11	2800	83271	18,19-11-5	67500
85273	15,16-11-11	2850	83283	18,19-11-5	67500
85287	15,16-11-11	2950	83297	18,19-11-5	65000
85294	15,16-11-11	2700	83305	18,19-11-5	62000
85301	15,16-11-11	2850	83311	18,19-11-5	64500
85308	15,16-11-11	2950	83318	18,19-11-5	62000
85316	15,16-11-11	2800	83325	18,19-11-5	62500
85322	15,16-11-11	3150	83332	18,19-11-5	62500
85329	15,16-11-11	2950	83339	18,19-11-5	62500
85343	15,16-11-11	2950	83346	18,19-11-5	62000
85350	15,16-11-11	3100	83353	18,19-11-5	61500
85357	15,16-11-11	3250	83361	18,19-11-5	60500
85364	15,16-11-11	3100	84003	18,19-11-5	62500
86006	15,16-11-11	3150	84009	18,19-11-5	61500
86013	15,16-11-11	3150	84016	18,19-11-5	59750
86027	15,16-11-11	3400	84030	18,19-11-5	63500
86034	15,16-11-11	3350	84037	18,19-11-5	62500
86041	15,16-11-11	3050	84044	18,19-11-5	62500
86049	15,16-11-11	3550	84052	18,19-11-5	63000
86055	15,16-11-11	3650	84058	18,19-11-5	62500
86062	15,16-11-11	3600	84065	18,19-11-5	62500
86069	15,16-11-11	3500	84072	18,19-11-5	61500
86076	15,16-11-11	3600	84079	18,19-11-5	61500
86083	15,16-11-11	3700	84086	18,19-11-5	60000
86090	15,16-11-11	3650	84093	18,19-11-5	59500
86097	15,16-11-11	3550	84100	18,19-11-5	59500
86104	15,16-11-11	3600	84107	18,19-11-5	58500
86111	15,16-11-11	3700	84114	18,19-11-5	55500
86118	15,16-11-11	3550	84121	18,19-11-5	57500
83192	18,19-11-5	112500	84128	18,19-11-5	56500
83200	18,19-11-5	105000	84135	18,19-11-5	52500
83206	18,19-11-5	95000	84142	18,19-11-5	52000
83213	18,19-11-5	90000	84151	18,19-11-5	52500
83220	18,19-11-5	82500	84156	18,19-11-5	51500
83227	18,19-11-5	110000	84163	18,19-11-5	49500
83241	18,19-11-5	74000	84170	18,19-11-5	51500
83250	18,19-11-5	72500	84177	18,19-11-5	53000
83255	18,19-11-5	72500	84184	18,19-11-5	53000
83262	18,19-11-5	67000	84191	18,19-11-5	48000

Table B1, Type: RC, continued.

Julian date	Sample#[a]	Reading (Ω)	Julian date	Sample#[a]	Reading (Ω)
84198	18,19-11-5	50000	85126	18,19-11-5	2700
84205	18,19-11-5	45000	85133	18,19-11-5	2900
84212	18,19-11-5	43000	85140	18,19-11-5	3000
84219	18,19-11-5	42000	85148	18,19-11-5	1150
84226	18,19-11-5	38500	85154	18,18-11-5	3450
84241	18,19-11-5	32500	85161	18,19-11-5	3650
84248	18,19-11-5	30000	85168	18,19-11-5	4850
84254	18,19-11-5	29000	85182	18,19-11-5	13000
84261	18,19-11-5	25000	85189	18,19-11-5	13000
84268	18,19-11-5	25000	85196	18,19-11-5	12900
84275	18,19-11-5	18000	85217	18,19-11-5	33500
84282	18,19-11-5	18000	85224	18,19-11-5	43500
84290	18,19-11-5	14000	85231	18,19-11-5	49500
84296	18,19-11-5	15000	85238	18,19-11-5	55500
84303	18,19-11-5	14000	85246	18,19-11-5	56500
84310	18,19-11-5	14500	85252	18,19-11-5	55000
84318	18,19-11-5	14000	85259	18,19-11-5	60500
84324	18,19-11-5	14000	85273	18,19-11-5	62000
84331	18,19-11-5	14000	85287	18,19-11-5	60000
84338	18,19-11-5	15750	85294	18,19-11-5	38000
84345	18,19-11-5	15750	85301	18,19-11-5	41000
84352	18,19-11-5	16000	85308	18,19-11-5	42000
84361	18,19-11-5	17500	85316	18,19-11-5	41000
85002	18,19-11-5	17500	85322	18,19-11-5	41000
85009	18,19-11-5	5850	85329	18,19-11-5	38000
85014	18,19-11-5	4700	85343	18,19-11-5	59500
85021	18,19-11-5	3650	85350	18,19-11-5	59500
85029	18,19-11-5	3350	85357	18,19-11-5	60000
85035	18,19-11-5	2950	85364	18,19-11-5	56000
85042	18,19-11-5	2800	86006	18,19-11-5	56500
85056	18,19-11-5	2600	86013	18,19-11-5	51500
85062	18,19-11-5	2500	86027	18,19-11-5	54000
85070	18,19-11-5	2500	86034	18,19-11-5	53500
85077	18,19-11-5	2500	86041	18,19-11-5	53500
85084	18,19-11-5	2500	86049	18,19-11-5	49500
85091	18,19-11-5	2400	86055	18,19-11-5	49500
85098	18,19-11-5	2450	86062	18,19-11-5	39250
85112	18,19-11-5	2600	86069	18,19-11-5	46000
85119	18,19-11-5	2700	86076	18,19-11-5	44500

Table B1, Type: RC, continued.

Julian date	Sample#[a]	Reading (Ω)	Julian date	Sample#[a]	Reading (Ω)
86083	18,19-11-5	44500	84086	9,12-11-7	4850
86090	18,19-11-5	44000	84093	9,12-11-7	4900
86097	18,19-11-5	43000	84100	9,12-11-7	4950
86104	18,19-11-5	40000	84107	9,12-11-7	5050
86111	18,19-11-5	41000	84114	9,12-11-7	4900
86118	18,19-11-5	38000	84121	9,12-11-7	5100
83192	9,12-11-7	4500	84128	9,12-11-7	5150
83200	9,12-11-7	4100	84135	9,12-11-7	5150
83206	9,12-11-7	3700	84142	9,12-11-7	4850
83213	9,12-11-7	3550	84151	9,12-11-7	4950
83220	9,12-11-7	3500	84156	9,12-11-7	4800
83227	9,12-11-7	3400	84163	9,12-11-7	4750
83241	9,12-11-7	3300	84170	9,12-11-7	4900
83250	9,12-11-7	3200	84177	9,12-11-7	4750
83255	9,12-11-7	3200	84184	9,12-11-7	4750
83262	9,12-11-7	3150	84191	9,12-11-7	4750
83271	9,12-11-7	3150	84198	9,12-11-7	4750
83283	9,12-11-7	3150	84205	9,12-11-7	4750
83297	9,12-11-7	3450	84212	9,12-11-7	4750
83305	9,12-11-7	3450	84219	9,12-11-7	4850
83311	9,12-11-7	3450	84226	9,12-11-7	4800
83318	9,12-11-7	3600	84241	9,12-11-7	4800
83325	9,12-11-7	3600	84248	9,12-11-7	4850
83332	9,12-11-7	3700	84254	9,12-11-7	4800
83339	9,12-11-7	3800	84261	9,12-11-7	4800
83346	9,12-11-7	3950	84268	9,12-11-7	4800
83353	9,12-11-7	3950	84275	9,12-11-7	4900
83361	9,12-11-7	4200	84282	9,12-11-7	5050
84003	9,12-11-7	4400	84290	9,12-11-7	5250
84009	9,12-11-7	4350	84296	9,12-11-7	5250
84016	9,12-11-7	4400	84303	9,12-11-7	5450
84030	9,12-11-7	4750	84310	9,12-11-7	5650
84037	9,12-11-7	5000	84318	9,12-11-7	5750
84044	9,12-11-7	4800	84324	9,12-11-7	5750
84052	9,12-11-7	4850	84331	9,12-11-7	5750
84058	9,12-11-7	5100	84338	9,12-11-7	6200
84065	9,12-11-7	4850	84345	9,12-11-7	6500
84072	9,12-11-7	4850	84352	9,12-11-7	6400
84079	9,12-11-7	4900	84361	9,12-11-7	6500

Table B1, Type: RC, continued.

Julian date	Sample#[a]	Reading (Ω)
85002	9,12-11-7	6750
85009	9,12-11-7	7150
85014	9,12-11-7	7150
85021	9,12-11-7	7150
85029	9,12-11-7	7500
85035	9,12-11-7	7150
85042	9,12-11-7	7300
85056	9,12-11-7	7350
85062	9,12-11-7	7500
85070	9,12-11-7	7350
85077	9,12-11-7	7000
85084	9,12-11-7	7450
85091	9,12-11-7	7300
85098	9,12-11-7	6850
85112	9,12-11-7	6600
85119	9,12-11-7	6550
85126	9,12-11-7	6450
85133	9,12-11-7	6250
85140	9,12-11-7	6200
85148	9,12-11-7	5900
85154	9,12-11-7	5900
85161	9,12-11-7	5700
85168	9,12-11-7	7050
85182	9,12-11-7	4550
85189	9,12-11-7	5200
85196	9,12-11-7	16500
85217	9,12-11-7	22500
85224	9,12-11-7	2350
85231	9,12-11-7	2600
85238	9,12-11-7	2550
85246	9,12-11-7	2600
85252	9,12-11-7	2100
85259	9,12-11-7	2800
85266	9,12-11-7	2600
85273	9,12-11-7	2650
85287	9,12-11-7	2750
85294	9,12-11-7	2600
85301	9,12-11-7	2900
85308	9,12-11-7	2950
85316	9,12-11-7	2900
85322	9,12-11-7	3150
85329	9,12-11-7	3100
85343	9,12-11-7	3250
85350	9,12-11-7	3400
85357	9,12-11-7	3450
85364	9,12-11-7	3550
86006	9,12-11-7	3550
86013	9,12-11-7	3550
86027	9,12-11-7	3850
86034	9,12-11-7	3800
86041	9,12-11-7	3450
86049	9,12-11-7	3950
86055	9,12-11-7	4100
86062	9,12-11-7	4300
86069	9,12-11-7	3800
86076	9,12-11-7	3950
86083	9,12-11-7	4000
86090	9,12-11-7	3850
86097	9,12-11-7	4050
86104	9,12-11-7	3800
86111	9,12-11-7	3850
86118	9,12-11-7	3950
83192	24,25-11-3	1150000
83200	24,25-11-3	1200000
83206	24,25-11-3	1125000
83213	24,25-11-3	1125000
83220	24,25-11-3	825000
83227	24,25-11-3	80000
83241	24,25-11-3	800000
83250	24,25-11-3	550000
83255	24,25-11-3	450000
83262	24,25-11-3	240000
83271	24,25-11-3	112500
83283	24,25-11-3	107000
83297	24,25-11-3	115000
83305	24,25-11-3	107500
83311	24,25-11-3	110000
83318	24,25-11-3	122500

Table B1, Type: RC, continued.

Julian date	Sample#[a]	Reading (Ω)
83325	24,25-11-3	125000
83332	24,25-11-3	140000
83339	24,25-11-3	145000
83346	24,25-11-3	160000
83353	24,25-11-3	145000
83361	24,25-11-3	155000
84003	24,25-11-3	155000
84009	24,25-11-3	145000
84016	24,25-11-3	147500
84030	24,25-11-3	145000
84037	24,25-11-3	140000
84044	24,25-11-3	130000
84052	24,25-11-3	135000
84058	24,25-11-3	130000
84065	24,25-11-3	125000
84072	24,25-11-3	125000
84079	24,25-11-3	112500
84086	24,25-11-3	110000
84093	24,25-11-3	109000
84100	24,25-11-3	104000
84107	24,25-11-3	94000
84114	24,25-11-3	95000
84121	24,25-11-3	95000
84128	24,25-11-3	94000
84135	24,25-11-3	86500
84142	24,25-11-3	86000
84151	24,25-11-3	83500
84156	24,25-11-3	89000
84163	24,25-11-3	94000
84170	24,25-11-3	102500
84177	24,25-11-3	110000
84184	24,25-11-3	115000
84191	24,25-11-3	120000
84198	24,25-11-3	117500
84205	24,25-11-3	117500
84212	24,25-11-3	110000
84219	24,25-11-3	105000
84226	24,25-11-3	96000
84241	24,25-11-3	95500
84248	24,25-11-3	90000
84254	24,25-11-3	72500
84261	24,25-11-3	60000
84268	24,25-11-3	60000
84275	24,25-11-3	60000
84282	24,25-11-3	64000
84290	24,25-11-3	67500
84296	24,25-11-3	66500
84303	24,25-11-3	72500
84310	24,25-11-3	80000
84318	24,25-11-3	80000
84324	24,25-11-3	82500
84331	24,25-11-3	85500
84338	24,25-11-38	8000
84345	24,25-11-3	95000
84352	24,25-11-3	95000
84361	24,25-11-3	45500
85002	24,25-11-3	4000
85009	24,25-11-3	2150
85014	24,25-11-3	1900
85021	24,25-11-3	1900
85029	24,25-11-3	1850
85035	24,25-11-3	2050
85042	24,25-11-3	2300
85056	24,25-11-3	2100
85062	24,25-11-3	2000
85070	24,25-11-3	2200
85077	24,25-11-3	2050
85084	24,25-11-3	2050
85091	24,25-11-3	2200
85098	24,25-11-3	2050
85112	24,25-11-3	2050
85119	24,25-11-3	2150
85126	24,25-11-3	2200
85133	24,25-11-3	2650
85140	24,25-11-3	4000
85148	24,25-11-3	10500
85154	24,25-11-3	27000
85161	24,25-11-3	67500

Table B1, Type: RC, continued.

Julian date	Sample#[a]	Reading (Ω)	Julian date	Sample#[a]	Reading (Ω)
85168	24,25-11-3	95000	86118	24,25-11-3	300000
85182	24,25-11-3	117500	83192	17,20-21-4	1400000
85189	24,25-11-3	135000	83200	17,20-21-4	1600000
85196	24,25-11-3	150000	83206	17,20-21-4	1750000
85217	24,25-11-3	170000	83213	17,20-21-4	1750000
85224	24,25-11-3	210000	83220	17,20-21-4	750000
85231	24,25-11-3	305000	83227	17,20-21-4	750000
85238	24,25-11-3	325000	83241	17,20-21-4	1500000
85246	24,25-11-3	335000	83250	17,20-21-4	1750000
85252	24,25-11-3	330000	83255	17,20-21-4	1500000
85259	24,25-11-3	385000	83262	17,20-21-4	1250000
85266	24,25-11-3	415000	83271	17,20-21-4	1250000
85273	24,25-11-3	425000	83283	17,20-21-4	1500000
85287	24,25-11-3	490000	83297	17,20-21-4	1500000
85294	24,25-11-3	520000	83305	17,20-21-4	1250000
85301	24,25-11-3	500000	83311	17,20-21-4	1250000
85308	24,25-11-3	560000	83318	17,20-21-4	1250000
85316	24,25-11-3	560000	83325	17,20-21-4	900000
85322	24,25-11-3	430000	83332	17,20-21-4	875000
85329	24,25-11-3	660000	83339	17,20-21-4	900000
85343	24,25-11-3	650000	83346	17,20-21-4	900000
85350	24,25-11-3	650000	83353	17,20-21-4	875000
85357	24,25-11-3	650000	83361	17,20-21-4	1000000
85364	24,25-11-3	650000	84003	17,20-21-4	875000
86006	24,25-11-3	650000	84009	17,20-21-4	1125000
86013	24,25-11-3	650000	84016	17,20-21-4	875000
86027	24,25-11-3	625000	84030	17,20-21-4	1250000
86034	24,25-11-3	600000	84037	17,20-21-4	1000000
86041	24,25-11-3	600000	84044	17,20-21-4	1200000
86049	24,25-11-3	560000	84052	17,20-21-4	1050000
86055	24,25-11-3	550000	84058	17,20-21-4	1200000
86062	24,25-11-3	500000	84065	17,20-21-4	875000
86069	24,25-11-3	425000	84072	17,20-21-4	875000
86076	24,25-11-3	425000	84079	17,20-21-4	875000
86083	24,25-11-3	475000	84086	17,20-21-4	875000
86090	24,25-11-3	385000	84093	17,20-21-4	875000
86097	24,25-11-3	405000	84100	17,20-21-4	875000
86104	24,25-11-3	345000	84107	17,20-21-4	875000
86111	24,25-11-3	340000	84114	17,20-21-4	800000

Table B1, Type: RC, continued.

Julian date	Sample#[a]	Reading (Ω)
84121	17,20-21-4	875000
84128	17,20-21-4	875000
84135	17,20-21-4	875000
84142	17,20-21-4	875000
84151	17,20-21-4	900000
84156	17,20-21-4	875000
84163	17,20-21-4	900000
84170	17,20-21-4	1000000
84177	17,20-21-4	900000
84184	17,20-21-4	1250000
84191	17,20-21-4	1150000
84198	17,20-21-4	1150000
84205	17,20-21-4	1150000
84212	17,20-21-4	1150000
84219	17,20-21-4	1000000
84226	17,20-21-4	1150000
84241	17,20-21-4	1000000
84248	17,20-21-4	900000
84254	17,20-21-4	875000
84261	17,20-21-4	875000
84268	17,20-21-4	875000
84275	17,20-21-4	750000
84282	17,20-21-4	750000
84290	17,20-21-4	800000
84296	17,20-21-4	800000
84303	17,20-21-4	800000
84310	17,20-21-4	800000
84318	17,20-21-4	875000
84324	17,20-21-4	850000
84331	17,20-21-4	1150000
84338	17,20-21-4	1150000
84345	17,20-21-4	1125000
84352	17,20-21-4	1150000
84361	17,20-21-4	1500000
85002	17,20-21-4	1200000
85009	17,20-21-4	136500
85014	17,20-21-4	26500
85021	17,20-21-4	16500
85029	17,20-21-4	12500
85035	17,20-21-4	12350
85042	17,20-21-4	10800
85056	17,20-21-4	10500
85062	17,20-21-4	8900
85070	17,20-21-4	8900
85077	17,20-21-4	9300
85084	17,20-21-4	8300
85091	17,20-21-4	7800
85098	17,20-21-4	7450
85112	17,20-21-4	9950
85119	17,20-21-4	14750
85126	17,20-21-4	54000
85133	17,20-21-4	101000
85140	17,20-21-4	180000
85148	17,20-21-4	265000
85154	17,20-21-4	285000
85161	17,20-21-4	335000
85168	17,20-21-4	385000
85182	17,20-21-4	425000
85189	17,20-21-4	425000
85196	17,20-21-4	535000
85217	17,20-21-4	110000
85224	17,20-21-4	500000
85231	17,20-21-4	1450000
85238	17,20-21-4	1550000
85246	17,20-21-4	1500000
85252	17,20-21-4	1500000
85259	17,20-21-4	1550000
85266	17,20-21-4	1600000
85273	17,20-21-4	1525000
85287	17,20-21-4	1550000
85294	17,20-21-4	1250000
85301	17,20-21-4	1100000
85308	17,20-21-4	2000000
85316	17,20-21-4	1550000
85322	17,20-21-4	2200000
85329	17,20-21-4	2150000
85343	17,20-21-4	2000000
85350	17,20-21-4	2250000

Table B1, Type: RC, continued.

Julian date	Sample#[a]	Reading (Ω)
85357	17,20-21-4	1900000
85364	17,20-21-4	2125000
86006	17,20-21-4	2125000
86013	17,20-21-4	2150000
86027	17,20-21-4	2400000
86034	17,20-21-4	2125000
86041	17,20-21-4	1600000
86049	17,20-21-4	2175000
86055	17,20-21-4	2000000
86062	17,20-21-4	1600000
86069	17,20-21-4	2000000
86076	17,20-21-4	1500000
86083	17,20-21-4	1500000
86090	17,20-21-4	2000000
86097	17,20-21-4	1650000
86104	17,20-21-4	1500000
86111	17,20-21-4	1500000
86118	17,20-21-4	1500000
83192	30,31-21-10	160000
83200	30,31-21-10	155000
83206	30,31-21-10	140000
83213	30,31-21-10	135000
83220	30,31-21-10	135000
83227	30,31-21-10	120000
83241	30,31-21-10	115000
83250	30,31-21-10	110000
83255	30,31-21-10	110000
83262	30,31-21-10	102500
83271	30,31-21-10	100000
83283	30,31-21-10	97500
83297	30,31-21-10	92500
83305	30,31-21-10	90000
83311	30,31-21-10	90000
83318	30,31-21-10	90000
83325	30,31-21-10	90000
83332	30,31-21-10	87500
83339	30,31-21-10	87500
83346	30,31-21-10	90000
83353	30,31-21-10	90000
83361	30,31-21-10	89500
84003	30,31-21-10	89500
84009	30,31-21-10	90000
84016	30,31-21-10	90000
84030	30,31-21-10	92500
84037	30,31-21-10	90000
84044	30,31-21-10	90000
84052	30,31-21-10	95000
84058	30,31-21-10	95000
84065	30,31-21-10	95000
84072	30,31-21-10	87500
84079	30,31-21-10	90000
84086	30,31-21-10	90000
84093	30,31-21-10	90000
84100	30,31-21-10	92500
84107	30,31-21-10	90000
84114	30,31-21-10	90000
84121	30,31-21-10	89000
84128	30,31-21-10	86500
84135	30,31-21-10	85000
84142	30,31-21-10	84000
84151	30,31-21-10	84000
84156	30,31-21-10	83500
84163	30,31-21-10	80000
84170	30,31-21-10	82500
84177	30,31-21-10	79000
84184	30,31-21-10	80000
84191	30,31-21-10	74000
84198	30,31-21-10	75000
84205	30,31-21-10	74000
84212	30,31-21-10	70000
84219	30,31-21-10	68500
84226	30,31-21-10	66500
84241	30,31-21-10	65000
84248	30,31-21-10	64000
84254	30,31-21-10	64000
84261	30,31-21-10	60000
84268	30,31-21-10	60000
84275	30,31-21-10	57500

Table B1, Type: RC, continued.

Julian date	Sample#[a]	Reading (Ω)
84282	30,31-21-10	600000
84290	30,31-21-10	56500
84296	30,31-21-10	56500
84303	30,31-21-10	56500
84310	30,31-21-10	55000
84318	30,31-21-10	57000
84324	30,31-21-10	57000
84331	30,31-21-10	55000
84338	30,31-21-10	56500
84345	30,31-21-10	56000
84352	30,31-21-10	57000
84361	30,31-21-10	58500
85002	30,31-21-10	58500
85009	30,31-21-10	58500
85014	30,31-21-10	60500
85021	30,31-21-10	60500
85029	30,31-21-10	63500
85035	30,31-21-10	62000
85042	30,31-21-10	62500
85056	30,31-21-10	62500
85062	30,31-21-10	70000
85070	30,31-21-10	65000
85077	30,31-21-10	63500
85084	30,31-21-10	65500
85091	30,31-21-10	63500
85098	30,31-21-10	63500
85112	30,31-21-10	63500
85119	30,31-21-10	62000
85126	30,31-21-10	61000
85133	30,31-21-10	60000
85140	30,31-21-10	63500
85148	30,31-21-10	57500
85154	30,31-21-10	55000
85161	30,31-21-10	53500
85168	30,31-21-10	51500
85182	30,31-21-10	47500
85189	30,31-21-10	45000
85196	30,31-21-10	44000
85217	30,31-21-10	62000
85224	30,31-21-10	78000
85231	30,31-21-10	98000
85238	30,31-21-10	73000
85246	30,31-21-10	51500
85252	30,31-21-10	34000
85259	30,31-21-10	30000
85266	30,31-21-10	28000
85273	30,31-21-10	27500
85287	30,31-21-10	27500
85294	30,31-21-10	24500
85301	30,31-21-10	27500
85308	30,31-21-10	27500
85316	30,31-21-10	26500
85322	30,31-21-10	28500
85329	30,31-21-10	27500
85343	30,31-21-10	28000
85350	30,31-21-10	27500
85357	30,31-21-10	28500
85364	30,31-21-10	28500
86006	30,31-21-10	28500
86013	30,31-21-10	29500
86027	30,31-21-10	31000
86034	30,31-21-10	31000
86041	30,31-21-10	28500
86049	30,31-21-10	31000
86055	30,31-21-10	32500
86062	30,31-21-10	32000
86069	30,31-21-10	31500
86076	30,31-21-10	32500
86083	30,31-21-10	33000
86090	30,31-21-10	32500
86097	30,31-21-10	32500
86104	30,31-21-10	33000
86111	30,31-21-10	32500
86118	30,31-21-10	33500
98192	1,2-11-15-	660
83200	1,2-11-15	1010
83206	1,2-11-15	1250
83213	1,2-11-15	1450

Table B1, Type: RC, continued.

Julian date	Sample#[a]	Reading (Ω)	Julian date	Sample#[a]	Reading (Ω)
83220	1,2-11-15	1550	84156	1,2-11-15	2450
83227	1,2-11-15	1700	84163	1,2-11-15	2450
83241	1,2-11-15	1725	84170	1,2-11-15	2350
83250	1,2-11-15	1740	84177	1,2-11-15	2450
83255	1,2-11-15	1790	84184	1,2-11-15	2400
83262	1,2-11-15	1800	84191	1,2-11-15	2450
83271	1,2-11-15	1800	84198	1,2-11-15	2550
83283	1,2-11-15	1900	84205	1,2-11-15	3000
83297	1,2-11-15	1900	84212	1,2-11-15	2450
83305	1,2-11-15	1950	84219	1,2-11-15	2450
83311	1,2-11-15	1850	84226	1,2-11-15	2450
83318	1,2-11-15	1900	84241	1,2-11-15	2450
83325	1,2-11-15	1400	84248	1,2-11-15	2500
83332	1,2-11-15	1850	84254	1,2-11-15	2500
83339	1,2-11-15	1900	84261	1,2-11-15	2450
83346	1,2-11-15	1950	84268	1,2-11-15	2450
83353	1,2-11-15	1950	84275	1,2-11-15	2500
83361	1,2-11-15	1875	84282	1,2-11-15	2500
84003	1,2-11-15	1875	84290	1,2-11-15	2500
84009	1,2-11-15	1925	84296	1,2-11-15	2350
84016	1,2-11-15	1925	84303	1,2-11-15	2550
84030	1,2-11-15	2100	84310	1,2-11-15	2600
84037	1,2-11-15	2050	84318	1,2-11-15	2500
84044	1,2-11-15	2013	84324	1,2-11-15	2550
84052	1,2-11-15	2200	84331	1,2-11-15	2450
84058	1,2-11-15	2200	84338	1,2-11-15	2600
84065	1,2-11-15	2400	84345	1,2-11-15	2600
84072	1,2-11-15	2350	84352	1,2-11-15	2500
84079	1,2-11-15	2300	84361	1,2-11-15	2600
84086	1,2-11-15	2300	85002	1,2-11-15	2650
84093	1,2-11-15	2300	85009	1,2-11-15	2700
84100	1,2-11-15	2350	85014	1,2-11-15	2750
84107	1,2-11-15	2450	85021	1,2-11-15	2800
84114	1,2-11-15	2450	85029	1,2-11-15	2850
84121	1,2-11-15	2450	85035	1,2-11-15	2750
84128	1,2-11-15	2350	85042	1,2-11-15	2950
84135	1,2-11-15	2450	85056	1,2-11-15	3000
84142	1,2-11-15	2450	85062	1,2-11-15	3050
84151	1,2-11-15	2450	85070	1,2-11-15	3150

Table B1, Type: RC, continued.

Julian date	Sample#[a]	Reading (Ω)	Julian date	Sample#[a]	Reading (Ω)
85077	1,2-11-15	3900	86034	1,2-11-15	3200
85084	1,2-11-15	3150	86041	1,2-11-15	3150
85091	1,2-11-15	3250	86049	1,2-11-15	3700
85098	1,2-11-15	3250	86055	1,2-11-15	3300
85112	1,2-11-15	3250	86062	1,2-11-15	3300
85119	1,2-11-15	3250	86069	1,2-11-15	3200
85126	1,2-11-15	3200	86076	1,2-11-15	3250
85133	1,2-11-15	3300	86083	1,2-11-15	3400
85140	1,2-11-15	3300	86090	1,2-11-15	3300
85148	1,2-11-15	3250	86097	1,2-11-15	3350
85154	1,2-11-15	3200	86104	1,2-11-15	3350
85161	1,2-11-15	3250	86111	1,2-11-15	3600
85168	1,2-11-15	3200	86118	1,2-11-15	4000
85182	1,2-11-15	3250	83192	7,8-11-10	9000
85189	1,2-11-15	2350	83200	7,8-11-10	8000
85196	1,2-11-15	3200	83206	7,8-11-10	7500
85217	1,2-11-15	2950	83213	7,8-11-10	7000
85224	1,2-11-15	2950	83220	7,8-11-10	6050
85231	1,2-11-15	2950	83227	7,8-11-10	5900
85238	1,2-11-15	2950	83241	7,8-11-10	5250
85246	1,2-11-15	2950	83250	7,8-11-10	5100
85252	1,2-11-15	2900	83255	7,8-11-10	5000
85259	1,2-11-15	3050	83262	7,8-11-10	6000
85266	1,2-11-15	2950	83271	7,8-11-10	5000
85273	1,2-11-15	2950	83283	7,8-11-10	4650
85287	1,2-11-15	2900	83297	7,8-11-10	4650
85294	1,2-11-15	2900	83305	7,8-11-10	4650
85301	1,2-11-15	3050	83311	7,8-11-10	4650
85308	1,2-11-15	2850	83318	7,8-11-10	4650
85316	1,2-11-15	2800	83325	7,8-11-10	4450
85322	1,2-11-15	2950	83332	7,8-11-10	4300
85329	1,2-11-15	2850	83339	7,8-11-10	4300
85343	1,2-11-15	2800	83346	7,8-11-10	4400
85350	1,2-11-15	2800	83353	7,8-11-10	4300
85357	1,2-11-15	2950	83361	7,8-11-10	4450
85364	1,2-11-15	3000	84003	7,8-11-10	4450
86006	1,2-11-15	3000	84009	7,8-11-10	4500
86013	1,2-11-15	3100	84016	7,8-11-10	4500
86027	1,2-11-15	3200	84030	7,8-11-10	4550

Table B1, Type: RC, continued.

Julian date	Sample#[a]	Reading (Ω)
84037	7,8-11-10	4550
84044	7,8-11-10	4925
84052	7,8-11-10	4800
84058	7,8-11-10	4850
84065	7,8-11-10	4900
84072	7,8-11-10	4850
84079	7,8-11-10	4900
84086	7,8-11-10	4850
84093	7,8-11-10	4700
84100	7,8-11-10	5150
84107	7,8-11-10	4900
84114	7,8-11-10	5100
84121	7,8-11-10	5300
84128	7,8-11-10	5000
84135	7,8-11-10	4800
84142	7,8-11-10	4900
84151	7,8-11-10	4800
84156	7,8-11-10	4650
84163	7,8-11-10	4650
84170	7,8-11-10	4550
84177	7,8-11-10	4550
84184	7,8-11-10	4500
84191	7,8-11-10	4750
84198	7,8-11-10	4400
84205	7,8-11-10	4400
84212	7,8-11-10	4250
84219	7,8-11-10	4250
84226	7,8-11-10	4050
84241	7,8-11-10	4050
84248	7,8-11-10	4750
84254	7,8-11-10	4050
84261	7,8-11-10	4000
84268	7,8-11-10	4000
84275	7,8-11-10	4150
84282	7,8-11-10	4150
84290	7,8-11-10	4050
84296	7,8-11-10	4000
84303	7,8-11-10	4050
84310	7,8-11-10	4050
84318	7,8-11-10	4050
84324	7,8-11-10	4050
84331	7,8-11-10	4100
84338	7,8-11-10	4200
84345	7,8-11-10	4350
84352	7,8-11-10	4150
84361	7,8-11-10	4250
85002	7,8-11-10	4100
85009	7,8-11-10	4400
85014	7,8-11-10	4450
85021	7,8-11-10	4500
85029	7,8-11-10	4500
85035	7,8-11-10	4500
85042	7,8-11-10	4550
85056	7,8-11-10	4750
85062	7,8-11-10	4700
85070	7,8-11-10	4950
85077	7,8-11-10	4550
85084	7,8-11-10	4750
85091	7,8-11-10	4650
85098	7,8-11-10	4850
85112	7,8-11-10	4750
85119	7,8-11-10	4600
85126	7,8-11-10	4550
85133	7,8-11-10	4300
85140	7,8-11-10	4500
85148	7,8-11-10	4250
85154	7,8-11-10	4100
85161	7,8-11-10	4150
85168	7,8-11-10	4200
85182	7,8-11-10	4050
85189	7,8-11-10	3750
85196	7,8-11-10	3900
85217	7,8-11-10	3700
85224	7,8-11-10	3700
85231	7,8-11-10	3600
85238	7,8-11-10	3700
85246	7,8-11-10	3600
85252	7,8-11-10	3150

Table B1, Type: RC, continued.

Julian date	Sample#[a]	Reading (Ω)
85259	7,8-11-10	3700
85266	7,8-11-10	3650
85273	7,8-11-10	3600
85287	7,8-11-10	3500
85294	7,8-11-10	3800
85301	7,8-11-10	3600
85308	7,8-11-10	3450
85316	7,8-11-10	3350
85322	7,8-11-10	3700
85329	7,8-11-10	3550
85343	7,8-11-10	3500
85350	7,8-11-10	3550
85357	7,8-11-10	3800
85364	7,8-11-10	3650
86006	7,8-11-10	3600
86013	7,8-11-10	3800
86027	7,8-11-10	4150
86034	7,8-11-10	3850
86041	7,8-11-10	3800
86049	7,8-11-10	4000
86055	7,8-11-10	4100
86062	7,8-11-10	4000
86069	7,8-11-10	3900
86076	7,8-11-10	4000
86083	7,8-11-10	4150
86090	7,8-11-10	4050
86097	7,8-11-10	4250
86104	7,8-11-10	4150
86111	7,8-11-10	4250
86118	7,8-11-10	4200
83192	10,11-11-5	230000
83200	10,11-11-5	235000
83206	10,11-11-5	250000
83213	10,11-11-5	235000
83220	10,11-11-5	18500
83227	10,11-11-5	17000
83241	10,11-11-5	145000
83250	10,11-11-5	140000
83255	10,11-11-5	130000
83262	10,11-11-5	120000
83271	10,11-11-5	115000
83283	10,11-11-5	110000
83297	10,11-11-5	105000
83305	10,11-11-5	100000
83311	10,11-11-5	100000
83318	10,11-11-5	100000
83325	10,11-11-5	100000
83332	10,11-11-5	100000
83339	10,11-11-5	100000
83346	10,11-11-5	100000
83353	10,11-11-5	97500
83361	10,11-11-5	100000
84003	10,11-11-5	99500
84009	10,11-11-5	105000
84016	10,11-11-5	97500
84030	10,11-11-5	104500
84037	10,11-11-5	101500
84044	10,11-11-5	100000
84052	10,11-11-5	100000
84058	10,11-11-5	100000
84065	10,11-11-5	100000
84072	10,11-11-5	89000
84079	10,11-11-5	89000
84086	10,11-11-5	88500
84093	10,11-11-5	83500
84100	10,11-11-5	83000
84107	10,11-11-5	78000
84114	10,11-11-5	75000
84121	10,11-11-5	73500
84128	10,11-11-5	68500
84135	10,11-11-5	66000
84142	10,11-11-5	62500
84151	10,11-11-5	58000
84156	10,11-11-5	56500
84163	10,11-11-5	54500
84170	10,11-11-5	51000
84177	10,11-11-5	47500
84184	10,11-11-5	45000

Table B1, Type: RC, continued.

Julian date	Sample#[a]	Reading (Ω)	Julian date	Sample#[a]	Reading (Ω)
84191	10,11-11-5	42500	85119	10,11-11-5	4050
84198	10,11-11-5	37500	85126	10,11-11-5	3950
84205	10,11-11-5	37500	85133	10,11-11-5	3800
84212	10,11-11-5	36000	85140	10,11-11-5	3800
84219	10,11-11-5	36000	85148	10,11-11-5	3650
84226	10,11-11-5	33000	85154	10,11-11-5	3600
84241	10,11-11-5	33500	85161	10,11-11-5	3550
84248	10,11-11-5	33000	85168	10,11-11-5	3550
84254	10,11-11-5	32000	85182	10,11-11-5	3350
84261	10,11-11-5	30000	85189	10,11-11-5	3450
84268	10,11-11-5	30000	85196	10,11-11-5	3300
84275	10,11-11-5	27000	85217	10,11-11-5	3300
84282	10,11-11-5	25500	85224	10,11-11-5	3500
84290	10,11-11-5	26500	85231	10,11-11-5	3600
84296	10,11-11-5	25500	85238	10,11-11-5	3700
84303	10,11-11-5	24000	85246	10,11-11-5	3850
84310	10,11-11-5	22000	85252	10,11-11-5	4150
84318	10,11-11-5	26000	85259	10,11-11-5	4350
84324	10,11-11-5	24000	85266	10,11-11-5	4400
84331	10,11-11-5	24500	85273	10,11-11-5	4750
84338	10,11-11-5	25500	85287	10,11-11-5	5050
84345	10,11-11-5	24500	85294	10,11-11-5	5900
84352	10,11-11-5	24500	85301	10,11-11-5	5350
84361	10,11-11-5	24500	85308	10,11-11-5	5600
85002	10,11-11-5	25500	85316	10,11-11-5	5600
85009	10,11-11-5	28000	85322	10,11-11-5	6600
85014	10,11-11-5	27000	85329	10,11-11-5	6250
85021	10,11-11-5	21500	85343	10,11-11-5	6550
85029	10,11-11-5	11500	85350	10,11-11-5	6750
85035	10,11-11-5	8000	85357	10,11-11-5	7250
85042	10,11-11-5	7000	85364	10,11-11-5	7100
85056	10,11-11-5	6150	86006	10,11-11-5	7200
85062	10,11-11-5	5550	86013	10,11-11-5	7500
85070	10,11-11-5	5450	86027	10,11-11-5	8000
85077	10,11-11-5	5050	86034	10,11-11-5	7450
85084	10,11-11-5	4850	86041	10,11-11-5	6750
85091	10,11-11-5	4750	86049	10,11-11-5	7750
85098	10,11-11-5	4650	86055	10,11-11-5	7950
85112	10,11-11-5	4150	86062	10,11-11-5	7900

Table B1, Type: RC, continued.

Julian date	Sample#[a]	Reading (Ω)
86069	10,11-11-5	6800
86076	10,11-11-5	7000
86083	10,11-11-5	7350
86090	10,11-11-5	7000
86097	10,11-11-5	7000
86104	10,11-11-5	6950
86111	10,11-11-5	6850
86118	10,11-11-5	6200

Table B1, continued.

(b) Type: NP

Julian date	Sample#[a]	Reading (Ω)	Julian date	Sample#[a]	Reading (Ω)
83192	11-5	12.00	84086	11-5	—
83200	11-5	12.7	84093	11-5	—
83206	11-5	12.7	84100	11-5	12.8
83213	11-5	12.3	84107	11-5	12.1
83220	11-5	13.0	84114	11-5	12.3
83227	11-5	12.5	84121	11-5	13.3
83241	11-5	13.3	84128	11-5	12.8
83250	11-5	13.0	84135	11-5	13.2
83255	11-5	13.1	84142	11-5	13.5
83262	11-5	15.2	84151	11-5	—
83271	11-5	13.0	84156	11-5	—
83283	11-5	13.7	84163	11-5	—
83297	11-5	13.0	84170	11-5	—
83305	11-5	14.0	84177	11-5	—
83311	11-5	12.9	84184	11-5	—
83318	11-5	13.6	84191	11-5	—
83325	11-5	13.1	84198	11-5	13.6
83332	11-5	13.1	84205	11-5	13.8
83339	11-5	13.1	84212	11-5	—
83346	11-5	13.2	84219	11-5	12.9
83353	11-5	12.7	84226	11-5	13.0
83361	11-5	13.0	83192	11-7.5	15.2
84003	11-5	12.5	83200	11-7.5	15.5
84009	11-5	13.2	83206	11-7.5	15.1
84016	11-5	13.5	83213	11-7.5	14.7
84030	11-5	—	83220	11-7.5	15.5
84037	11-5	—	83227	11-7.5	14.7
84044	11-5	—	83241	11-7.5	14.8
84052	11-5	—	83250	11-7.5	14.9
84058	11-5	—	83255	11-7.5	15.3
84065	11-5	—	83262	11-7.5	13.0
84072	11-5	—	83271	11-7.5	14.9
84079	11-5	—	83283	11-7.5	14.3

[a] Final two numbers of the Sample # identify the location and depth of the instrument. See Sec. 3 and references cited therein for details of locations and descriptions.

Table B1, Type: NP, continued.

Julian date	Sample#[a]	Reading (%VM)
83297	11-7.5	14.4
83305	11-7.5	14.6
83311	11-7.5	14.3
83318	11-7.5	14.4
83325	11-7.5	14.5
83332	11-7.5	14.6
83339	11-7.5	14.3
83346	11-7.5	15.0
83353	11-7.5	14.2
83361	11-7.5	14.2
84003	11-7.5	14.6
84009	11-7.5	14.8
84016	11-7.5	14.8
84030	11-7.5	—
84037	11-7.5	—
84044	11-7.5	—
84052	11-7.5	—
84058	11-7.5	—
84065	11-7.5	—
84072	11-7.5	—
84079	11-7.5	—
84086	11-7.5	—
84093	11-7.5	—
84100	11-7.5	15.5
84107	11-7.5	14.8
84114	11-7.5	14.6
84121	11-7.5	15.3
84128	11-7.5	15.7
84135	11-7.5	14.4
84142	11-7.5	15.3
84151	11-7.5	—
84156	11-7.5	—
84163	11-7.5	—
84170	11-7.5	—
84177	11-7.5	—
84184	11-7.5	—
84191	11-7.5	—
84198	11-7.5	15.1
84205	11-7.5	14.7
84212	11-7.5	—
84219	11-7.5	16.3
84226	11-7.5	13.3
83192	11-10	14.8
83200	11-10	15.0
83206	11-10	14.8
83213	11-10	14.6
83220	11-10	15.3
83227	11-10	14.5
83241	11-10	14.7
83250	11-10	14.7
83255	11-10	13.3
83262	11-10	15.1
83271	11-10	13.7
83283	11-10	14.6
83297	11-10	14.2
83305	11-10	13.3
83311	11-10	13.7
83318	11-10	14.8
83325	11-10	13.2
83332	11-10	14.4
83339	11-10	15.3
83346	11-10	14.8
83353	11-10	13.6
83361	11-10	14.2
84003	11-10	14.0
84009	11-10	14.1
84016	11-10	14.3
84030	11-10	—
84037	11-10	—
84044	11-10	—
84052	11-10	—
84058	11-10	—
84065	11-10	—
84072	11-10	—
84079	11-10	—
84086	11-10	—
84093	11-10	—
84100	11-10	14.5

Table B1, Type: NP, continued.

Julian date	Sample#[a]	Reading (%VM)
84107	11-10	13.7
84114	11-10	13.9
84121	11-10	13.4
84128	11-10	14.0
84135	11-10	13.6
84142	11-10	13.3
84151	11-10	—
84156	11-10	—
84163	11-10	—
84170	11-10	—
84177	11-10	—
84184	11-10	—
84191	11-10	—
84198	11-10	13.2
84205	11-10	14.4
84212	11-10	—
84219	11-10	13.1
84226	11-10	11.1
83192	11-12.5	14.6
83200	11-12.5	14.7
83206	11-12.5	15.5
83213	11-12.5	14.5
83220	11-12.5	15.0
83227	11-12.5	14.8
83241	11-12.5	14.5
83250	11-12.5	15.1
83255	11-12.5	14.4
83262	11-12.5	14.0
83271	11-12.5	14.8
83283	11-12.5	14.2
83297	11-12.5	15.4
83305	11-12.5	14.3
83311	11-12.5	14.2
83318	11-12.5	15.6
83325	11-12.5	14.5
83332	11-12.5	14.3
83339	11-12.5	14.6
83346	11-12.5	15.0
83353	11-12.5	14.6
83361	11-12.5	14.6
84003	11-12.5	15.8
84009	11-12.5	14.5
84016	11-12.5	15.0
84030	11-12.5	—
84037	11-12.5	—
84044	11-12.5	—
84052	11-12.5	—
84058	11-12.5	—
84065	11-12.5	—
84072	11-12.5	—
84079	11-12.5	—
84086	11-12.5	—
84093	11-12.5	—
84100	11-12.5	14.9
84107	11-12.5	15.1
84114	11-12.5	13.9
84121	11-12.5	14.8
84128	11-12.5	15.1
84135	11-12.5	15.1
84142	11-12.5	13.8
84151	11-12.5	—
84156	11-12.5	—
84163	11-12.5	—
84170	11-12.5	—
84177	11-12.5	—
84184	11-12.5	—
84191	11-12.5	—
84198	11-12.5	14.7
84205	11-12.5	14.6
84212	11-12.5	—
84219	11-12.5	14.1
84226	11-12.5	12.5
83192	11-15	14.0
83200	11-15	14.2
83206	11-15	13.5
83213	11-15	13.0
83220	11-15	13.8
83227	11-15	13.3

Table B1, Type: NP, continued.

Julian date	Sample#[a]	Reading (%VM)
83241	11-15	14.4
83250	11-15	14.7
83255	11-15	14.1
83262	11-15	13.9
83271	11-15	13.9
83283	11-15	14.5
83297	11-15	14.4
83305	11-15	14.5
83311	11-15	14.4
83318	11-15	13.9
83325	11-15	13.8
83332	11-15	13.7
83339	11-15	13.3
83346	11-15	12.9
83353	11-15	13.7
83361	11-15	14.1
84003	11-15	13.0
84009	11-15	13.9
84016	11-15	13.7
84030	11-15	—
84037	11-15	—
84044	11-15	—
84052	11-15	—
84058	11-15	—
84065	11-15	—
84072	11-15	—
84079	11-15	—
84086	11-15	—
84093	11-15	—
84100	11-15	—
84107	11-15	13.6
84114	11-15	13.7
84121	11-15	13.3
84128	11-15	13.8
84135	11-15	12.9
84142	11-15	13.1
84151	11-15	—
84156	11-15	—
84163	11-15	—
84170	11-15	—
84177	11-15	—
84184	11-15	—
84191	11-15	—
84198	11-15	13.1
84205	11-15	13.3
84212	11-15	—
84219	11-15	12.5
84226	11-15	10.9

Table B1: continued.

(c) Type: T

Julian date	Sample#[a]	Reading (Ω)
83192	1,6-0-3	7
83200	1,6-0-3	8
83206	1,6-0-3	9
83213	1,6-0-3	8
83220	1,6-0-3	8
83227	1,6-0-3	8
83241	1,6-0-3	7
83250	1,6-0-3	8
83255	1,6-0-3	8
83262	1,6-0-3	8
83271	1,6-0-3	7
83283	1,6-0-3	7
83297	1,6-0-3	7
83305	1,6-0-3	8
83311	1,6-0-3	7
83318	1,6-0-3	7
83325	1,6-0-3	8
83332	1,6-0-3	0
83339	1,6-0-3	—
83346	1,6-0-3	—
83353	1,6-0-3	—
83361	1,6-0-3	—
84003	1,6-0-3	—
84009	1,6-0-3	—
84016	1,6-0-3	—
84030	1,6-0-3	—
84037	1,6-0-3	—
84044	1,6-0-3	—
84052	1,6-0-3	—
84058	1,6-0-3	—
84065	1,6-0-3	—
84072	1,6-0-3	—
84079	1,6-0-3	0
84086	1,6-0-3	0
84093	1,6-0-3	0
84100	1,6-0-3	0
84107	1,6-0-3	0
84114	1,6-0-3	0
84121	1,6-0-3	0
84128	1,6-0-3	0
84135	1,6-0-3	0
84142	1,6-0-3	0
84151	1,6-0-3	0
84156	1,6-0-3	0
84163	1,6-0-3	0
84170	1,6-0-3	4
84177	1,6-0-3	3
84184	1,6-0-3	4
84191	1,6-0-3	4
84198	1,6-0-3	3
84205	1,6-0-3	4
84212	1,6-0-3	—
84219	1,6-0-3	4
84226	1,6-0-3	3
83192	2,7-1.5-5	5
83200	2,7-1.5-5	7
83206	2,7-1.5-5	8
83213	2,7-1.5-5	9
83220	2,7-1.5-5	8
83227	2,7-1.5-5	9
83241	2,7-1.5-5	6
83250	2,7-1.5-5	6
83255	2,7-1.5-5	7
83262	2,7-1.5-5	8
83271	2,7-1.5-5	8
83283	2,7-1.5-5	8

[a] Final two numbers of the Sample # identify the location and depth of the instrument. See Sec. 3 and references cited therein for details of locations and descriptions.

Table B1, Type: T, continued.

Julian date	Sample#[a]	Reading (cbar)
83297	2,7-1.5-5	8
83305	2,7-1.5-5	9
83311	2,7-1.5-5	9
83318	2,7-1.5-5	8
83325	2,7-1.5-5	0
83332	2,7-1.5-5	0
83339	2,7-1.5-5	—
83346	2,7-1.5-5	—
83353	2,7-1.5-5	—
83361	2,7-1.5-5	—
84003	2,7-1.5-5	—
84009	2,7-1.5-5	—
84016	2,7-1.5-5	—
84030	2,7-1.5-5	—
84037	2,7-1.5-5	—
84044	2,7-1.5-5	0
84052	2,7-1.5-5	—
84058	2,7-1.5-5	—
84065	2,7-1.5-5	—
84072	2,7-1.5-5	0
84079	2,7-1.5-5	0
84086	2,7-1.5-5	1
84093	2,7-1.5-5	0
84100	2,7-1.5-5	0
84107	2,7-1.5-5	0
84114	2,7-1.5-5	0
84121	2,7-1.5-5	0
84128	2,7-1.5-5	0
84135	2,7-1.5-5	0
84142	2,7-1.5-5	0
84151	2,7-1.5-5	0
84156	2,7-1.5-5	0
84163	2,7-1.5-5	0
84170	2,7-1.5-5	5
84177	2,7-1.5-5	5
84184	2,7-1.5-5	5
84191	2,7-1.5-5	4
84198	2,7-1.5-5	4
84205	2,7-1.5-5	3
84212	2,7-1.5-5	—
84219	2,7-1.5-5	3
84226	2,7-1.5-5	4
83200	3,8-5-3	22
83206	3,8-5-3	24
83213	3,8-5-3	29
83220	3,8-5-3	28
83227	3,8-5-3	27
83241	3,8-5-3	13
83250	3,8-5-3	13
83255	3,8-5-3	15
83262	3,8-5-3	16
83271	3,8-5-3	16
83283	3,8-5-3	14
83297	3,8-5-3	16
83305	3,8-5-3	15
83311	3,8-5-3	15
83318	3,8-5-3	15
83325	3,8-5-3	16
83332	3,8-5-3	0
83339	3,8-5-3	—
83346	3,8-5-3	—
83353	3,8-5-3	—
83361	3,8-5-3	—
84003	3,8-5-3	—
84009	3,8-5-3	—
84016	3,8-5-3	—
84030	3,8-5-3	—
84037	3,8-5-3	—
84044	3,8-5-3	0
84052	3,8-5-3	—
84058	3,8-5-3	0
84065	3,8-5-3	0
84072	3,8-5-3	0
84079	3,8-5-3	0
84086	3,8-5-3	0
84093	3,8-5-3	0
84100	3,8-5-3	0
84107	3,8-5-3	1

Table B1, Type: T, continued.

Julian date	Sample#[a]	Reading (cbar)
84114	3,8-5-3	1
84121	3,8-5-3	1
84128	3,8-5-3	2
84135	3,8-5-3	3
84142	3,8-5-3	3
84151	3,8-5-3	6
84156	3,8-5-3	6
84163	3,8-5-3	6
84170	3,8-5-3	15
84177	3,8-5-3	19
84184	3,8-5-3	20
84191	3,8-5-3	15
84198	3,8-5-3	17
84205	3,8-5-3	20
84212	3,8-5-3	—
84219	3,8-5-3	8
84226	3,8-5-3	8
83192	4,9-6-5	16
83200	4,9-6-5	15
83206	4,9-6-5	19
83213	4,9-6-5	20
83220	4,9-6-5	20
83227	4,9-6-5	20
83241	4,9-6-5	13
83250	4,9-6-5	11
83255	4,9-6-5	12
83262	4,9-6-5	14
83271	4,9-6-5	15
83283	4,9-6-5	15
83297	4,9-6-5	15
83305	4,9-6-5	15
83311	4,9-6-5	16
83318	4,9-6-5	16
83325	4,9-6-5	17
83332	4,9-6-5	0
83339	4,9-6-5	—
83346	4,9-6-5	—
83353	4,9-6-5	—
83361	4,9-6-5	—
84003	4,9-6-5	—
84009	4,9-6-5	—
84016	4,9-6-5	—
84030	4,9-6-5	—
84037	4,9-6-5	—
84044	4,9-6-5	4
84052	4,9-6-5	4
84058	4,9-6-5	5
84065	4,9-6-5	6
84072	4,9-6-5	7
84079	4,9-6-5	8
84086	4,9-6-5	11
84093	4,9-6-5	12
84100	4,9-6-5	14
84107	4,9-6-5	14
84114	4,9-6-5	9
84121	4,9-6-5	16
84128	4,9-6-5	15
84135	4,9-6-5	16
84142	4,9-6-5	14
84151	4,9-6-5	16
84156	4,9-6-5	16
84163	4,9-6-5	16
84170	4,9-6-5	15
84177	4,9-6-5	15
84184	4,9-6-5	13
84191	4,9-6-5	14
84198	4,9-6-5	16
84205	4,9-6-5	19
84212	4,9-6-5	—
84219	4,9-6-5	15
84226	4,9-6-5	12
83192	5,10-11-10	6
83200	5,10-11-10	6
83206	5,10-11-10	5
83213	5,10-11-10	11
83220	5,10-11-10	8
83227	5,10-11-10	11
83241	5,10-11-10	6

Table B1, Type: T, continued.

Julian date	Sample#[a]	Reading (cbar)
83250	5,10-11-10	6
83255	5,10-11-10	9
83262	5,10-11-10	10
83271	5,10-11-10	12
83283	5,10-11-10	11
83297	5,10-11-10	10
83305	5,10-11-10	12
83311	5,10-11-10	13
83318	5,10-11-10	13
83325	5,10-11-10	14
83332	5,10-11-10	0
83339	5,10-11-10	—
83346	5,10-11-10	—
83353	5,10-11-10	—
83361	5,10-11-10	—
84003	5,10-11-10	—
84009	5,10-11-10	—
84016	5,10-11-10	—
84030	5,10-11-10	—
84037	5,10-11-10	—
84044	5,10-11-10	0
84052	5,10-11-10	0
84058	5,10-11-10	0
84065	5,10-11-10	0
84072	5,10-11-10	0
84079	5,10-11-10	1
84086	5,10-11-10	2
84093	5,10-11-10	2
84100	5,10-11-10	2
84107	5,10-11-10	2
84114	5,10-11-10	1
84121	5,10-11-10	3
84128	5,10-11-10	4
84135	5,10-11-10	4
84142	5,10-11-10	3
84151	5,10-11-10	5
84156	5,10-11-10	4
84163	5,10-11-10	4
84170	5,10-11-10	4
84177	5,10-11-10	4
84184	5,10-11-10	2
84191	5,10-11-10	4
84198	5,10-11-10	3
84205	5,10-11-10	1
84212	5,10-11-10	—
84219	5,10-11-10	2
84226	5,10-11-10	2

Table B2. Cambric tritium data.[a]
(a) Type: L

Location	Date	dpm/mL	Error	Decay-corr	D(‰)
A6	83241	4206	ND	4227	—
	83250	4258	19	4279	—
	83255	4204	19	4225	—
	83272	4268	20	4307	—
	83272	4206	19	4244	—
	83292	4395	21	4435	—
	83297	4360	ND	4408	—
	83311	4090	41	4186	—
	83315	4366	ND	4415	—
	83318	3971	40	4064	—
	83325	4002	40	4096	—
	83332	3967	40	4060	—
	83339	3955	40	4048	—
	84003	3953	39	4046	-104
	84030	3771	38	3932	—
	84065	3694	37	3852	—
	84114	3881	39	4047	—
	84121	3832	38	3996	—
	84156	3898	20	4125	—
	84212	4032	20	4267	—
	84248	3437	17	3637	—
	84275	3443	17	3659	—
	84310	3120	31	3410	—
	84337	3095	31	3383	—
	85002	3068	31	3353	—
	85062	3121	31	3411	—
	85091	2802	28	3093	—
	85182	2870	29	3214	—
	85217	2697	27	—	—
	85248	2723	27	—	—
	85280	2753	27	—	—
	85308	2635	26	—	—
	85336	2464	24	—	—
	86006	2509	24	—	—

[a] The results of LLNL tritium determinations are expressed in disintegrations per minute per milliliter of water (dpm/mL). Errors reported are in dpm/mL, and are two standard deviations based on counting statistics alone. DRI deuterium determinations are expressed in per mille relative to the Standard Mean Ocean Water (SMOW) standard.

Table B2, (a) Type L, continued.

Location	Date	dpm/mL	Error	Decay-corr	D(‰)
A6	86034	2531	24	—	—
	86062	2531	24	—	—
	86097	2420	24	—	—
	86125	1770	18	Note decrease	
	86153	2260	9	—	—
	86203	2150	22	—	—
	86224	2120	21	—	—
	86253	2110	21	—	—
	86282	2090	20	—	—
C12	83241	5029	ND	5054	—
	83250	5010	21	5035	—
	83255	5048	21	5073	—
	83262	5151	22	5198	—
	83272	5029	20	5054	—
	83272	5047	21	5072	—
	83283	5181	23	5228	—
	83297	5228	ND	5286	—
	83311	4842	48	4956	—
	83325	4739	48	4851	—
	83332	4858	49	4972	—
	83339	4849	49	4963	—
	84030	4669	47	4869	—
	84065	4613	46	4810	—
	84121	4596	46	4792	—
	84156	3667	20	3880	—
	84248	4282	22	4531	—
	84275	4231	21	4496	—
	84310	4080	41	4459	—
	84337	3988	40	4358	—
	85002	3947	39	4314	—
	85035	3878	39	4238	—
	85062	3886	38	4247	—
	85091	3670	37	4051	—
	85154	3598	36	3982	—
	85217	3536	35	—	—
	85280	3419	33	—	—
	85308	3368	33	—	—
	86006	3108	31	—	—
	86034	3108	31	—	—

Table B2, (a) Type L, continued.

Location	Date	dpm/mL	Error	Decay-corr	D(‰)
C12	86062	3041	30	—	—
	86097	2910	29	—	—
	86125	2840	28	—	—
	86203	2690	27	—	—
	86224	2600	26	—	—
	86253	2640	26	—	—
	86282	2550	26	—	—
D6	83255	353.8	3.3	356	—
	83262	494.9	4.1	504	—
	83271	374.4	3.4	378	—
	83297	430	ND	435	—
	83325	443	11	453	—
	83332	338	9	346	—
	84065	568	6	592	—
	84121	672	7	701	—
	84212	871.1	9.8	922	—
	84275	1150	10	1222	—
	84310	1100	11	1202	—
	84337	570.3	5.2	623	—
	85035	891.9	9.0	975	—
	85062	695.6	7.0	760	—
	85091	550.6	5.6	608	—
	85126	524	5	575	—
	85154	520	5	574	—
	86125	1700	—	15	—
E12	84212	852.7	9.8	903	—
	84310	787.9	7.9	861	—
	84337	801.7	8.1	876	—
	85002	864.6	8.7	945	—
	85035	893.8	9.0	977	—
	85062	1005	10	1098	—
	85091	921.5	9.3	1017	—
	85126	1178	12	1293	—
	85154	921	9	1017	—
	85182	955	10	1069	—
	85248	935	9	—	—
	85280	1137	—	11	—
	86006	1190	—	12	—
	86308	1061	—	11	—

Table B2, (a) Type L, continued.

Location	Date	dpm/mL	Error	Decay-corr	D(‰)
E12	86062	1361	—	14	—
	86125	1620	—	16	—
	86153	1600	—	6.4	—
	86224	1760	—	18	—
F5	85091	10.91	0.61	12.04	—
	85062	34.08	0.91	37.23	—
G11	84310	10.70	0.61	11.69	—
	85002	8.35	0.57	9.13	—
	85091	1.02	0.42	1.13	—
	85182	1.42	0.46	1.59	—
	85280	9.90	0.60	—	—
	85308	5.39	0.53	—	—
	86006	2.29	0.44	—	—
	86034	6.95	0.58	—	—
	86062	0.71	0.44	—	—
	86097	0.73	0.40	—	—
	86125	1.01	0.42	—	—
	86153	1.41	0.44	—	—
L-1	83332	2270	25	2323	—
	83339	2267	25	2320	—
	84003	3000	30	3071	—
	84065	2929	29	3054	—
	84307	2392	24	2614	—
	85035	2352	24	2570	—
	85091	2194	22	2422	—
	85126	2219	22	2436	—
	85154	2200	22	2429	—
	85182	2650	27	2968	—
	85280	2575	27	—	—
	85308	2453	24	—	—
	86062	2353	24	—	—
	86097	2400	24	—	—
	86125	2290	23	—	—
	86153	2330	40	—	—
L-2	83332	1294	18	1324	—
	83339	1391	19	1424	—
	84065	1993	20	2078	—

Table B2, (a) Type L, continued.

Location	Date	dpm/mL	Error	Decay-corr	D(‰)
L-2	84337	1841	18	2012	—
	85002	1640	16	1792	—
	85091	708.6	7.2	782	—
L-100	85203	2191	22	—	—
	85203	2674	27	—	—
	85217	2695	27	—	—
	85231	2704	27	—	—
	85238	2697	27	—	—
	85246	2711	27	—	—
	85252	2731	27	—	—
	85259	2686	27	—	—
	85273	2708	27	—	—
	85280	2731	27	—	—
	85287	2686	27	—	—
	85294	2691	27	—	—
	85301	2717	27	—	—
	85324	2597	27	—	—
	85329	2575	27	—	—
	85343	2553	27	—	—
	85350	2553	27	—	—
	85357	2531	24	—	—
	85364	2553	27	—	—
	86013	2575	27	—	—
	86021	2553	27	—	—
	86027	2575	27	—	—
	86041	2553	27	—	—
	86049	2575	27	—	—
	86055	2553	27	—	—
	86069	2530	24	—	—
	86076	2571	11	—	—
	86081	2533	11	—	—
	86083	2522	11	—	—
	86084-1	2513	11	—	—
	86084-2	2544	11	—	—
	86085-1	2533	11	—	—
	86085-2	2546	11	—	—
	86086-1	2529	11	—	—
	86086-2	2524	11	—	—
	86087-1	2513	11	—	—

Table B2, (a) Type L, continued.

Location	Date	dpm/mL	Error	Decay-corr	D(‰)
L-100	86087-2	2502	11	—	—
	86088	2529	11	—	—
	86089	2526	11	—	—
	86090-1	2522	11	—	—
	86090-2	2509	11	—	—
	86091	2540	11	—	—
	86092	2511	11	—	—
	86093-1	2546	11	—	—
	86093-2	2517	11	—	—
	86094	2533	11	—	—
	86097-1	2513	11	—	—
	86097-2	2515	11	—	—
	86098-1	2509	11	—	—
	86098-2	2517	11	—	—
	86100	2498	11	—	—
	86101-1	2480	11	—	—
	86101-2	2493	11	—	—
	86104-1	2493	11	—	—
	86104-2	2462	11	—	—
	86105	2511	11	—	—
	86107-1	2506	11	—	—
	86107-2	2460	11	—	—
	86111-1	2473	11	—	—
	86111-2	2504	11	—	—
	86113	2364	11	—	—
	86114	2389	11	—	—
	86118-1	2391	11	—	—
	86118-2	2364	11	—	—
	86121-1	2367	11	—	—
	86121-2	2378	11	—	—
	86125-1	2373	11	—	—
	86125-2	2362	11	—	—
	86147-1	2350	9.1	—	—
	86147-2	2350	9.1	—	—
	86149	2310	9.3	—	—
	86153-1	2330	9.3	—	—
	86153-2	2330	9.3	—	—
	86160-1	2330	9.3	—	—
	86160-2	2330	9.3	—	—

Table B2, (a) Type L, continued.

Location	Date	dpm/mL	Error	Decay-corr	D(‰)
L-100	86174	2310	9.1	—	—
	86177	2310	9.3	—	—
	86188	2290	9.1	—	—
	86203	2260	9.1	—	—
	86216	2210	22	—	—
	86224	2190	22	—	—
	86246	2200	22	—	—
	86253	2200	22	—	—
	86275	2160	22	—	—
	86282	2140	22	—	—

Table B2, (b) Type: CCW

Location	Date	dpm/mL	Error	Decay-corr	D(‰)
OUT	83154	4427	20	—	—
F-1	83154	4455	20	4455	—
F-2	83154	4445	20	4445	—
F-1	83271	4186	20	4207	-101
F-2	83271	4170	19	4191	-103
	84030	3754	38	3914	—
	84065	3680	37	3837	—
	84114	3594	36	3748	—
	84121	3557	36	3709	—
	84156	3863	20	4088	—
	84212	3759	20	3978	—
	84220	3756	20	3975	—
F-3	84220	3770	20	3989	—
	84221	3754	20	3972	—
	84221	3814	20	4036	—
	84248	3279	16	3499	—
	84282	3073	31	3297	—
	84310	3048	30	3270	—
	84337	3021	30	3287	—
	85002	2957	30	3218	—
	85035	2957	29	3232	—
	85062	2916	29	3187	—
	85091	2877	29	3175	—

Table B2, (b) Type: CCW, continued.

Location	Date	dpm/mL	Error	Decay-corr	D(‰)
	85126	2730	27	3040	—
	85154	2693	27	2999	—
	85182	2684	27	3017	—
	85217	2624	26	—	—
	85248	2561	26	—	—
	85280	2509	24	—	—
	85308	2494	25	—	—
	86034	2464	24	—	—
	86062	2398	24	—	—
	86084	2313	11	—	—
	86085-1	2311	11	—	—
	86085-2	2307	11	—	—
	86085-3	2291	11	—	—
	86085-4	2249	11	—	—
	86087	2293	11	—	—
	86097	2295	11	—	—
	86105	2253	11	—	—
	86107	2269	11	—	—
	86111	2278	11	—	—
	86113	2207	11	—	—
	86114	2202	11	—	—
	86116	2267	11	—	—
	86118	2204	11	—	—
	86121	2213	11	—	—
	86125	2204	11	—	—
	86147	2200	8.9	—	—
	86149	2200	8.9	—	—
	86153	2200	8.9	—	—
	86160	2170	8.7	—	—
	86168	2160	8.7	—	—
	86174	2160	8.7	—	—
	86177	2170	8.7	—	—
	86188	2160	8.7	—	—
	86203	2150	8.7	—	—
	86216	2100	9.4	—	—
	86224	2080	21	—	—
	86246	2020	20	—	—
	86253	2050	20	—	—
	86275	2030	20	—	—
	86282	2020	20	—	—

Table B2, (c) Type: LANL CCW

Date	dpm/mL	Decay-corr
83131	4375	4292
83145	4356	4273
83154	4294	4234
83154	4455	4393
83160	4296	4236
83168	4264	4204
83173	4268	4208
83181	4238	4179
83188	4215	4177
83195	4161	4124
83202	4183	4145
83215	4113	4092
83223	4093	4073
83229	4196	4175
83237	4249	4228
83245	4210	4210
83250	4232	4232
83258	4064	4064
83265	4051	4051
83271	4020	4020
83271	4186	4186
83287	4026	4046
83300	3965	3985
83306	4028	4065
83314	4021	4058
83320	4019	4055
83326	3895	3930
83335	3857	3912
83343	3854	3909
83348	3857	3912
83356	3812	3866
83363	3784	3838
84012	3760	3833
84018	3742	3814
84026	3764	3837
84033	3768	3857
84040	3769	3858
84047	3732	3820
84054	3712	3799
84061	3710	3817
84069	3691	3797
84156	3863	4011
84212	3759	3920
84220	3756	3937
84221	3754	3935
84230	3241	3430
84263	3197	3397

Table B2, (d) Type: FDSW

Location	Date	dpm/mL	Error
4-5	83153	5056	23
10-5	83153	189	2
20-5	83153	1.03	0.04
0-7	83153	4141	21
0-3	83153	4021	20
0-5	83153	4074	20
4-10	83153	4922	22
10-10	83153	145.6	2.0
20-10	83153	4.7	0.13
11-15	83153	1984	12
FF-1,1	83145	24.0	1.1
FF-1,2	83145	22.3	1.0
FF-1,3	83145	14.2	0.7
FF-1,4	83145	9.4	0.5
FF-1,5	83145	6.1	0.4
FF-1,7	83145	4.1	0.2
L-100-6.5	85123	2758	28
L-100-11	85123	2826	28
L-100-21.5	85123	2787	28
L-100-31.5	85123	2745	27
L-100-42	85123	2768	28
L-100-57	85123	2789	28
L-100-71.5	85123	2780	28
L-100-100	85123	2764	28

Table B2, (e) Type: RW

Location	Date	dpm/mL	Error
plot	84267	1.40	0.45
plot	84282	10.0	0.7
plot	85254	5.65	0.56

Table B2, (f) Type: SAW

Location	Date	dpm/mL	Error
A	—	4.03	0.48
B	—	10.2	0.6
A	85093	12.7	0.62
B	85093	4.60	0.49
B	85224	4.44	0.48
A	86013	22.9	0.76
B	86013	30.4	0.84

Table B2, (g) Type: CPW

Location	Date	dpm/mL	Error	D(‰)
EEOL	83154	2850	16	—
	83271	2753	15	–88
SEOL	83154	3749	18	—
	83271	3179	17	–93
SOL	83154	4177	19	—
	83271	2561	15	–82
W-1	84039	3786	38	—
W-2	84039	3789	38	—
	84220	3530	20	—
W-3	84039	3807	38	—
	84220	3732	20	—
W-4	84039	3787	38	—
	84220	3743	20	—
W-5	84039	3716	37	—
W-6	84039	3537	36	—
W-7	84039	3541	35	—
W-8	84039	3477	35	—
W-9	84039	3780	38	—
W-10	84039	3787	38	—
	84220	3623	20	—
W-11	84039	3755	38	—
	84220	3561	20	—
W-12	84039	3776	38	—
	84220	3712	20	—
W-13	84039	3800	38	—
	84220	3403	20	—
W-14	84039	3824	38	—
	84220	3712	20	—
W-15	84039	3802	38	—

Table B2, (h) Type: AMS

Location	Date	dpm/mL	Error	D(‰)
Ditch	84220	748	9	–108
Ditch	84220	333	6	–112
Remote	84220	30.9	2.9	–108
Remote	84220	62.8	3.3	–82

Table B2, (i) Type: TPS[b]

Location	dpm/mL	Error
DRI01	1065	7
DRI02	1543	10
DRI03	1703	11
DRI04	838	8
DRI05	1363	10
DRI06	1140	7
DRI07	614	6
DRI08	713	8
DRI09	1337	11
DRI10	1395	10
DRI11	972	8
DRI12	935	8
DRI13	1318	10
DRI14	1138	7
DRI15	700	7
DRI16	602	10
DRI17	1447	10
DRI18	1853	12
DRI19	855	8
DRI20	828	8
DRI21	258	4
DRI22	314	5
DRI23	748	8
DRI24	640	6
DRI25	853	8
DRI26	770	13
DRI27	1045	20
DRI28	1125	9
DRI29	2697	55
DRI31	904	8
DRI32	865	9
DRI33	1038	17
DRI34	208014	
DRI35	919	8
DRI36	936	8
DRI37	1226	20
DRI38	1608	11
DRI39	42	1
DRI40	52	2
DRI41	27	1
DRI42	25	1
DRI43	1176	9
DRI44	732	7
DRI45	62	2
DRI46	58	2
DRI47	34	1
DRI48	34	1
DRI49	22	1
DRI50	26	1
DRI51	2435	14
DRI52	2272	13
DRI53	950	8
DRI54	974	8
DRI55	2383	14
DRI56	2183	13
DRI57	1368	10
DRI58	1769	11

[b] See Table B3 for descriptions of these samples.

Table B2, (j) Type: FDPW

Code/Location	Date	Time	dpm/mL	Error	D(‰)
F1-1	83154	—	2531	15	—
F1-2	83154	—	2898	16	—
EOL-1	83154	—	2136	12	—
MC01/1-4	83271	0730	1336	8	–85
MC02/5-6	83271	0730	1776	10	–90
MC03/7-8	83271	0730	911	6	–78
MC04/9-10	83271	0730	2030	12	–75
MC05/11-12	83271	0730	829	5	–92
MC06/21-22	83271	—	331	3	–61
MC07/23-24	83271	—	669	5	–80
MC08/25-26	83271	—	1217	7	–62
MC09/27-28	83271	—	1422	8	–69
MC10/37-38	83271	—	1969	11	–78
MC11/39-40	83271	—	41.2	1.1	–58
MC12/41-42	83271	—	17.4	0.4	–63
MC13/51-52	83271	1200	2597	15	–77
MC14/53-54	83271	1200	1306	8	–63
MC15/55-56	83271	1200	2777	16	–73
MC16/57-58	83271	1200	1169	7	–78
1/CT	84220	0800	1852	13	–2
2/SC	84220	0800	2646	18	–67
3/CT6-7	84220	0830	1645	13	0
4/CT3-4	84220	0830	2635	18	–49
5/CT1-2	84220	0830	3337	20	–119
6/CT	84220	1200	2804	18	+35
7/SC	84220	1200	3481	20	–67
8/CT	84220	1600	3374	20	+21
9/SC	84220	1600	3576	20	–85
10/CT6-7	84220	1630	3514	20	+19
11/CT3-4	84220	1630	3787	20	–80
12/CT1-2	84220	1630	3858	20	–97

Table B3. Toluene Plant Samples (TPS).

DRI Sample #	Sample (28 Sept 84)
1–4[a]	Methods-comparisons sample: taken near dawn using *Conyza coulteri*
5–12[a]	0700 h diurnal C_3– C_4 comparisons
(5–6)	*Conyza coulteri* (leafy C_3 dicot weed; common in moist places)
(7–8)	*Salsola iberica* (C_4 dicot weed; most common in open waste places)
(9–10)	*Typha domingensis* (C_3 monocot wetland plant; cattail)
(11–12)	*Euphorbia albomarginata* (mat-like C_4 perennial herb)
13–20	0830 h diurnal
(13–14)	*Conyza coulteri*
(15–16)	*Salsola iberica*
(17–18)	*Typha domingensis*
(19–20)	*Euphorbia albomarginata*
21–28[a]	Near Frenchman Flat berm, from marsh ca. 200 m from end of canal
(21–22)	*Typha domingensis*, 200 m N of canal line, 0930 h
(23–24)	*Tamarix pentandra* (C_3 tree; salt cedar), same as above
(25–26)	*Typha domingensis*, in line with canal, 1000 h
(27–28)	*Tamarix pentandra*, same as above
29–36	1030 h diurnal
(29–30)	*Conyza coulteri*
(31–32)	*Salsola iberica*
(33–34)	*Typha domingensis*
(35–36)	*Euphorbia albomarginata*

[a] Duplicate samples taken by LLNL.

Table B3. Continued.

DRI Sample #	Sample (28 Sept 84)
37–42[a]	C_3 species transect from berm; *Sphaeralcea coulteri* (globe mallow), a leafy herbaceous "roadside" weed used in transect
(37–38)	Next to berm (but outside it), a 50 x 50 cm plant
(39–40)	6-7 m from berm (berm side of road), population of small plants
(41–42)	12 m from berm (across road), population of small plants
43–50	C_4 species transect from berm; *Atriplex canescens* (four-wing saltbush) used in transect
(43–44)	Inside berm, 2 shrubs each 60 x 40 cm
(45–46)	6-7 m from berm (berm side of road), 40 x 60 cm bush
(47–48)	12 m from berm (across road), 2 bushes each 50 x 50 cm
(49–50)	30 m from berm, two large bushes each 100 x 100 cm
51–58[a]	1200 h diurnal
(51–52)	*Conyza coulteri*
(53–54)	*Salsola iberica*
(55–56)	*Typha domingensis*
(57–58)	*Euphorbia albomarginata*

[a] Duplicate samples taken by LLNL.